EXTENDING AND FORMALIZING THE ENERGY SIGNATURE METHOD FOR CALIBRATING SIMULATIONS AND ILLUSTRATING WITH APPLICATION FOR THREE CALIFORNIA CLIMATES

A Thesis

by

NABIL BENSOUDA

Submitted to the Office of Graduate Studies of
Texas A&M University
in partial fulfillment of the requirements for the degree of

MASTER OF SCIENCE

August 2004

Major Subject: Mechanical Engineering

EXTENDING AND FORMALIZING THE ENERGY SIGNATURE METHOD FOR CALIBRATING SIMULATIONS AND ILLUSTRATING WITH APPLICATION FOR THREE CALIFORNIA CLIMATES

A Thesis

by

NABIL BENSOUDA

Submitted to the Office of Graduate Studies of
Texas A&M University
in partial fulfillment of the requirements for the degree of

MASTER OF SCIENCE

Approved as to style and content by:

David E. Claridge (Chair of Committee)	W. Dan Turner (Member)
Jeff S. Haberl (Member)	Charles H. Culp (Member)
Dennis O'Neal (Head of Department)	

August 2004

Major Subject: Mechanical Engineering

ABSTRACT

Extending and Formalizing the Energy Signature Method for Calibrating Simulations and Illustrating with Application for Three California Climates.

(August 2004)

Nabil Bensouda, B.S.,

Ecole Nationale de l'Industrie Minérale, Rabat, Morocco

Chair of Advisory Committee: Dr. David E. Claridge

This thesis extends and formalizes the energy signature method developed by Wei et al. (1998) for the rapid calibration of cooling and heating energy consumption simulations for commercial buildings. This method is based on the use of "calibration signatures" which characterize the difference between measured and simulated performance.

By creating a library of shapes for certain known errors, clues can be provided to the analyst to use in identifying what simulation input errors may be causing the discrepancies. These are referred to as "characteristic signatures". In this thesis, sets of characteristic signatures are produced for the climates typified by Pasadena, Sacramento and Oakland, California for each of the four major system types: single-duct variable-air-volume, single-duct constant-volume, dual-duct variable-air-volume and dual-duct constant-volume.

A detailed step-by-step description is given for the proposed methodology, and two examples and a real-world case study serve to illustrate the use of the signature method.

ACKNOWLEDGEMENTS

I would like to acknowledge and express my gratitude to my advisor and committee chair Dr. David E. Claridge. He introduced me to this research field and continuously guided and assisted me.

My sincere thanks go to my committee members Dr. Dan Turner, Dr. Jeff Haberl, and Dr. Charles Culp for all of their help, guidance and insight.

I greatly appreciate the contributions of Mr. Seung Uk Lee and Mr. Guanghua Wei of the Energy Systems Lab of Texas A&M University, Dr. Kristin Heinemeier of the Brooks Energy and Sustainability Laboratory, and Mr. Naoya Motegi of the Lawrence Berkeley National Laboratory. Some of the work in this thesis was conducted concurrently with Mr. Lee for the sake of verifying results. Mr. Wei (with Dr. Liu and Dr. Claridge) developed the energy signature method on which this research work was based. Mr. Wei also facilitated the calibration process in the second illustrative example by generating the "synthetic measured data" so I did not know which simulation parameters had been altered while calibrating the simulation. Mr. Motegi was the contact person at the Lawrence Berkeley National Laboratory. He provided me with valuable information on the Dalziel building for the case study.

TABLE OF CONTENTS

Page

Page

LIST OF FIGURES

Page

Page

LIST OF TABLES

Page

CHAPTER I

INTRODUCTION AND LITERATURE REVIEW

I.1 Introduction

The calibration of a cooling and heating energy consumption simulation typically consists of closely matching the simulation results to measured consumption from utility bills or actual data. However, the calibration processes used to achieve agreement have generally been quite time-consuming. There would be tremendous value in having a procedure that can quickly and reliably calibrate simulations of large commercial buildings with built-up HVAC systems. With such a procedure, it would be practical to use a calibrated simulation for energy audits (to determine the potential savings from proposed retrofit measures), to explore the potential savings from changing building operational strategies or to track the building's performance over time in support of fault detection activities.

The objective of this thesis is to extend and formalize the energy signature method developed by Wei et al. (1998) for the rapid calibration of cooling and heating energy consumption simulations for commercial buildings. This method is based on the use of "calibration signatures", which characterize the difference between measured and simulated performance.

This thesis follows the style of *Journal of Solar Energy Engineering*.

It will be extended for use for the climates typified by Pasadena, Sacramento, and Oakland, California. Separate sets of characteristic calibration signatures will be published for these climates for four major system types: single-duct variable-air-volume, single-duct constant-volume, dual-duct variable-air-volume and dual-duct constant-volume.

The procedure will be formalized so that it can be easily learned and applied by any person familiar with simulation. A detailed step-by-step description will be provided, with hints and discussions for the steps that require the analyst to make more judgment.

The use of the proposed method is to be demonstrated in illustrative examples, and a real-world case study.

I.2 Literature review

a. Energy simulation

The formation of the ASHRAE Task Group on Energy Requirements in 1965 was recognition of the growing interest in building energy simulations. Mainframe computers had already been used for building thermal environmental calculations in universities, national laboratories, and to a limited extent in consulting firms.

In the late 1960s and early 1970s, the first hourly energy simulation programs were developed, and important papers were published on load calculations, system and equipment simulation, and hourly weather data for energy analysis (Kusuda 2001).

The oil crisis of 1972 heightened the need for energy conservation when it was pointed out that the building sector was consuming almost one third of the total energy consumption in the United States. Many researchers became more attracted to energy conservation areas, especially due to the shift in the availability of the government's research funding.

Computer simulations started to be used for studying the effectiveness of various energy conservation strategies, and comparing the calculated energy consumption with the metered values. The difficult task was to simulate the interactions between HVAC system components while they responded to the changes in heating and cooling requirements of the building under changing operating conditions.

Energy simulation programs continue to be developed and improved since then, while the building sector continues to represent a big share in the total energy consumption in the United States, with approximately 4.6 million commercial buildings containing about 5.5 billion m^2 of floor area in 1995 (EIA 1997).

Simulation tools include detailed whole building simulations, such as DOE-2 (Winkelmann et al. 1993) and BLAST (BSL 1999); detailed system simulations, such as

HVACSIM+ (Clark 1985); and simplified models, such as ASEAM (Fleming 1983) and AirModel (Liu et al. 1997).

According to Kusuda (2001), two of the most renowned simulation programs, DOE-2 and BLAST, originated from methods and codes that trace back respectively to the late 1960s and the early 1970s. DOE-2, sponsored by the United States Department of Energy (DOE), has its origins in a program written for the United States Post Office; and BLAST sponsored by the United States Department of Defense (DOD), has its origins in a program developed at the United States National Bureau of Standards (now NIST).

A new generation of building energy simulation programs is about to begin with the advent of EnergyPlus (Crawley 2001), a simulation program sponsored by the United States Department of Energy.

b. Calibration of energy simulation

Historically, the inputs for energy simulations of commercial buildings have been based on design data. Differences between simulation results based on design data and measured consumption can reach 100% (Norford et al. 1994), or even 150% (Ahmad 2003). These errors are not thought to be due to errors in the simulation software itself or to undescribed input parameters but to errors in the input assumptions for a particular building, due to misunderstanding of the building's design or to the differences between design and as-built conditions or operations.

Numerous organizations and individuals have developed procedures to adjust the inputs used to "calibrate" a simulation so the simulated results more closely match measured consumption (e.g., Diamond and Hunn 1981, Kaplan et al. 1992, Haberl and Bou-Saada 1998 and Liu and Claridge 1998). These procedures employ a variety of techniques to either measure or infer the characteristics of individual buildings as they were built and operated and identify candidate changes in model inputs that may resolve the differences. These efforts have been quite successful in achieving simulated results that agreed with the measured consumption, typically to less than 5% on an annual basis. Agreement within 5-10% has often been achieved on a monthly basis, and sometimes on a daily basis.

Once a probable error (or errors) in a simulation input has been identified, the analyst must typically assess whether the change makes physical and intuitive sense. This sometimes requires revisiting the building or conducting some other investigation. It must then be decided whether it is appropriate to revise the model inputs before accepting the model.

A simulation that will be useful for large commercial buildings with built-up HVAC systems can require hundreds of input variables, and will have at least a few dozen crucial input parameters. If monthly values of measured consumption data were used for calibration, there would be more parameters that may be varied than the number of data points being fit with a typical year of data and the problem would be mathematically "over-determined" (more equations than unknowns). This has the consequence that the

calibration achieved might fit past data very well, but will not necessarily fit future data very well. Hence, a calibration based on monthly data is not suitable for use in tuning HVAC operating parameters. The use of several months of daily consumption data eliminates this problem and has been shown to be suitable for use in calibrating models that were subsequently used to develop improved operating strategies (Liu and Claridge 1998). Hourly data can also be used, although dynamic effects of the thermal mass of the building and system will become evident. In some calibration methods, this could present a problem, although the differences will tend to average out over the course of a day, so some statistical analysis will not be affected by these differences. Hourly data can also be used to "fine tune" a calibration that was done mostly with daily data (Liu et al. 1998). This is achieved by introducing a daily load profile.

The simulation period should cover most of the annual ambient temperature range. It may vary from several weeks to a whole year depending on the fluctuations of weather conditions throughout the year. Haberl and Bou-Saada (1998) recommend that measured energy data should cover at least seven to nine months. As far as weather data is concerned, Haberl et al. (1995) found that using on-site measured weather data improved the simulation; however, standard weather data may be used when no site measured data is available. The impact of using different types of standard weather data on cooling and heating energy consumption has been investigated by Haberl et al. (1995), and Huang and Crawley (1996).

The measured performance data used for calibration must closely match the simulated data when calibration is complete. It must include the same physical factors (e.g. thermal load or energy consumption, whole building or system-based, hourly, daily or monthly) over the same period of time. Measured data can be obtained from any of a number of sources:

- Utility billing data (typically monthly, or something close to monthly).
- Utility interval meter data (available from the utility for some larger buildings).
- Interval pulse-data obtained from a utility meter.
- Data from an Energy Management and Control System.
- Data from an installed data logger (with Btu or kWh sensors/transducers).

Data quality must be assessed for any use of measured data. Identifying erroneous data points is important. Particularly for shorter interval data, an approach to identifying and "fixing" any erroneous or missing data must be designed. Chen (1999) evaluated four interpolation techniques for filling in short periods of missing data: Single regression, polynomial models, Lagrange interpolation and linear interpolation. He found that linear and polynomial techniques were the most reliable. Order 8 and order 10 polynomials offered the best results respectively for energy data and weather data, with 24 measured existing data points around the missing data. Baltazar-Cervantes (2000) evaluated spline and Fourier series mathematical techniques to interpolate missing data. He concluded that linear interpolation was the most reliable for weather data. As for energy data, the Fourier series approach with 24 data points before and after and six constants was found to be the

most suitable. Linear interpolation was recommended where there are not enough measured data to apply the Fourier series approach.

There has been an increased level of interest in applications for calibrated simulation in recent years (IPMVP 2001, Liu and Claridge 1998). They discussed potential uses for calibrated simulation, which include:

- energy audits, to determine the potential savings from proposed retrofit measures;
- energy savings estimation, to explore the potential savings from changing building operational strategies ("what-if" analysis);
- existing building and new construction commissioning;
- fault detection and diagnostics;
- model-based optimization; and
- program evaluation.

c. Calibration techniques

Procedures for calibrating hourly simulations have evolved in the 1990s (Claridge 1998). This section describes some of the calibration techniques that have been developed to assist the simulation engineer in visualizing the difference between simulated and measured data, perform the calibration, and evaluate the adequacy of the calibrated simulation.

A graphical procedure was developed by Bronson et al. (1992) for visualizing hourly differences between the simulated and measured data over the entire simulation period. The procedure relies on four three-dimensional comparative plots. The x and y axes represent the day of the year and the hour of the day respectively, and the z axis represents measured data, simulated data, positive residuals, and negative residuals respectively for the four comparative plots. The utilization of these plots permitted the analyst to visualize small differences between the simulated and measured data, and therefore be able to produce a more fine-tuned calibration.

Haberl and Bou-Saada (1998) improved the graphical procedure described above. In addition to 3-D comparative plots, a more detailed statistical analysis was conducted and box-whisker-mean plots were used to compare simulated and measured data in more detail. Several statistical goodness-of-fit parameters were also used to provide more tools to evaluate the adequacy of the calibrated simulation. Box-whisker-mean plots were used to show energy use as a function of binned dry-bulb temperature, hour of the day, and weekly time series displaying maximum, minimum, mean, median, 10th, 25th, 75th, and 90th percentile points for each data bin.

Earlier, Manke and Hittle (1996) developed a short-term hourly energy use calibration procedure. Four or five selected simulation input parameters were varied one at a time from 10% to 200% of their nominal values with 10% increments. The minimum Root Mean Square Error (RMSE) was sought for each parameter. The parameter was returned to its nominal value before testing the next parameter. After a set of 19 runs was

conducted for each parameter, the values that produced the minimum RMSEs were used as the new nominal values, and the process was iterated until an acceptable RMSE was reached. The procedure was tested with two small single-story buildings (less than 10,000 ft^2 of floor area) for short-term simulation periods (less than 4 days).

In order to compare simulated and measured data, Thamilseran (1999) used “residual plots” and “comparison plots” to test an inverse bin method for baselining hourly energy use. The “residual plot” is a time series plot that shows simulated data, measured data, and the differences between them (residuals). The “comparison plot” shows simulated data in the y-axis as a function of measured data in the x-axis with the cloud of data points compared to the line x=y.

Wei et al. (1998) developed a "signature" calibration procedure and published input parameter "signatures" to assist the calibrator in identifying input parameter(s) to be altered at each calibration step. The "signatures" are graphical representations of the impact of changing an input parameter on the total energy use as a function of ambient temperature. Nine or ten selected input parameters were varied one at a time from the baseline value to another selected value, which produced an impact within ±10% over the entire ambient temperature range (except for switching to an economizer mode, which produces much bigger changes in the low ambient temperature range). The percent change caused by altering the input parameter on both cooling and heating energy consumption was then plotted as a function of ambient temperature. Sets of signatures were generated and published for the selected input parameters for four major AHU types

with San Antonio, Texas weather data. The calibration procedure consists in generating a first simulation and producing two graphs of the normalized difference between simulated and measured data as a function of ambient temperature for both cooling and heating. This pair of graphs is then compared to published "signatures" for the corresponding AHU type to help identify an input parameter(s) that has a comparable curve, and can therefore be altered to improve the calibration for cooling and/or heating over the entire or part of the temperature range. The process is iterated until the calibration is adequate.

The calibration procedure described in this thesis is based on the signature method mentioned above. This method was reviewed and improved. It was then extended, formalized, and tested with a real building simulation.

A different approach was taken by Subbarao (2000) in their patented work. In order to calibrate an hourly simulation, the approach consists in correcting heat flows in the energy balance, rather than modifying input parameters. A software package was developed to predict heating and cooling loads from corrected heat flows using a simplified program, and convert them to electrical and gas energy consumption using simple models of systems and plants.

I.3 Purpose and objective

The objective of this thesis is to extend and formalize the energy signature method developed by Wei et al. (1998). It will be extended for use in the climates typified by Pasadena, Sacramento, and Oakland, California; and for four major system types: single-duct variable-air-volume, single-duct constant-volume, dual-duct variable-air-volume and dual-duct constant-volume. The procedure will be formalized so that it can be easily learned and applied by any person familiar with simulation.

The purpose is to provide a simple step-by-step procedure to assist the calibrator in visualizing the difference between simulated and measured data and identifying input parameter(s) to be altered at each calibration step for the rapid calibration of cooling and heating energy consumption simulations for commercial buildings.

I.4 Significance of this work

The calibration procedure described in this thesis is based on the signature method developed by Wei et al. (1998). As a first step, the signatures published in Wei et al.'s paper were regenerated using the same simulation program (AirModel). The results matched perfectly, except for the hot deck temperature heating signature for the constant volume variable air volume system. Investigation discovered an error in the original published signature. The program's output was then verified against a spreadsheet with simplified load calculations. Some load calculation errors and AirModel bugs were

reported to and corrected by the program developer (Liu 2001). The definition of the "characteristic signature" was reviewed and its sign was reversed in order to make it easier for the user to compare the simulation's "calibration signature" to published "characteristic signatures". The user now can look for "characteristic signatures" that have the same shape as the "calibration signature" instead of the mirror shape. Some of the selected input parameters for which characteristic signatures were generated were changed. The minimum air flow rate, for example, was used instead of the design flow rate for variable air volume systems. The Envelope U-value (including walls, windows and the roof) was also used in lieu of the window U-value.

This thesis presents the definitions of the calibration signature and characteristic signature. It provides sets of characteristic calibration signatures for the four AHU types and the three climates mentioned above. It also describes in detail the four major AHU types by providing a flow chart of operational equations. It also provides a procedure to generate one's own characteristic signatures for use with other AHU types, climates, or simulation input variables.

A detailed step-by-step description of the energy signature calibration process is provided, with hints and discussions for the steps that require the analyst to use judgment. Two statistical variables used to evaluate calibrated simulations are also presented. The use of the proposed method is demonstrated in illustrative examples, and a real-world case study.

I.5 Limitations

The proposed calibration procedure was not tested with simulation programs other than AirModel, systems other than the four major types described in section III.3, or buildings with more than one AHU type.

CHAPTER II

ENERGY SIGNATURE METHOD

The calibration procedure presented in this thesis is based on the energy signature method developed by Wei et al. (1998) for the rapid calibration of cooling and heating energy simulation for commercial buildings. This calibration procedure is based on the use of a pair of cooling and heating "calibration signatures" for the uncalibrated simulation, and a library of published pairs of cooling and heating "characteristic signatures".

The cooling and heating "calibration signatures" graphically represent the normalized difference between measured and simulated cooling and heating energy consumption as a function of ambient temperature. The library consists of pairs of cooling and heating "calibration signatures" generated and published for major input parameters. Each pair graphically represents, as a function of ambient temperature, the normalized change introduced in cooling and heating simulation results when the input parameter is altered.

Wei et al. (1998) found that comparing the pair of cooling and heating calibration signatures to pairs of cooling and heating characteristic signatures provides important information about the input variable change(s) needed to achieve calibration.

This section presents the formal definitions of the calibration signature and the characteristic signature.

II.1 Definition of the calibration signature

The calibration signature is a normalized plot of the difference between measured and simulated energy consumption values as a function of ambient temperature. This normalization does not affect the RMSE. The calibration signature values for cooling and heating energy consumption are calculated for each data point as follows:

$$\text{Cooling Calibration signature value} = \frac{\text{- Cooling Residual}}{\text{Maximum measured cooling energy consumption}} \text{ x } 100\% \quad (1)$$

$$\text{Heating Calibration signature value} = \frac{\text{- Heating Residual}}{\text{Maximum measured heating energy consumption}} \text{ x } 100\% \quad (2)$$

$$\text{where} \qquad \text{Residual} = \text{Simulated consumption} - \text{Measured consumption} \quad (3)$$

Cooling and heating calibration signature values are then plotted versus ambient temperature as shown in Figure 1 for an uncalibrated simulation.

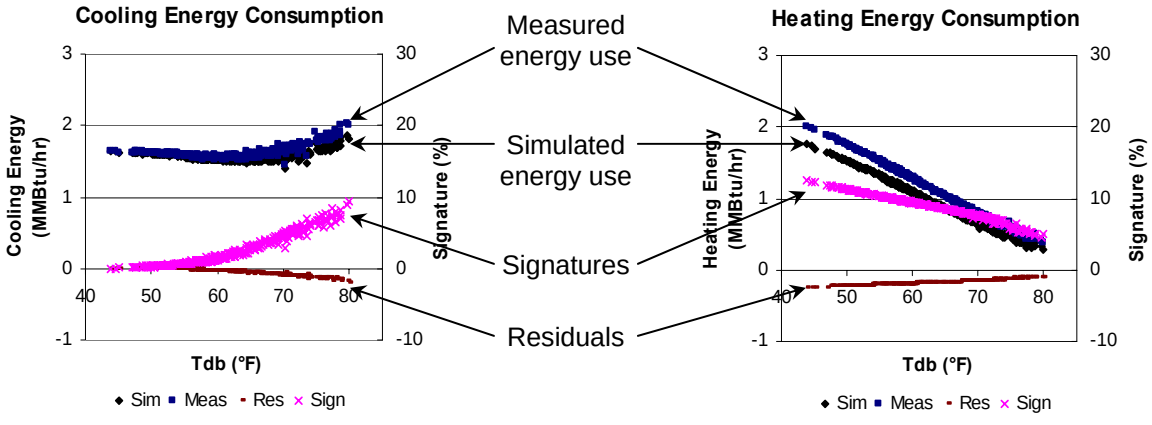

Figure 1. Example of cooling and heating calibration signatures

Note that calibration signature values are read on the right hand side vertical axis for each graph.

The cooling and heating calibration signatures shown in Figure 1 have the same sign and have opposite slopes. The cooling calibration signature increases from zero at low ambient temperatures to about 10% at high ambient temperatures, while the heating calibration signature decreases from about 12% at low ambient temperatures to about 5% at high ambient temperatures. These characteristics will be useful in trying to determine which input parameters need to be altered when comparing this pair of calibration signatures to pairs of characteristic signatures.

II.2 Definition of the characteristic signature

Any particular uncalibrated (or partially calibrated) simulation will have a pair of cooling and heating calibration signatures, as described in the previous section and illustrated in Figure 1.

By creating a library of shapes for certain known changes introduced by individual simulation input parameters, clues can be provided to the analyst to identify what simulation input errors may be causing the discrepancies between measured and simulated consumption. These are referred to as “characteristic signatures”.

The pair of calibration signatures needs to be compared to published characteristic signatures for the corresponding climate and air handling unit (AHU) type. In this thesis, sets of characteristic signatures are produced for the climates typified by Pasadena, Sacramento and Oakland, California for each of the four major system types: Single-Duct Constant-Volume (SDCV), Single-Duct Variable-Air-Volume (SDVAV), Dual-Duct Constant-Volume (DDCV) and Dual-Duct Variable-Air-Volume (DDVAV).

This was done for each climate and AHU type by simulating a prototypical 6-floor office building with an initial value for an input parameter (the "baseline" run), then changing that input by a given amount and rerunning the simulation. The characteristic signature values for cooling and heating energy consumption are calculated for each data point as follows:

$$\text{Cooling Characteristic signature value} = \frac{\text{Change in cooling energy consumption}}{\text{Maximum baseline cooling energy consumption}} \text{ x } 100\% \quad (4)$$

$$\text{Heating Characteristic signature value} = \frac{\text{Change in heating energy consumption}}{\text{Maximum baseline heating energy consumption}} \text{ x } 100\% \quad (5)$$

where the change in energy consumption is taken as the cooling or heating energy consumption value from the simulation with the changed input minus the baseline value at the same temperature. The denominator is the maximum baseline energy consumption determined over the entire range of ambient temperatures contained in the weather file being used.

Characteristic signatures present the impact of an input parameter on cooling and heating energy consumption as the percent change relative to the maximum baseline cooling and heating energy consumption respectively.

Figures 2 to 5 illustrate how cooling and heating characteristic signatures were generated for the outside air flow rate for a single duct constant volume AHU with Sacramento, California weather data.

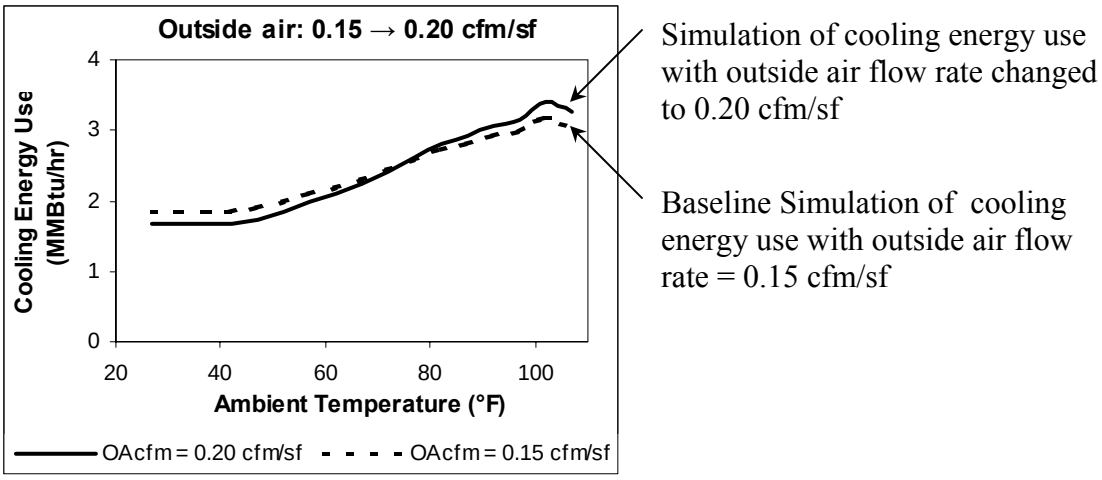

Figure 2. Simulated cooling energy use with baseline and altered outside air flow rate

The outside air flow rate was changed from 0.15 cfm/sf for the baseline simulation to 0.20 cfm/sf. Figure 2 shows cooling energy use as a function of ambient temperature for both values.

The cooling characteristic signature values were calculated for each data point according to equation 4, and plotted as a function of ambient temperature as shown in Figure 3.

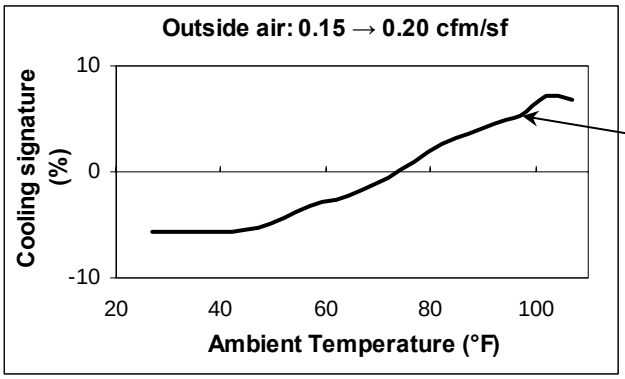

Figure 3. Cooling characteristic signature for outside air flow rate produced from data in Figure 2

Figure 4 shows heating energy use as a function of ambient temperature for the baseline simulation with outside air flow rate = 0.15 cfm/sf, and the simulation with the outside air flow rate altered to 0.20 cfm/sf.

The heating characteristic signature values were calculated for each data point according to equation 5, and plotted as a function of ambient temperature as shown in Figure 5.

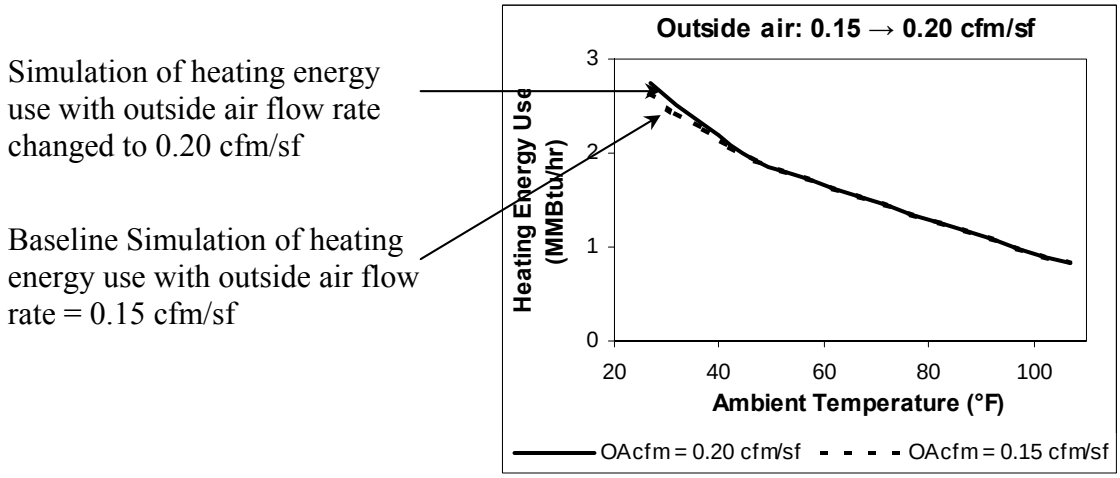

Figure 4. Simulated heating energy use with baseline and altered outside air flow rate

Calculated outside air flow rate heating characteristic signature with a change from 0.15 to 0.20 cfm/sf

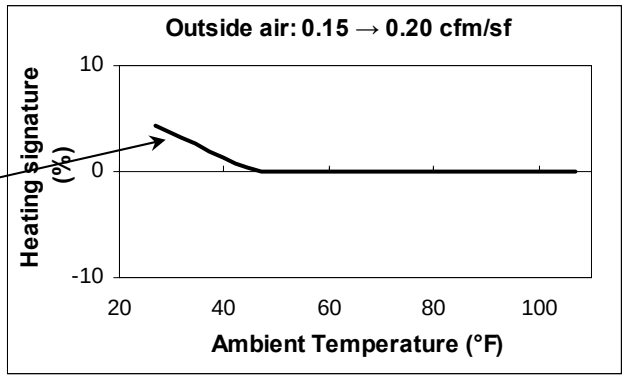

Figure 5. Heating characteristic signature for outside air flow rate produced from data in Figure 4

The pair of outside air flow rate cooling and heating characteristic signatures is shown in Figure 6. It is one of the pairs of published characteristic signatures, among those of other input parameters shown in Figure 17 for a single duct constant volume system with Sacramento, CA weather data. Published characteristic signatures are presented in the next chapter.

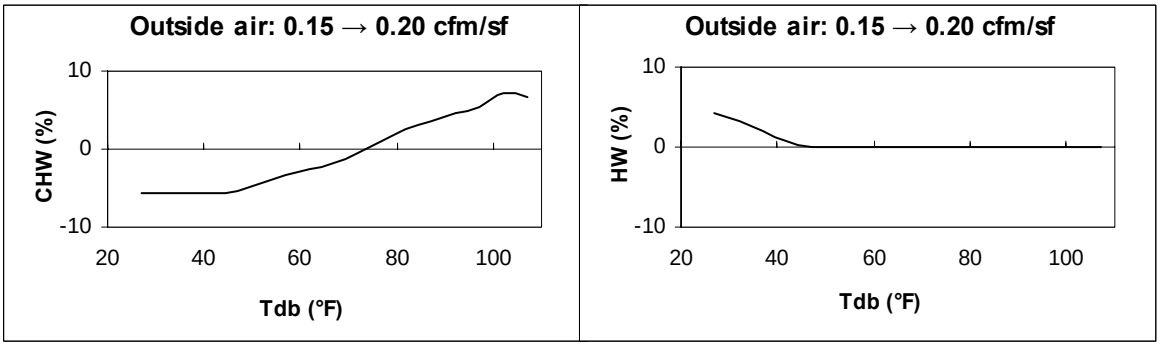

Figure 6. Published outside air flow rate cooling and heating characteristic signatures for a SDCV system with Sacramento, CA, weather data

CHAPTER III

PUBLISHED CHARACTERISTIC SIGNATURES

This chapter presents the sets of published characteristic signatures for the climates typified by Pasadena, Sacramento and Oakland, California for each of the four major system types: single-duct constant-volume, single-duct variable-air-volume, dual-duct constant-volume and dual-duct variable-air-volume.

This chapter also describes weather conditions for the three California cities, the building and system models, and the simulation program used to generate these characteristic signatures.

III.1 Simulation program

The characteristic signatures were generated as described in the previous chapter using AirModel, an HVAC software package for simulation of building cooling and heating consumption. AirModel was developed at the Energy Systems Laboratory at Texas A&M University (Liu 1997). AirModel is based on simplified steady state models. It is not a dynamic hourly simulation program, such as DOE-2. It is rather a bin model run with hourly data. Therefore, one of its limitations is that it doesn't capture the dynamics related to the thermal mass. The signatures and calibration methodology may also be used with other simulation packages that can provide daily values of heating and cooling consumption.

III.2 Weather implications

The characteristic signatures shown in Figure 6 clearly depend on outside temperature. Though not explicitly shown, they also depend on the ambient humidity level when it is high enough to induce latent cooling loads. This is treated by simply using the mean of the humidity values present at each temperature in the weather data for the site in question to define the characteristic signatures. Humidity-sub-binning is a way of revealing the effect of latent loads if necessary. Thamilseran (1999) used this approach by separating energy data into four humidity groups before separating them into temperature bins. He concluded that sub-binning improved the simulation when latent loads are large, as in a hot and humid climate, but is rather unnecessary when latent loads are small.

This humidity dependence suggests that separate sets of signatures may be needed for sites with significantly different temperature and humidity combinations. Separate sets of signatures are also required for different air handler types.

Characteristic signatures depend on the correlation between relative humidity and dry-bulb temperature for the location of interest. Figure 7 shows the average measured relative humidity as a function of ambient temperature for the three California cities used to generate the sets of characteristic signatures presented in this thesis. The weather data used was provided by Motegi (2002). 5°F dry-bulb temperature bins and mean coincident wet-bulb temperatures were used. Figure 7 shows that dry-bulb temperatures range from 32°F to 82°F, 32°F to 97°F and 27°F to 107°F respectively for Oakland, Pasadena and

Sacramento. Relative humidity ranges from 35 to 83%, 17 to 75% and 22 to 83% respectively.

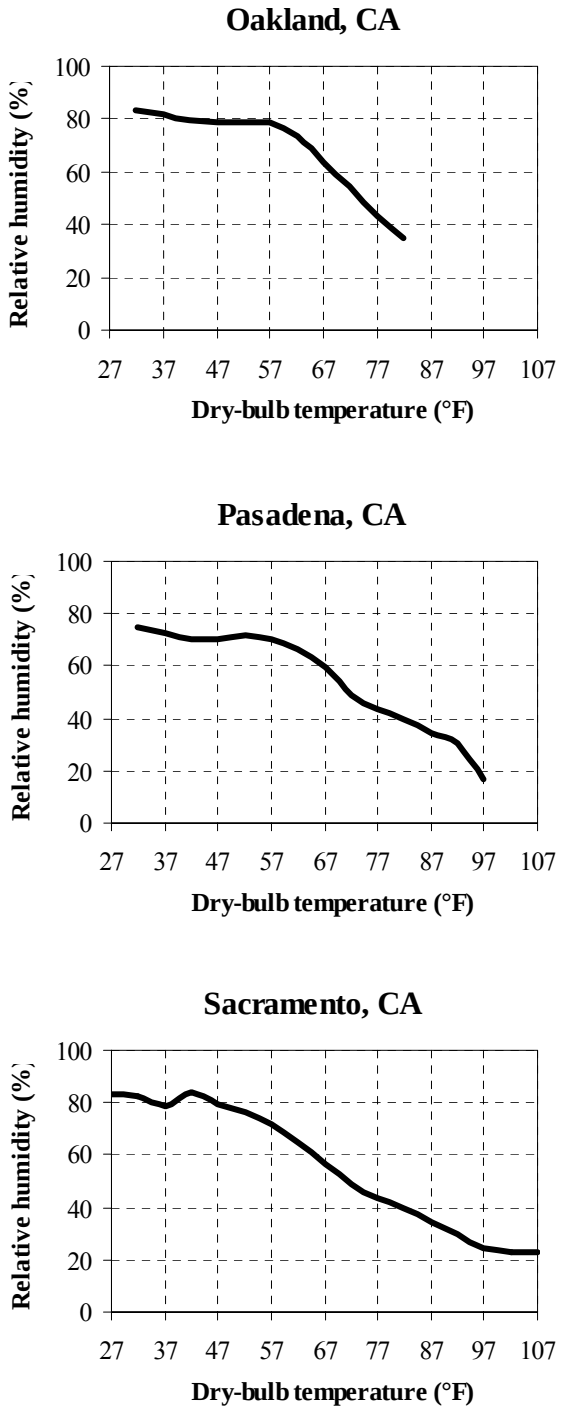

Figure 7. Weather data for three representative California cities

It can be noticed that Sacramento has the widest ranges of both temperature and relative humidity. It is the coldest city in the winter and the hottest in the summer. Oakland has the narrowest ranges of temperatures and relative humidity. It is the warmest in the winter and the coolest in the summer. Pasadena weather conditions fall between the extremes of the weather conditions of the other two cities.

III.3 System models used to generate characteristic signatures

Published characteristic signatures are provided for four AHU types: single-duct constant-volume, single-duct variable-air-volume, dual-duct constant-volume and dual-duct variable-air-volume. Figures 8 and 9 show schematics of the single-duct and dual-duct system models used to generate the published characteristic signatures. Constant-volume systems have constant air flow rate fans, while variable-air-volume systems have variable air flow rate fans.

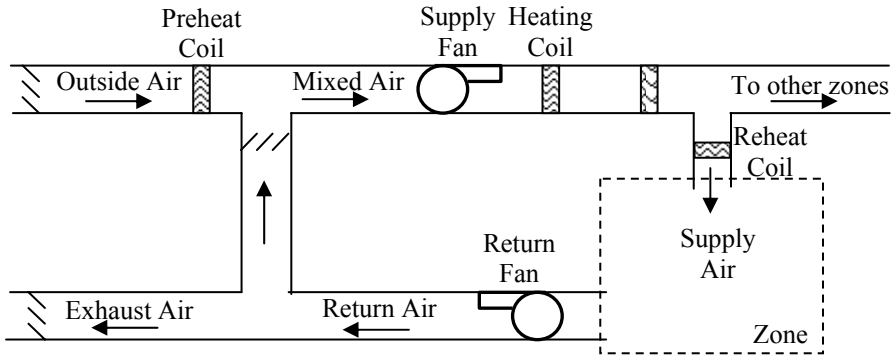

Figure 8. Schematic of a single-duct air handler

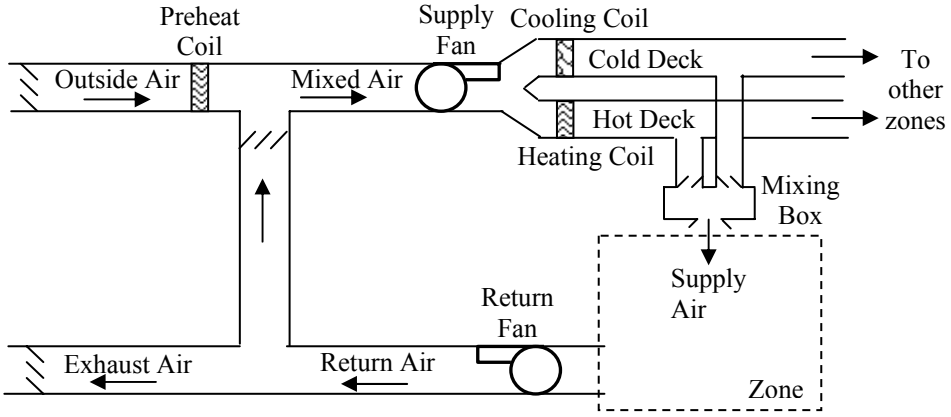

Figure 9. Schematic of a dual-duct air handler

The operational equations that define the models used for SDCV, SDVAV, DDCV and DDVAV systems are shown respectively in Figures 10 to 13, with the nomenclature defined in Table 1.

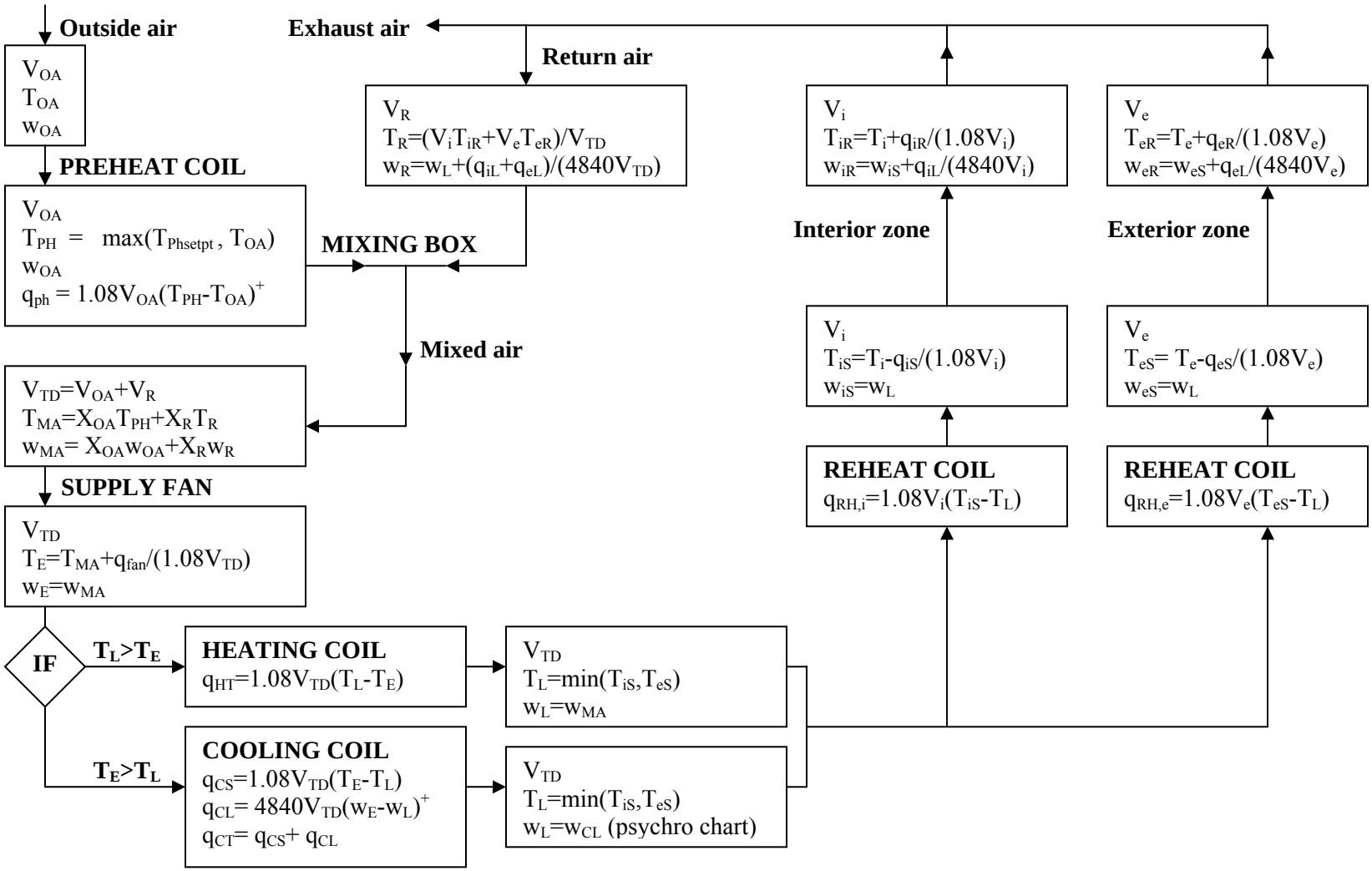

Figure 10. Operational equations for the SDCV system model

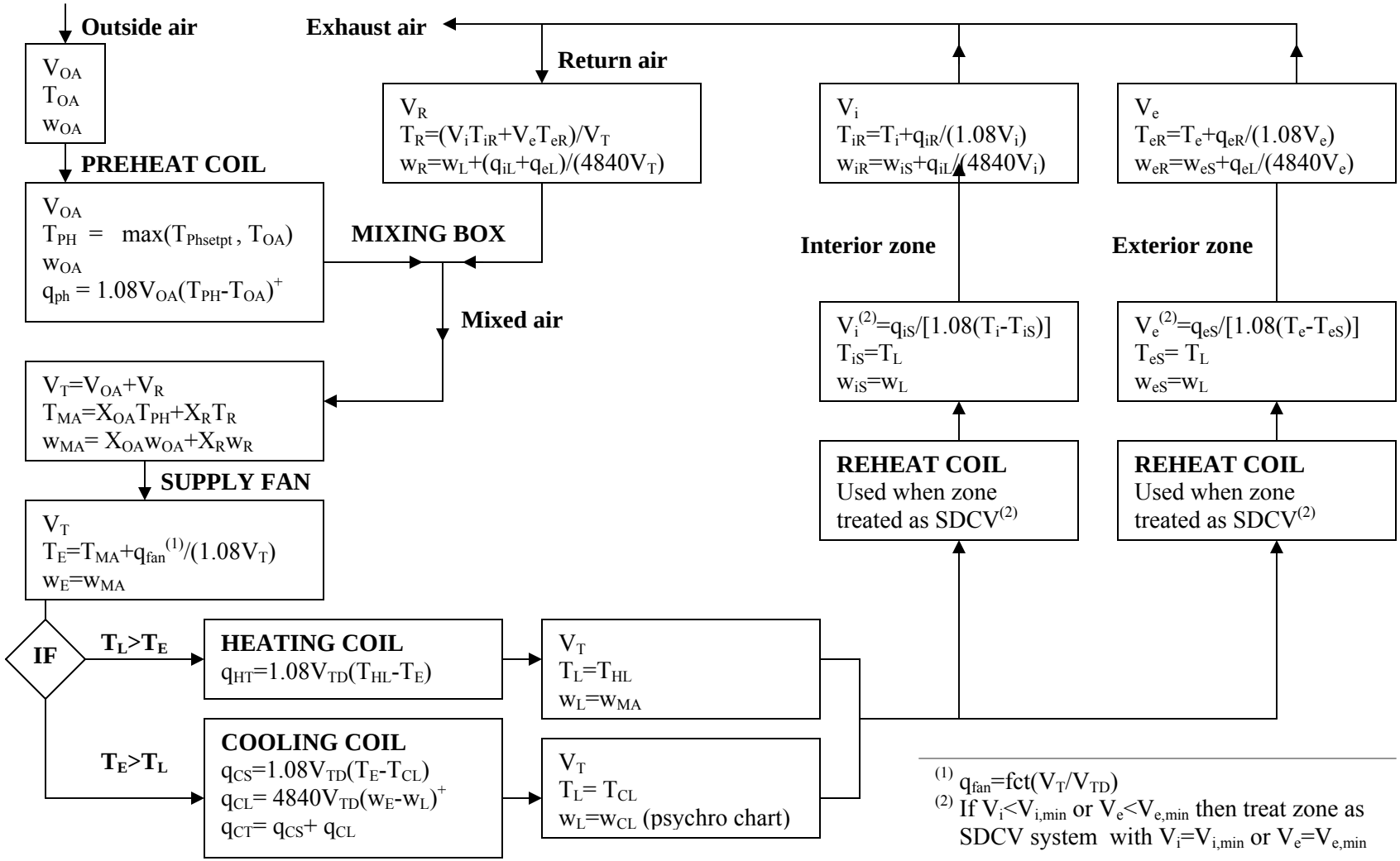

Figure 11. Operational equations for the SDVAV system model

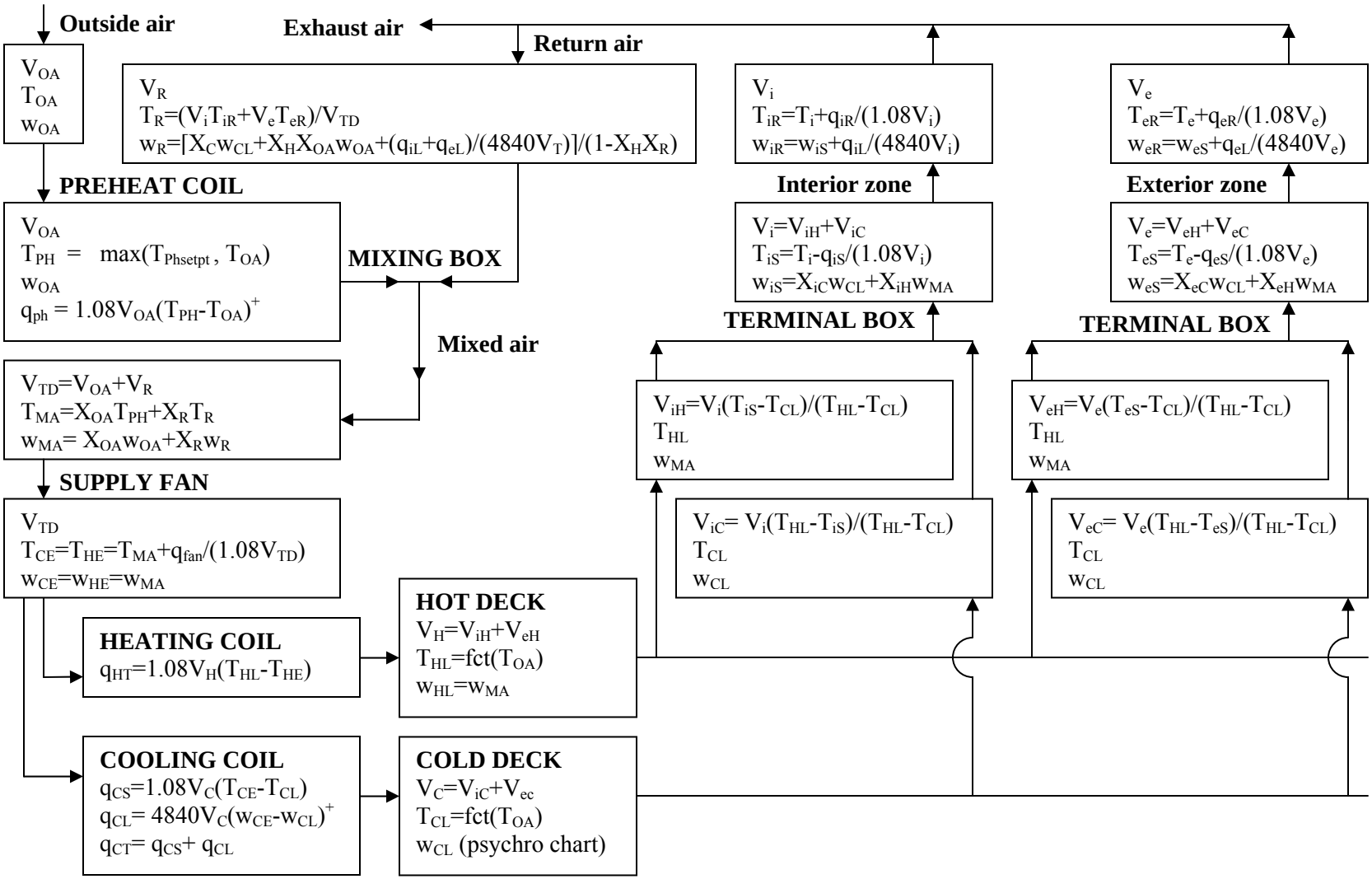

Figure 12. Operational equations for the DDCV system model

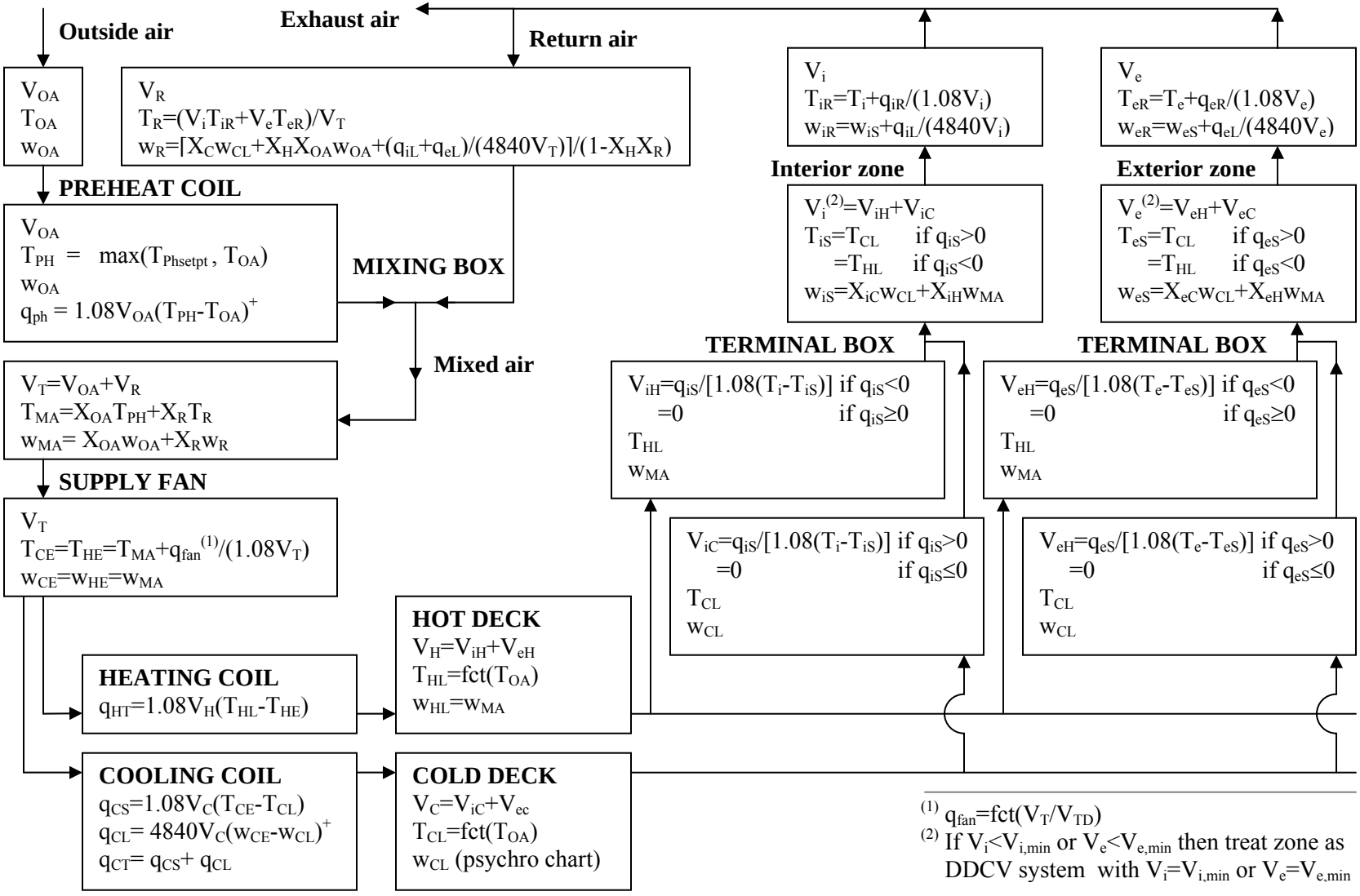

Figure 13. Operational equations for the DDVAV system model

Table 1. Nomenclature for operational equations

Variable	Definition	Unit
ΔT_{SF}	Supply air fan Temperature rise	°F
q_{CL}	Cooling coil latent load	Btu/hr
q_{CS}	Cooling coil sensible load	Btu/hr
q_{CT}	Cooling coil total load	Btu/hr
q_{eL}	Exterior zone latent load	Btu/hr
q_{eR}	Exterior zone return air heat gain	Btu/hr
q_{eS}	Exterior zone sensible load	Btu/hr
q_{HT}	Heating coil sensible load	Btu/hr
q_{iL}	Interior zone latent load	Btu/hr
q_{iR}	Interior zone return air heat gain	Btu/hr
q_{iS}	Interior zone sensible load	Btu/hr
q_{ph}	Preheat coil load	Btu/hr
$q_{RH,i}$	Interior zone reheat coil load	Btu/hr
$q_{RH,e}$	Exterior zone reheat coil load	Btu/hr
T_{CE}	Cooling coil entering air dry bulb Temperature	°F
T_{CL}	Cooling coil leaving air dry bulb Temperature	°F
T_e	Exterior zone design air dry bulb Temperature	°F
T_E	Coil entering air dry bulb Temperature	°F
T_{eR}	Exterior zone return air dry bulb Temperature	°F
T_{eS}	Exterior zone supply air dry bulb Temperature	°F
T_{HE}	Heating coil entering air dry bulb Temperature	°F
T_{HL}	Heating coil leaving air dry bulb Temperature	°F
T_i	Interior zone design air dry bulb Temperature	°F
T_{iR}	Interior zone return air dry bulb Temperature	°F
T_{iS}	Interior zone supply air dry bulb Temperature	°F
T_L	Coil leaving air dry bulb Temperature	°F
T_{MA}	Mixed air dry bulb Temperature	°F
T_{OA}	Outside air dry bulb Temperature	°F
T_{PH}	Preheat coil leaving air dry bulb Temperature	°F
T_R	Return air dry bulb Temperature	°F
V_C	Cold Deck air volume	ft^3/min
V_e	Exterior zone supply air volume	ft^3/min
$V_{e,min}$	Exterior zone minimum supply air volume	ft^3/min

Table 1. Continued

Variable	Definition	Unit
V_{eC}	Exterior zone cold air volume	ft^3/min
V_{eH}	Exterior zone hot air volume	ft^3/min
V_H	Hot Deck air volume	ft^3/min
V_i	Interior zone supply air volume	ft^3/min
$V_{i,min}$	Interior zone minimum supply air volume	ft^3/min
V_{iC}	Interior zone cold air volume	ft^3/min
V_{iH}	Interior zone hot air volume	ft^3/min
V_{OA}	Outside air volume	ft^3/min
V_R	Return air volume	ft^3/min
V_T	Total air volume	ft^3/min
V_{TD}	Design total air volume	ft^3/min
w_{CE}	Cooling coil entering air humidity ratio	lb_w/lb_a
w_{CL}	Cooling coil leaving air humidity ratio	lb_w/lb_a
w_E	Coil entering air humidity ratio	lb_w/lb_a
w_{eR}	Exterior zone return air humidity ratio	lb_w/lb_a
w_{eS}	Exterior zone supply air humidity ratio	lb_w/lb_a
w_{HE}	Heating coil entering air humidity ratio	lb_w/lb_a
w_{HL}	Heating coil leaving air humidity ratio	lb_w/lb_a
w_{iR}	Interior zone return air humidity ratio	lb_w/lb_a
w_{iS}	Interior zone supply air humidity ratio	lb_w/lb_a
w_L	Coil leaving air humidity ratio	lb_w/lb_a
w_{MA}	Mixed air humidity ratio	lb_w/lb_a
w_{OA}	Outside air humidity ratio	lb_w/lb_a
w_R	Return air humidity ratio	lb_w/lb_a
X_C	Cold Deck air volume ratio = V_C/V_T	Dimensionless
X_{eC}	Exterior zone cold air volume ratio = V_{eC}/V_e	Dimensionless
X_{eH}	Exterior zone hot air volume ratio = V_{eH}/V_e	Dimensionless
X_H	Hot Deck air volume ratio = V_H/V_T	Dimensionless
X_{iC}	Interior zone cold air volume ratio = V_{iC}/V_i	Dimensionless
X_{iH}	Interior zone hot air volume ratio = V_{iH}/V_i	Dimensionless
X_{OA}	Ouside air volume ratio = V_{OA}/V_T	Dimensionless
X_R	Return air volume ratio = V_R/V_T	Dimensionless

III.4 Building model used to generate characteristic signatures

A prototypical 6-floor office building was simulated to generate the published characteristic signatures. Figure 14 shows the floor plan of the building. Major characteristics of the building and its systems are shown in Table 2.

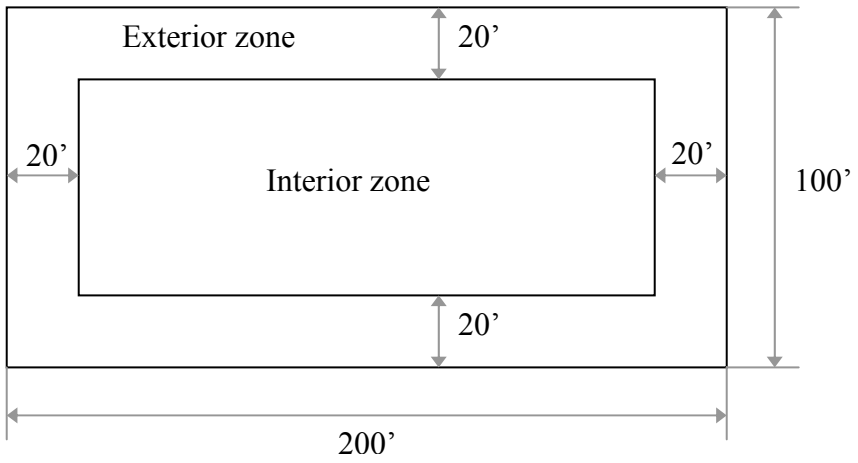

Figure 14. Building floor plan

The AirModel simulation program approximates solar gains as a linear function of outside air temperature as recommended by Knebel (1983). Required inputs of solar gains for the three cities were calculated using the Klein-Theilacker method (Duffie and Beckman 1991), as described in Appendix A.

Table 2. Baseline building and system characteristics

Parameter	Baseline value
Conditioned floor area	120,000 ft^2
Interior zone ratio	0.5
Exterior wall area	37,800 ft^2
Exterior wall U-value	0.1 $Btu/ft^2.hr.°F$
Window area	16,200 ft^2
Window U-value	0.7 $Btu/ft^2.hr.°F$
Roof area	20,000 ft^2
Roof U-value	0.09 $Btu/ft^2.hr.°F$
Design room temperature T_{room}	73 °F
Total air flow rate	1 cfm/ft^2
Minimum air flow rate -VAV systems-	0.5 cfm/ft^2
Outside air flow rate	0.15 cfm/ft^2
Economizer	None
Average internal heat gain Q_{int}	1.4 W/ft^2
Solar gains in $Btu/hr/ft^2$ of building floor area (linear between defined points)	◆ Pasadena: 0.77 at $T_{OA\text{-}min}$=32 °F 0.98 at $T_{OA\text{-}max}$=97 °F ◆ Sacramento: 0.49 at $T_{OA\text{-}min}$=27 °F 1.27 at $T_{OA\text{-}max}$=107 °F ◆ Oakland: 0.54 at $T_{OA\text{-}min}$=32 °F 1.08 at $T_{OA\text{-}max}$=82 °F
Air infiltration	None – building positively pressurized
Average occupancy	200 ft^2/person
Return air and room air temperature difference	2 °F
Cold deck temperature T_c	55 °F
Hot deck schedule T_h -DD systems- (linear between defined points and constant outside lower and higher limits)	110 °F at T_{OA}=40 °F 80 °F at T_{OA}=70 °F 70 °F at T_{OA}=100 °F
Preheat location	Outside air
Preheat temperature T_{ph} schedule	45 °F for T_{OA}<45 °F

The characteristic signatures were generated by running the baseline simulation, then altering key calibration parameters one by one and calculating the cooling and heating characteristic signatures as described in the previous chapter.

Table 3 shows the alterations of the key calibration parameters used to generate the characteristic signatures for the four AHU types. These calibration parameters have a significant influence on energy consumption, are perceived as having a significant influence (and thus are commonly considered for making calibration changes) or are those in which errors have frequently been seen.

Calibration parameter values have been altered to values that were reasonable and produced characteristic signatures within ± 10% when possible.

Table 3. Alterations of calibration parameters used to generate characteristic signatures for the four AHU types

Calibration parameter	Baseline	Alteration			
		SDVAV	SDCV	DDVAV	DDCV
Cold deck temperature T_c (°F)	55	54	54	53	52
Hot deck temperature T_h (°F) vs. outdoor temperature T_{OA}:					
◆ **At T_{OA}= 40 °F**	110			Increased by 3 °F	Increased by 2 °F
◆ **At T_{OA}= 70 °F**	80				
◆ **At T_{OA}= 100 °F**	70				
Minimum air flow rate (cfm/ft^2)	0.5	0.47		0.40	
Supply air flow rate (cfm/ft^2)	1		1.08		1.08
Conditioned floor area (ft^2)	120,000	130,000			
Pre-heat temperature T_{ph} (°F)	45	55			
Internal gains Q_{int} (W/ft^2)	1.4	1.2	1	1.2	1
Outside air flow rate (cfm/ft^2)	0.15	0.20			
Room Temperature T_{room} (°F)	73	74	74	73	74
Envelope U-value (Btu/ft^2.hr.°F)					
◆ **Window**	0.7	Decreased by 15%	Decreased by 20%	Decreased by 15%	Decreased by 20%
◆ **Exterior wall**	0.1				
◆ **Roof**	0.09				
Economizer	None	Temperature economizer at [40,58°F]			

III.5 Published characteristic signatures

This thesis provides characteristic signatures for single-duct constant- volume (SDCV), single-duct variable-air-volume (SDVAV), dual-duct constant-volume (DDCV) and dual-duct variable-air-volume (DDVAV) air handling Unit (AHU) types. The signatures are given for three representative climates in California: Pasadena, Sacramento and Oakland. The twelve sets of characteristic signatures are provided in Figures 15 to 26. Figure numbers for each AHU type and climate are shown in Table 4.

Table 4. Figure numbers for characteristic signatures corresponding to each AHU type and climate

Climate / AHU	Oakland, CA	Pasadena, CA	Sacramento, CA
SDCV	Figure 15	Figure 16	Figure 17
SDVAV	Figure 18	Figure 19	Figure 20
DDCV	Figure 21	Figure 22	Figure 23
DDVAV	Figure 24	Figure 25	Figure 26

The left-hand column shows the chilled water (CHW) characteristic signature and the right-hand column shows the hot water (HW) characteristic signature for the input variable noted in each figure.

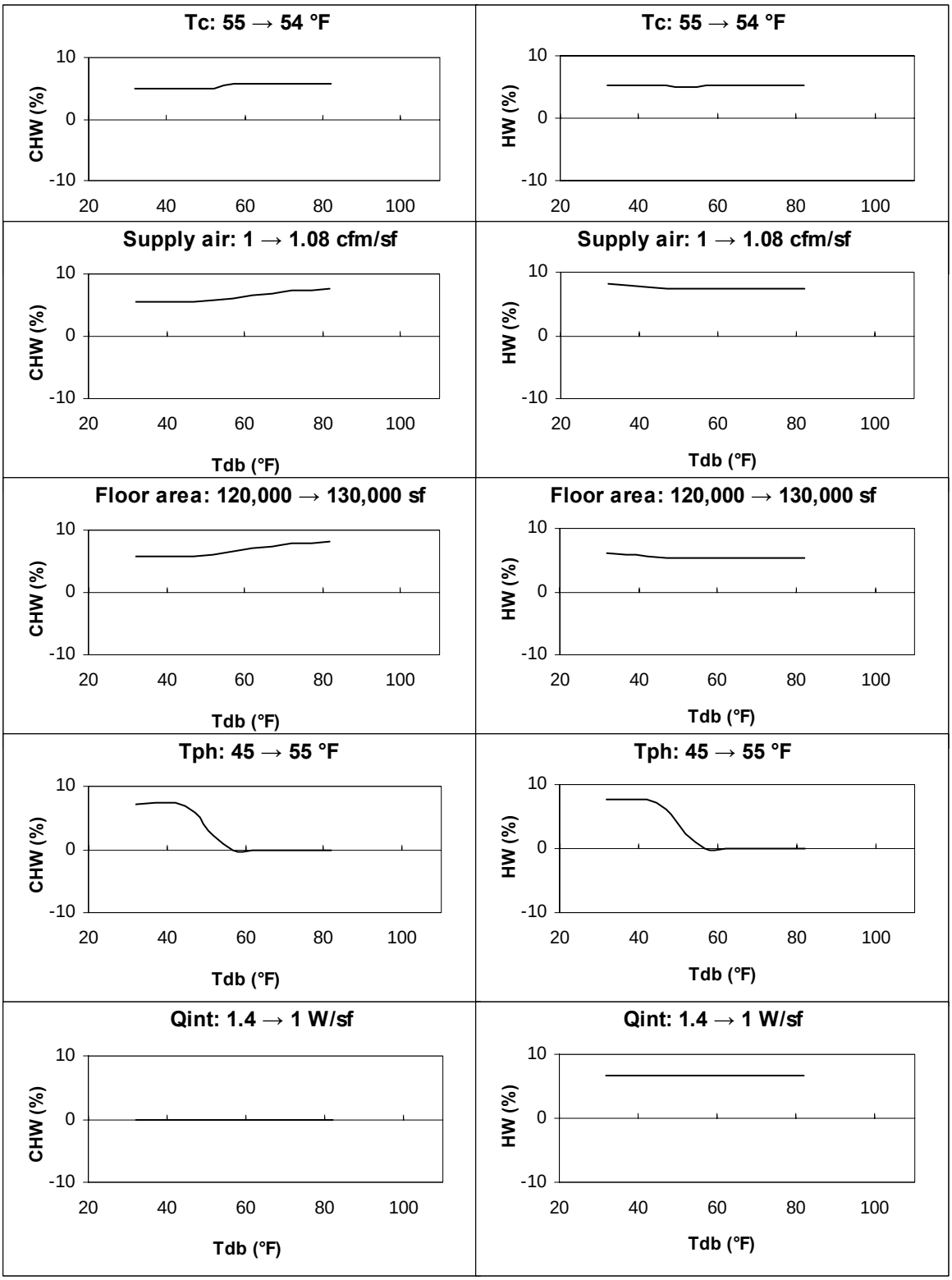

Figure 15. Characteristic signatures for SDCV systems in Oakland

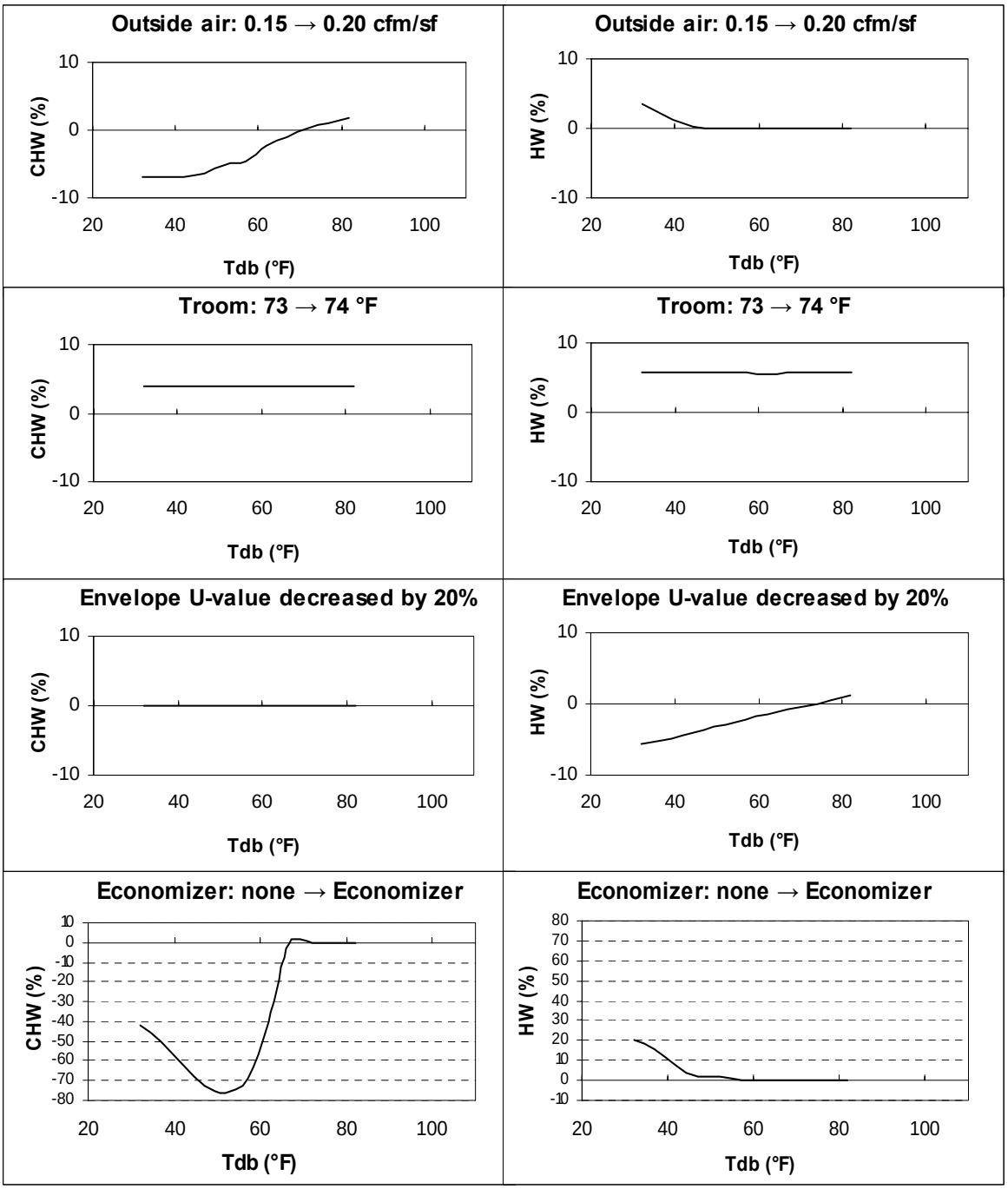

Figure 15. Continued

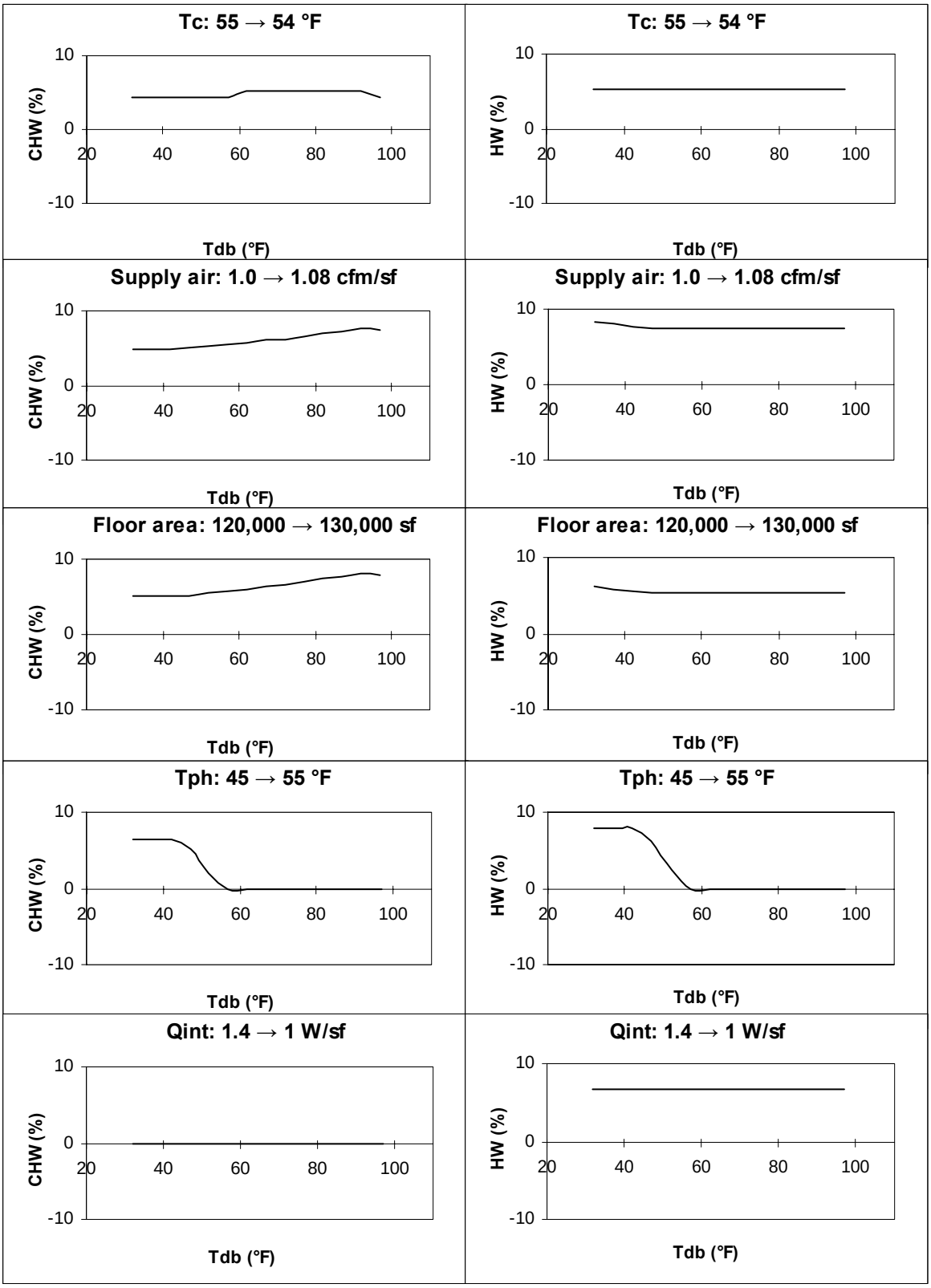

Figure 16. Characteristic signatures for SDCV systems in Pasadena

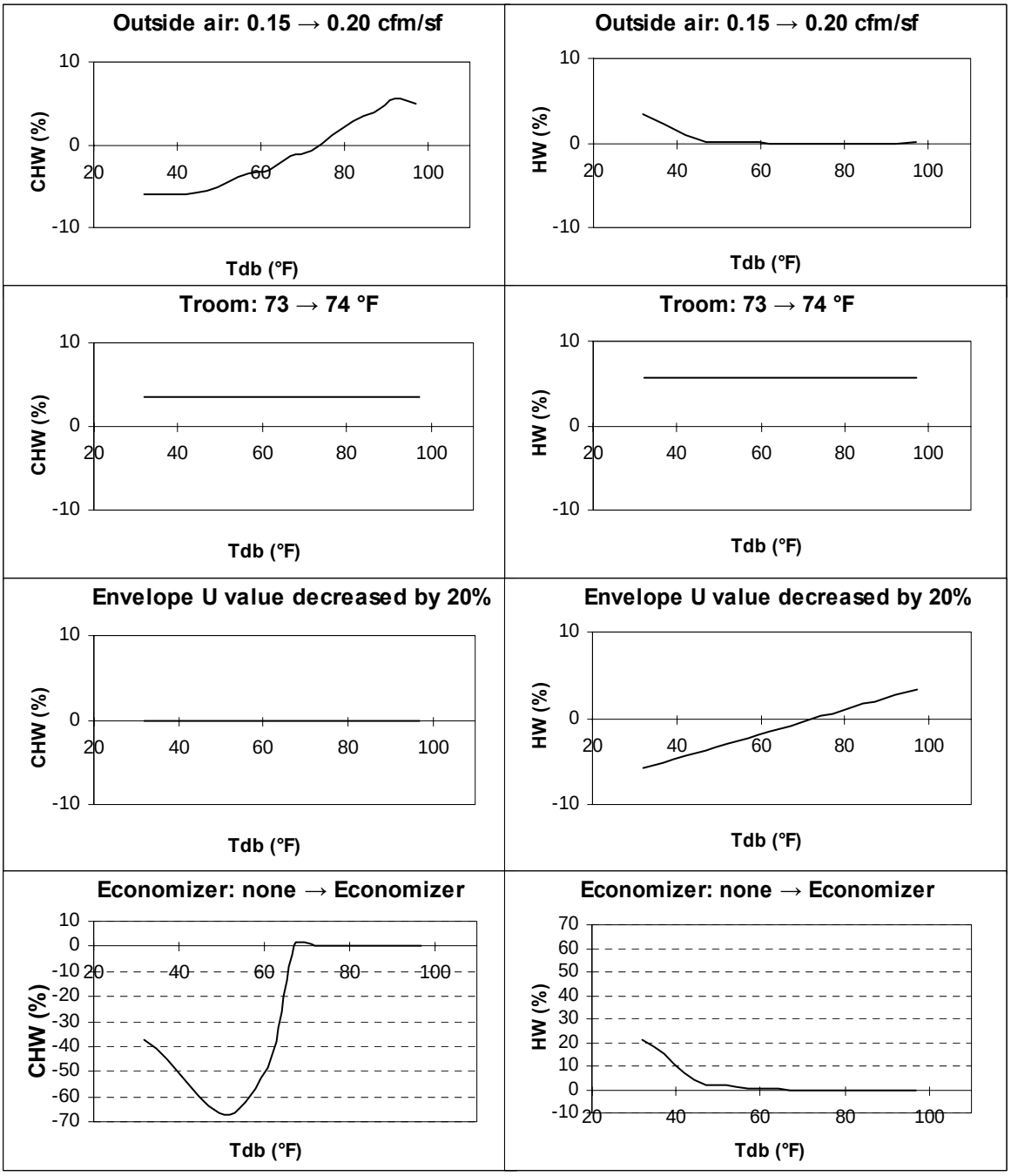

Figure 16. Continued

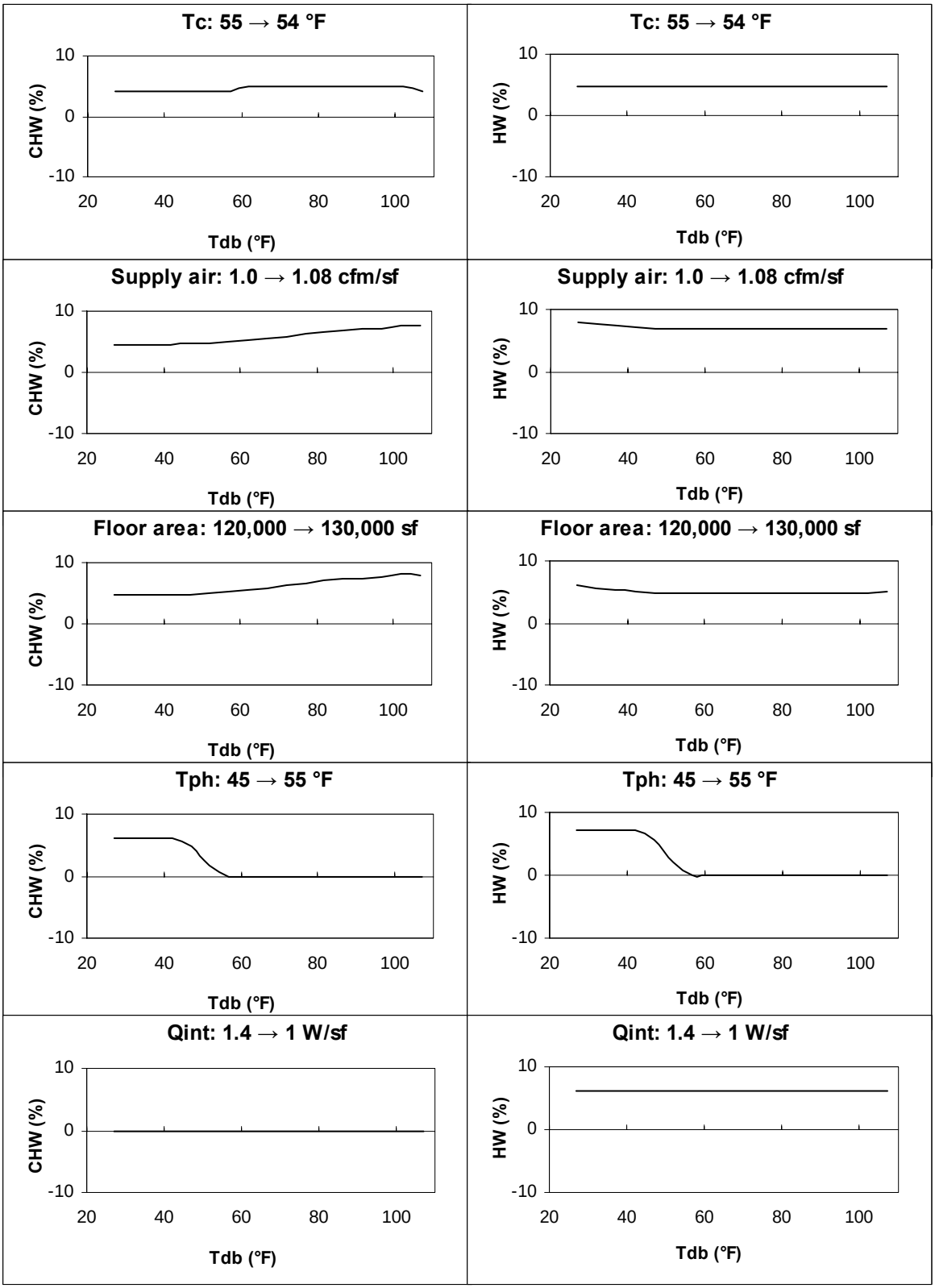

Figure 17. Characteristic signatures for SDCV systems in Sacramento

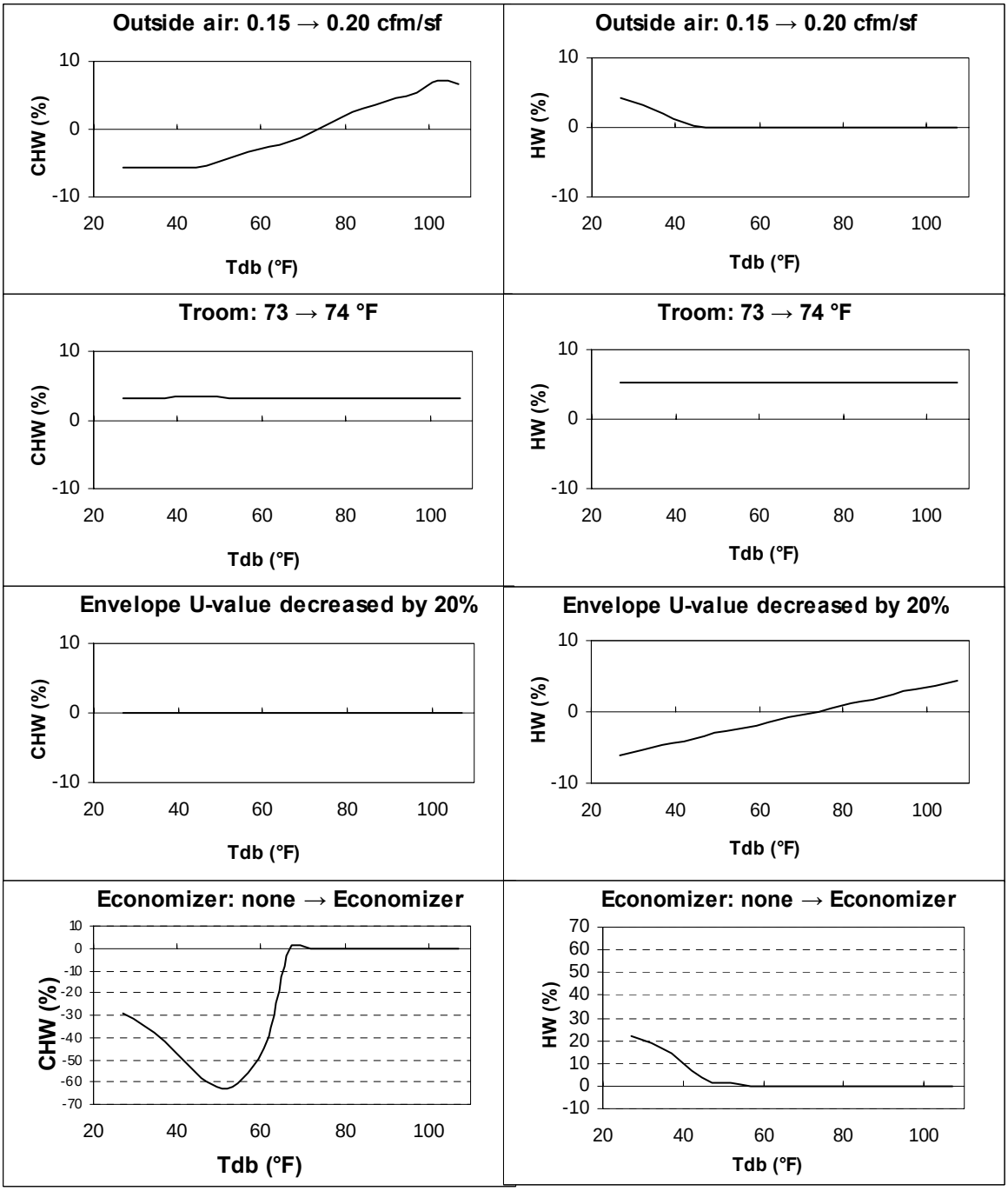

Figure 17. Continued

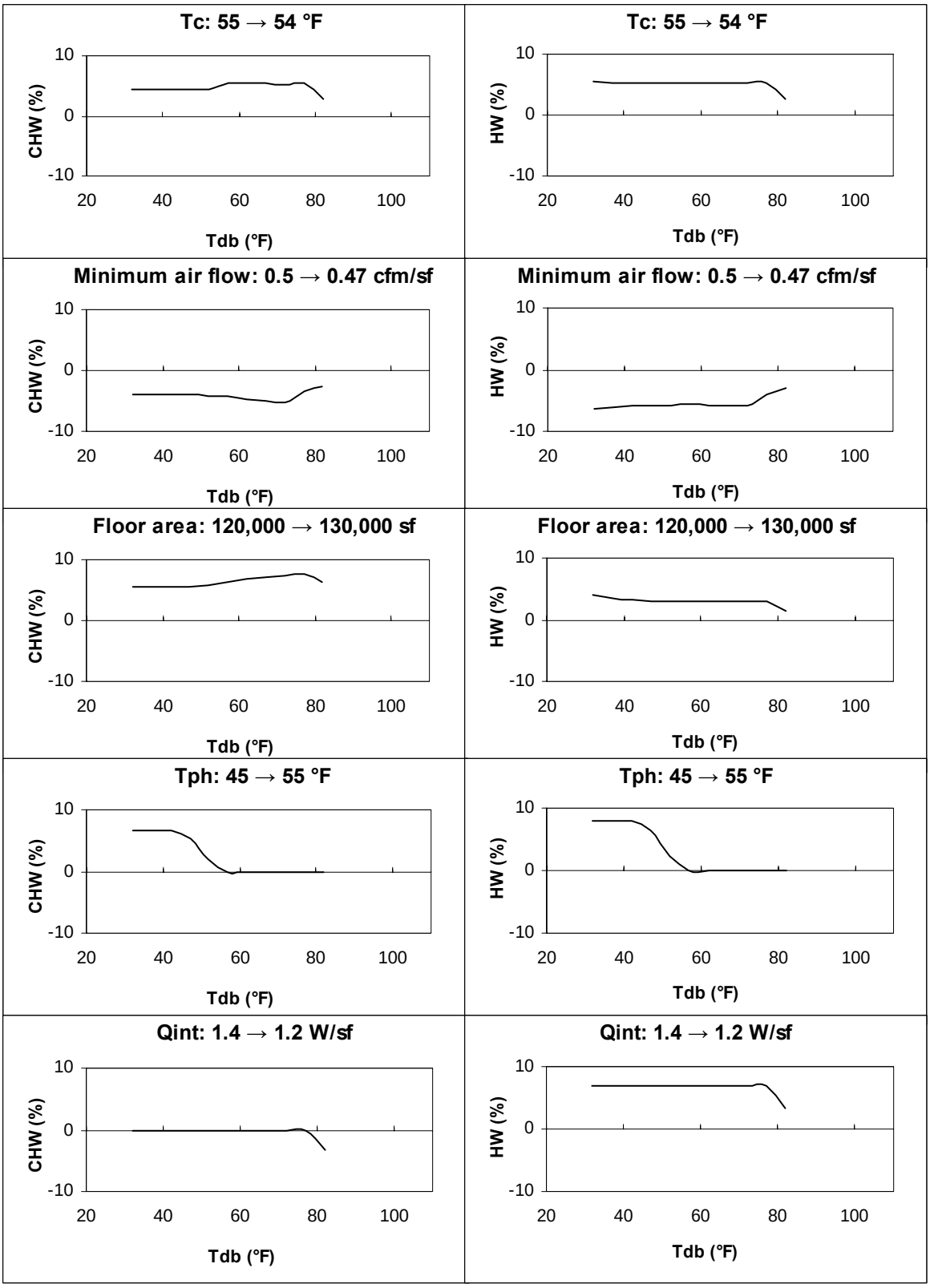

Figure 18. Characteristic signatures for SDVAV systems in Oakland

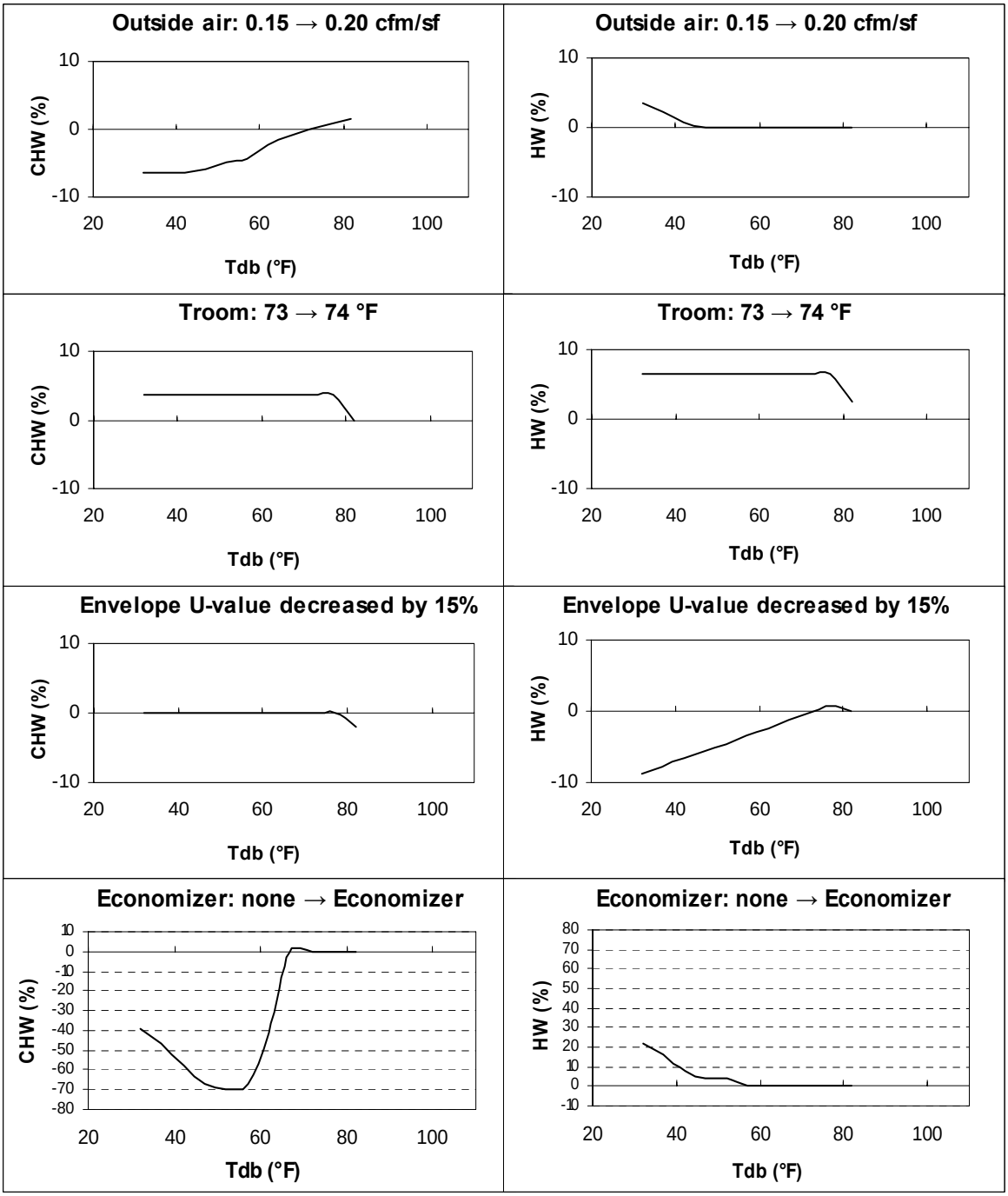

Figure 18. Continued

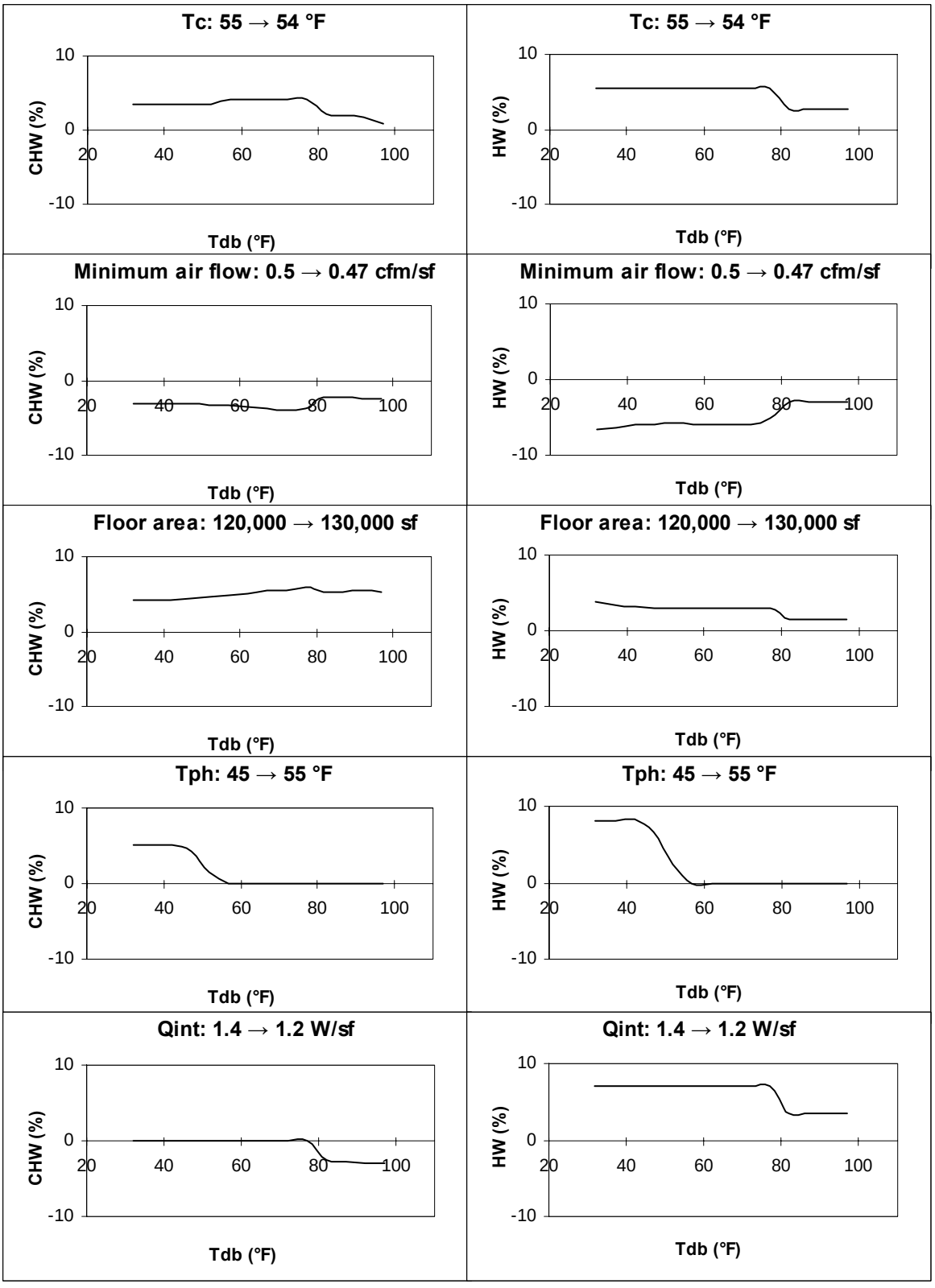

Figure 19. Characteristic signatures for SDVAV systems in Pasadena

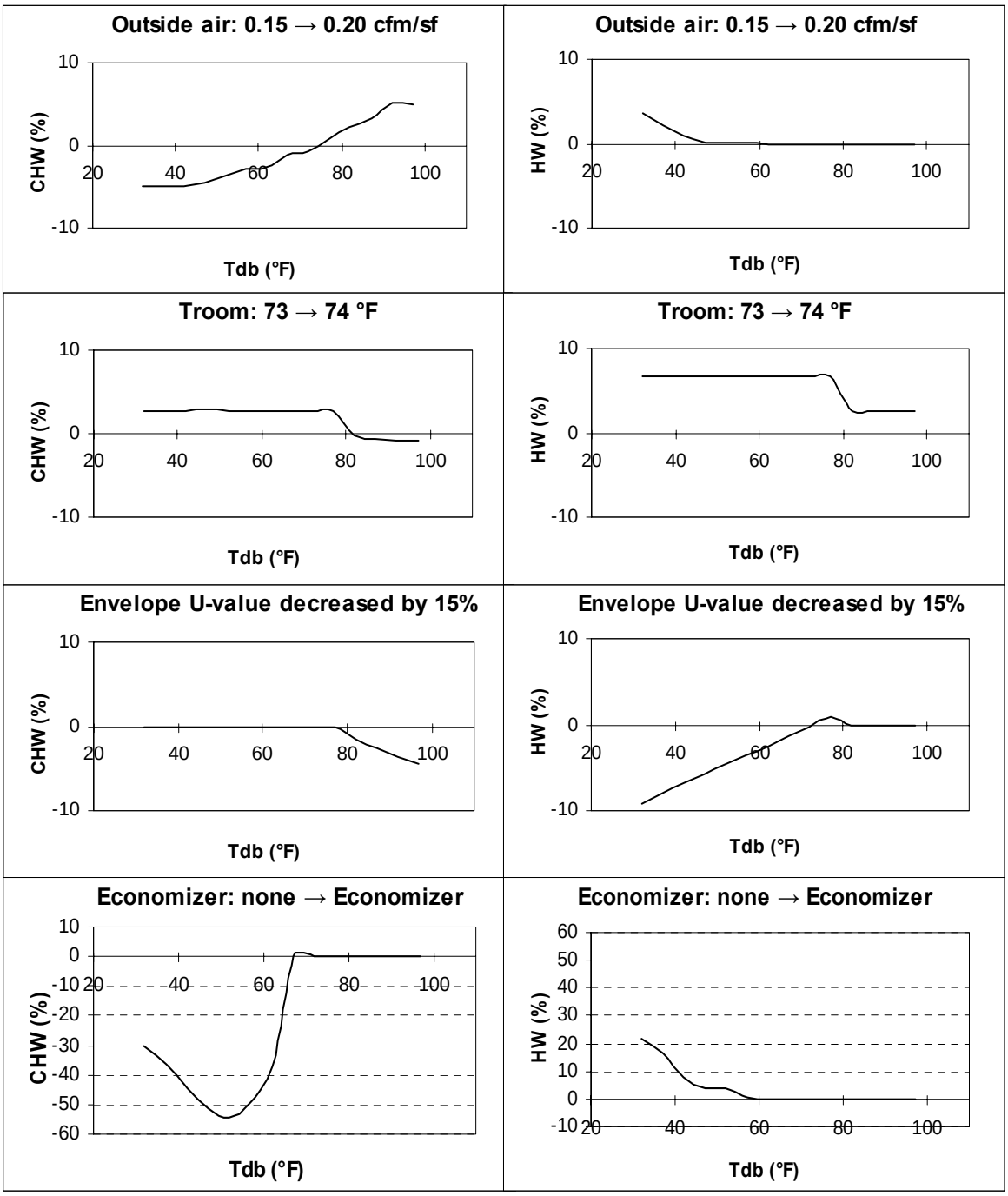

Figure 19. Continued

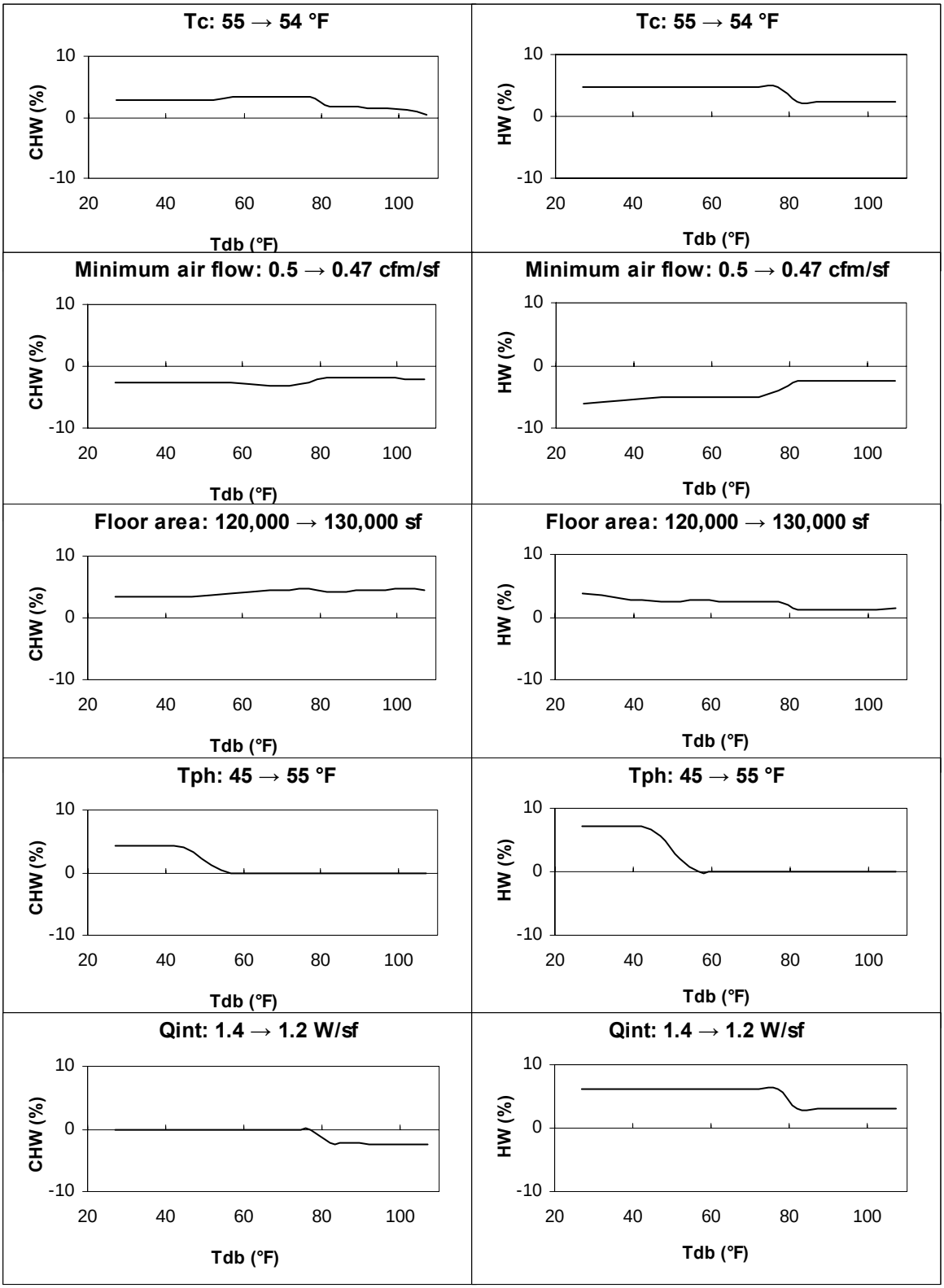

Figure 20. Characteristic signatures for SDVAV systems in Sacramento

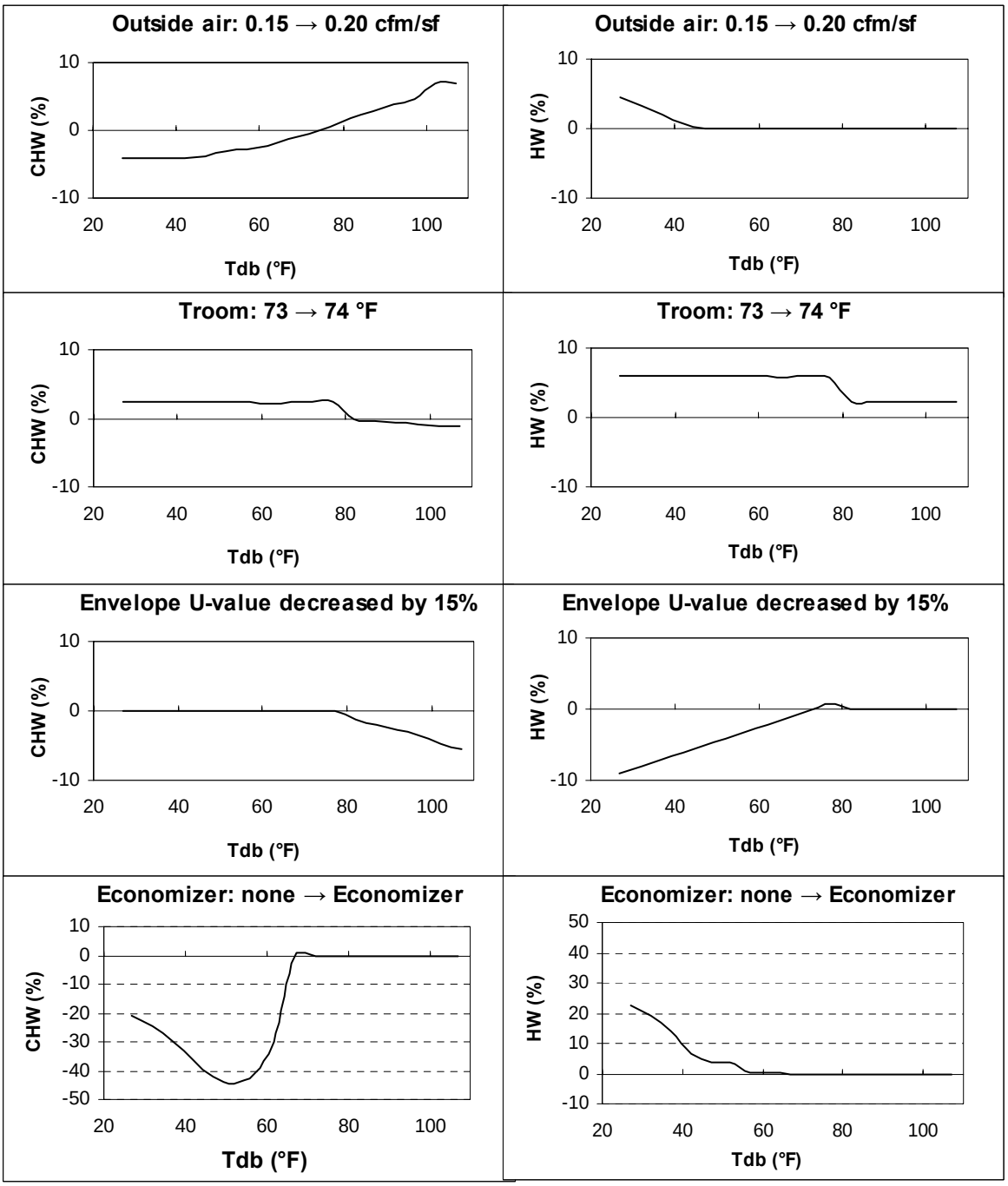

Figure 20. Continued

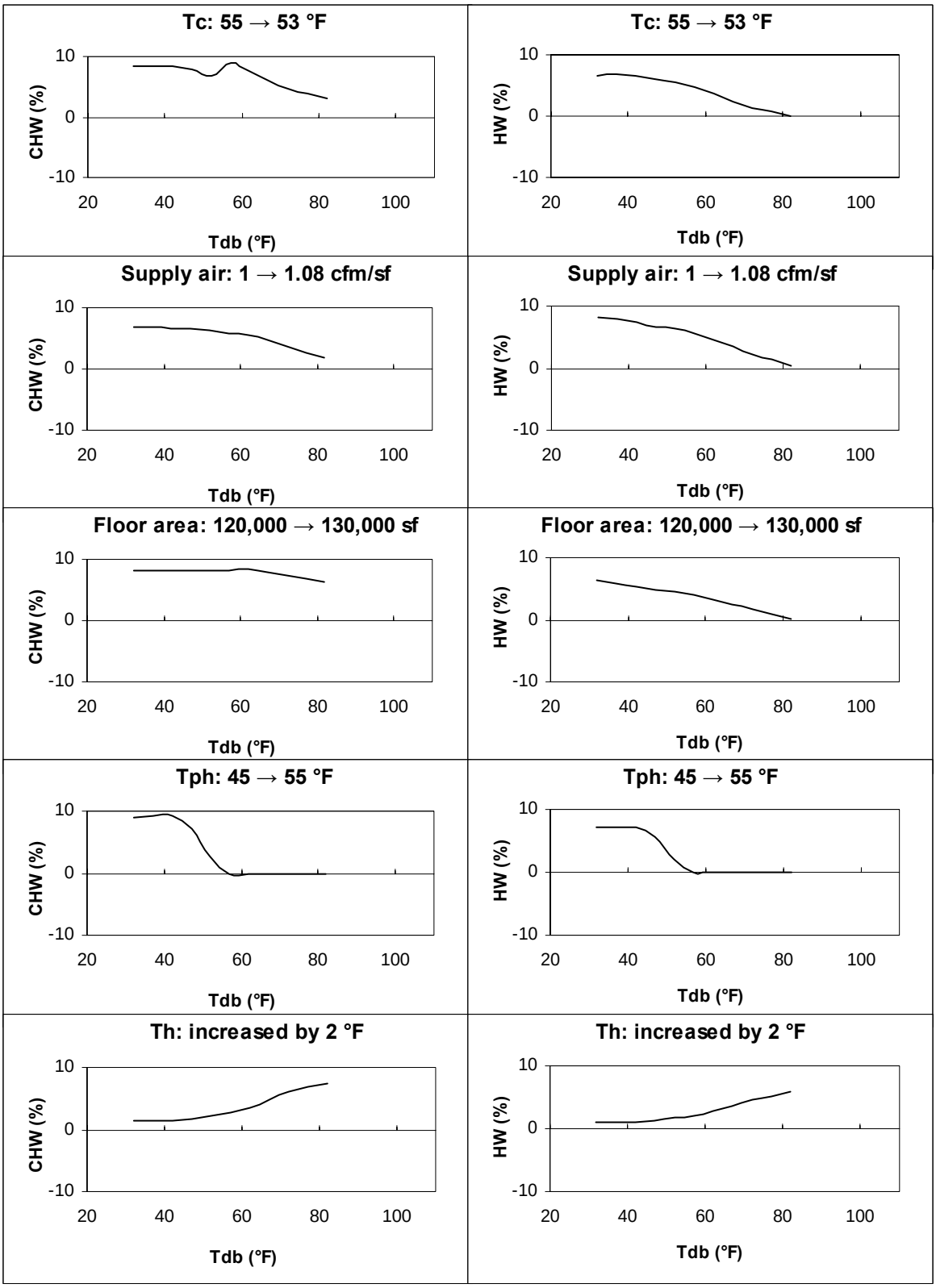

Figure 21. Characteristic signatures for DDCV systems in Oakland

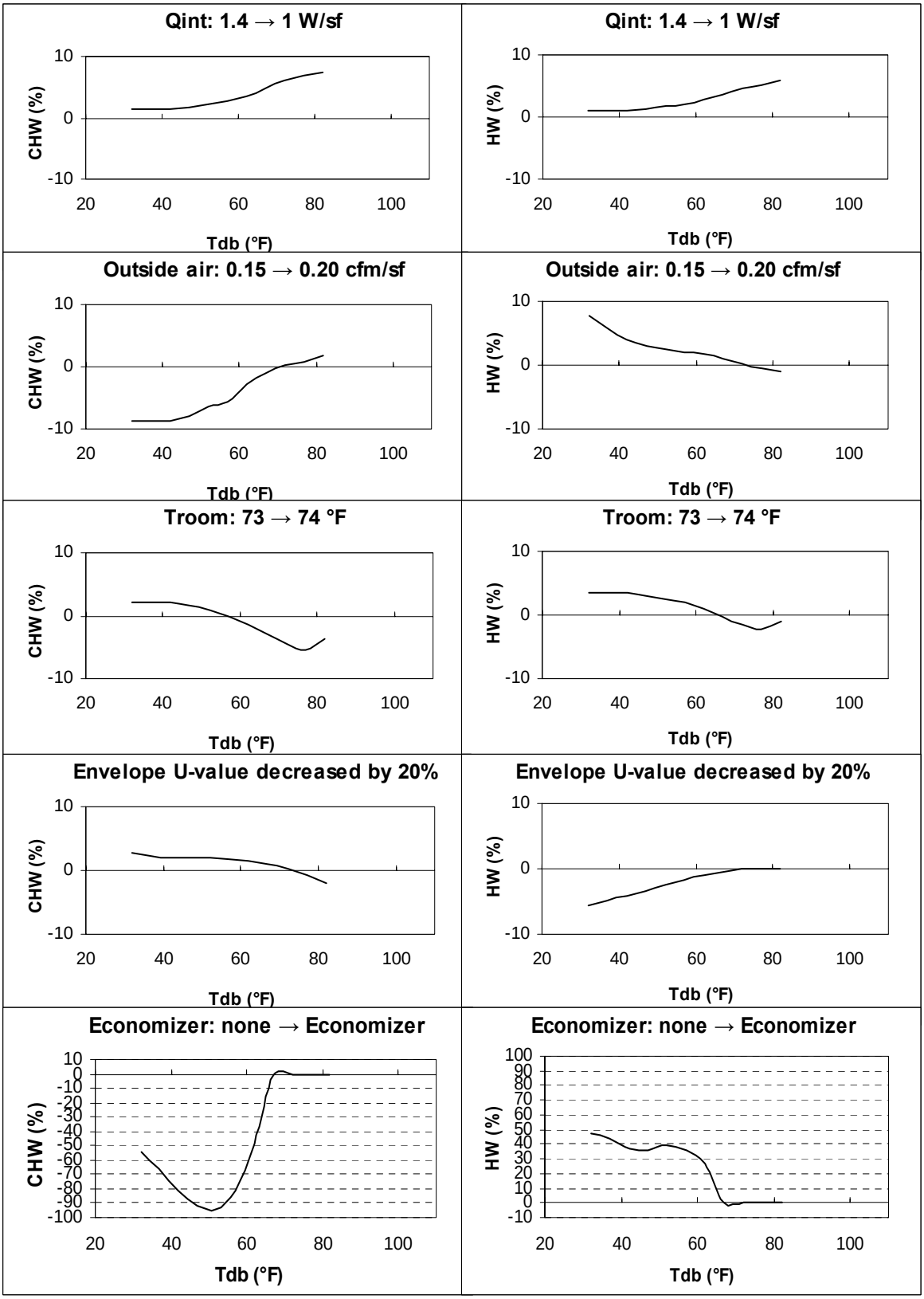

Figure 21. Continued

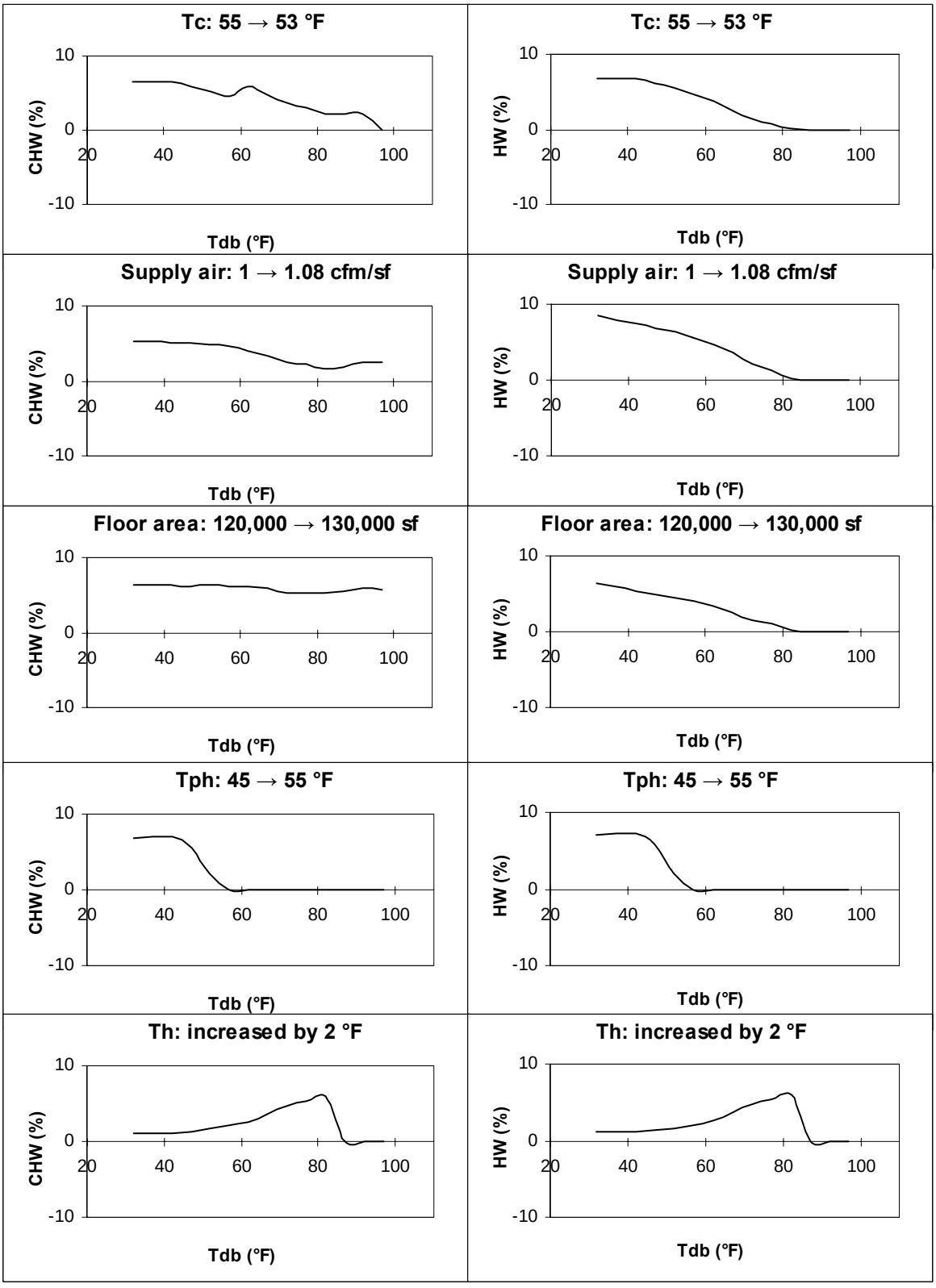

Figure 22. Characteristic signatures for DDCV systems in Pasadena

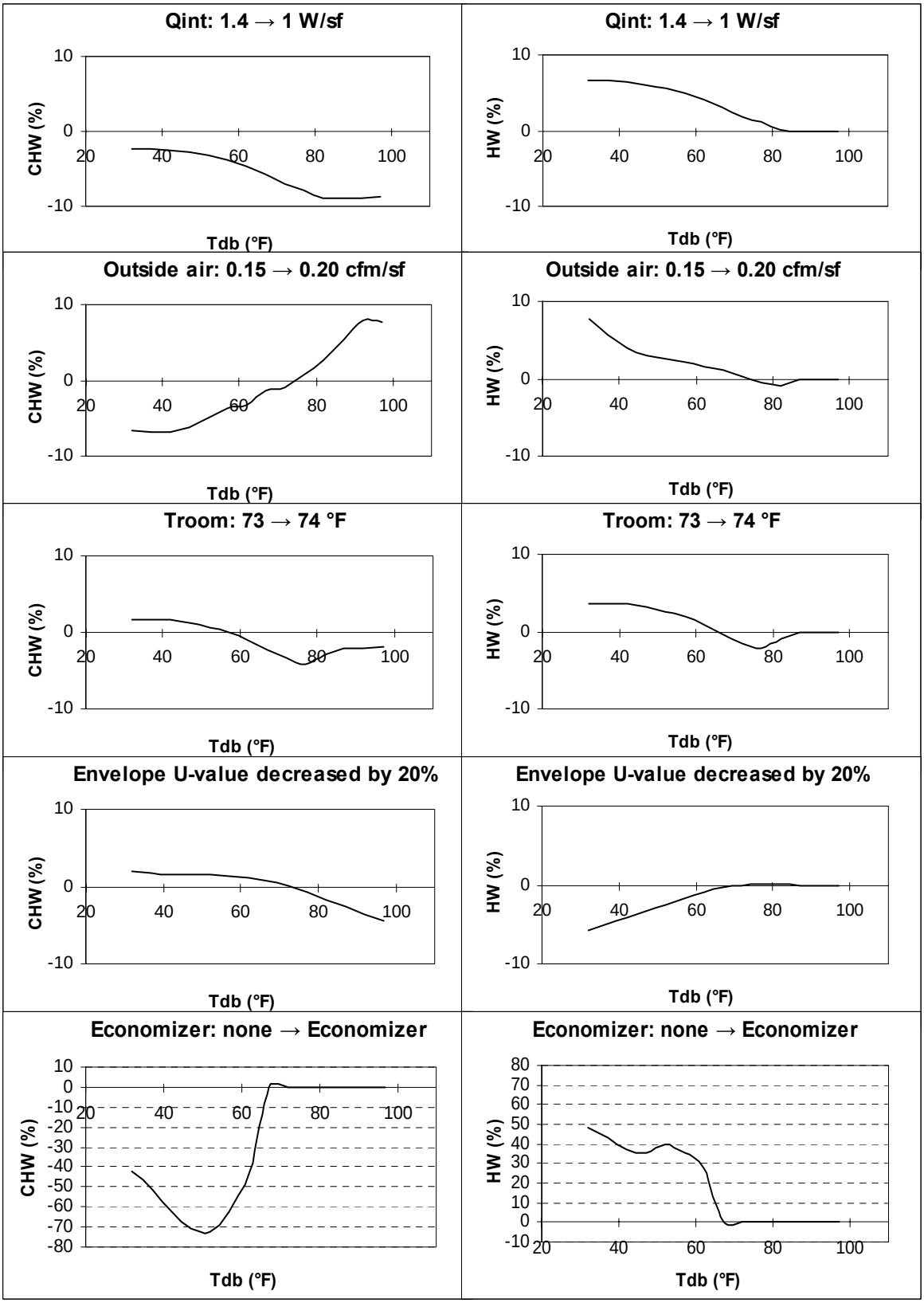

Figure 22. Continued

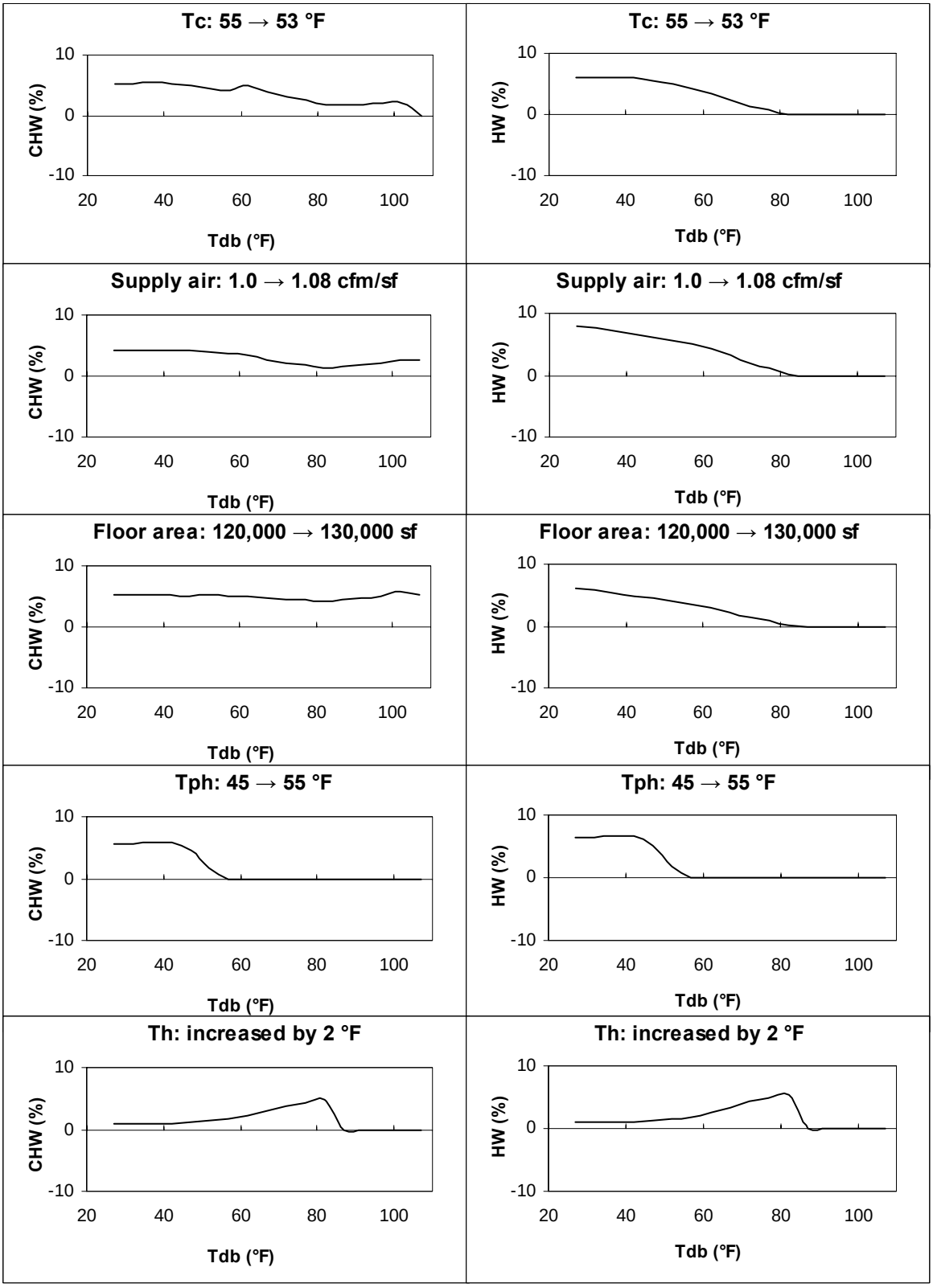

Figure 23. Characteristic signatures for DDCV systems in Sacramento

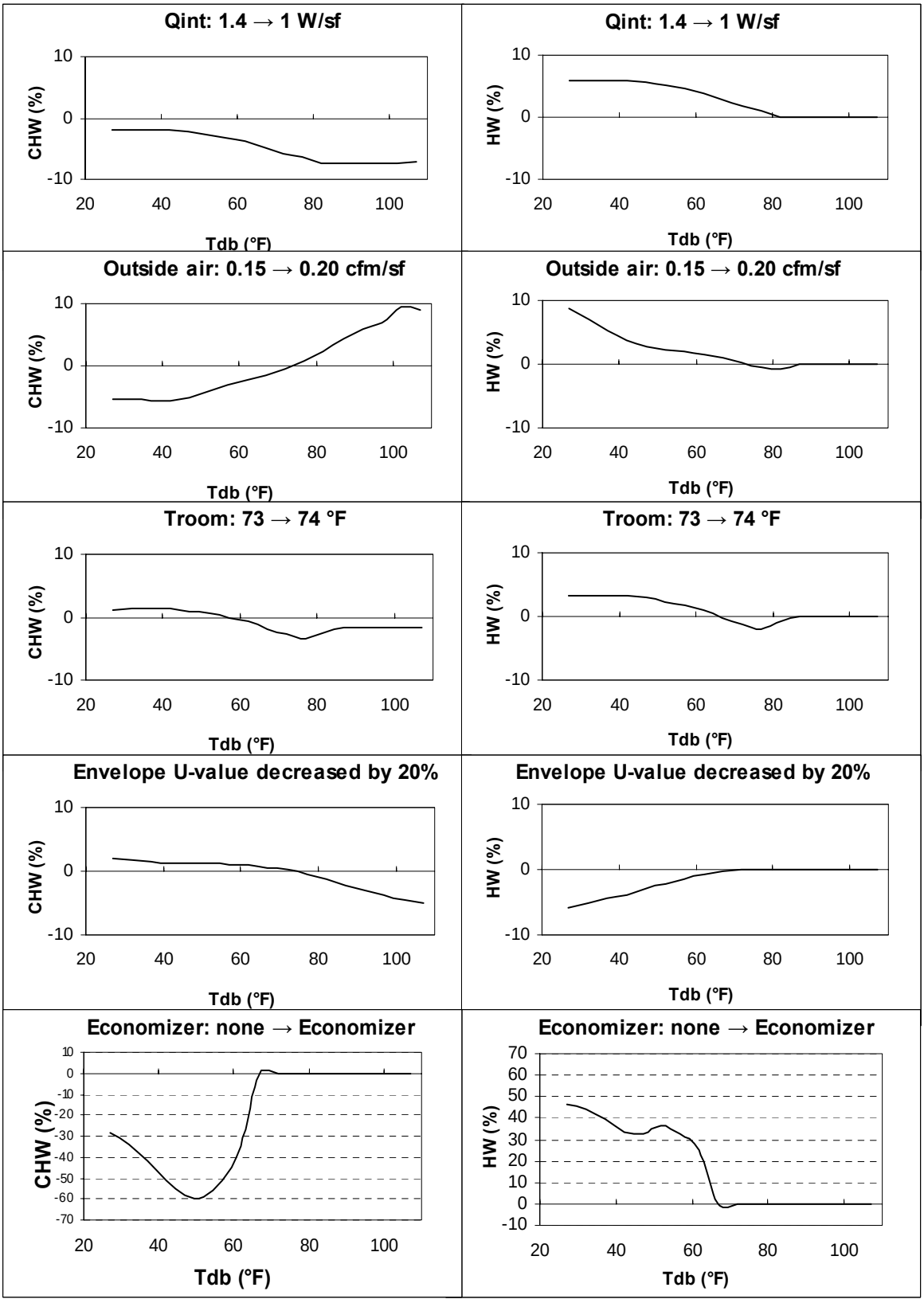

Figure 23. Continued

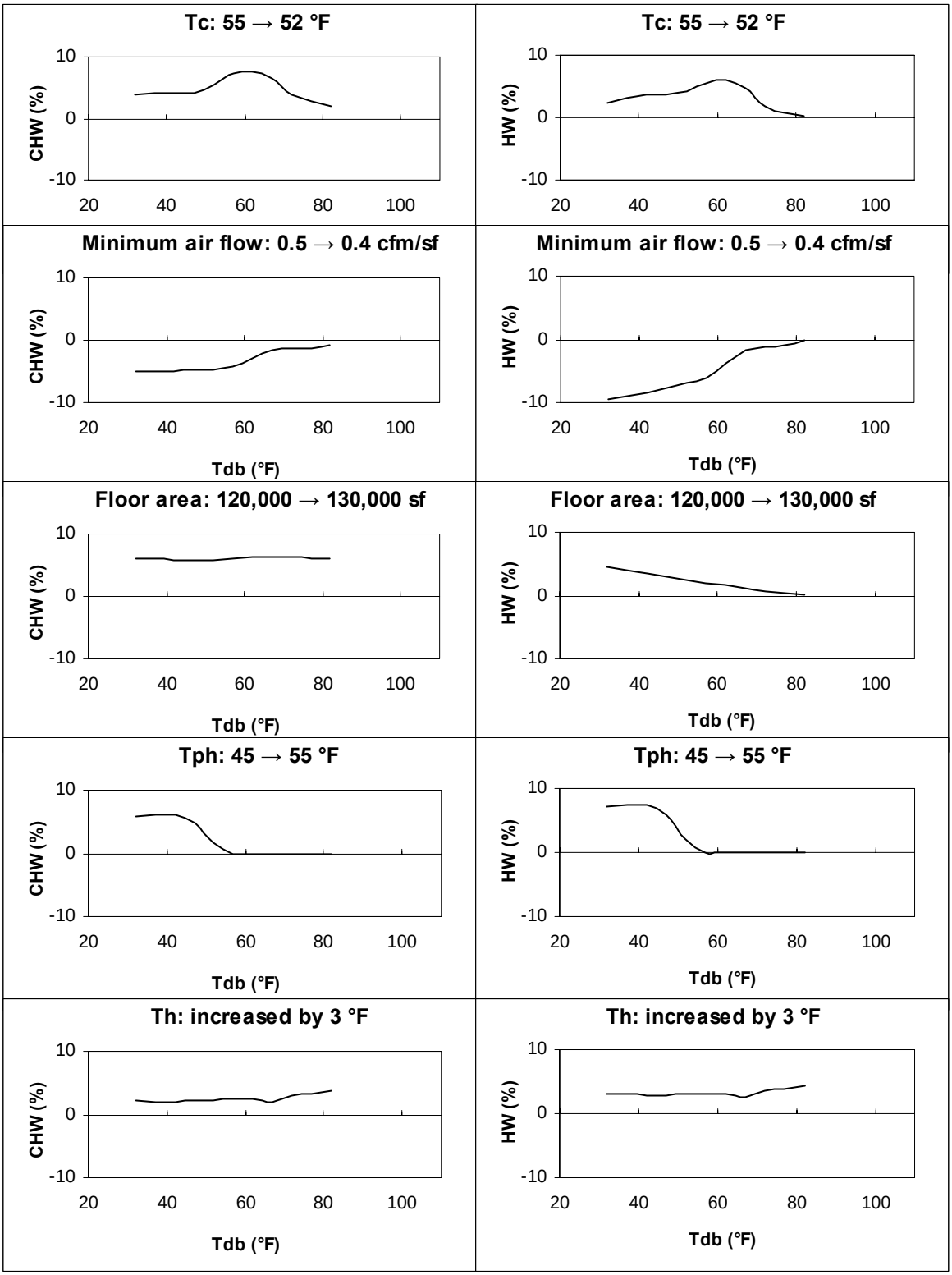

Figure 24. Characteristic signatures for DDVAV systems in Oakland

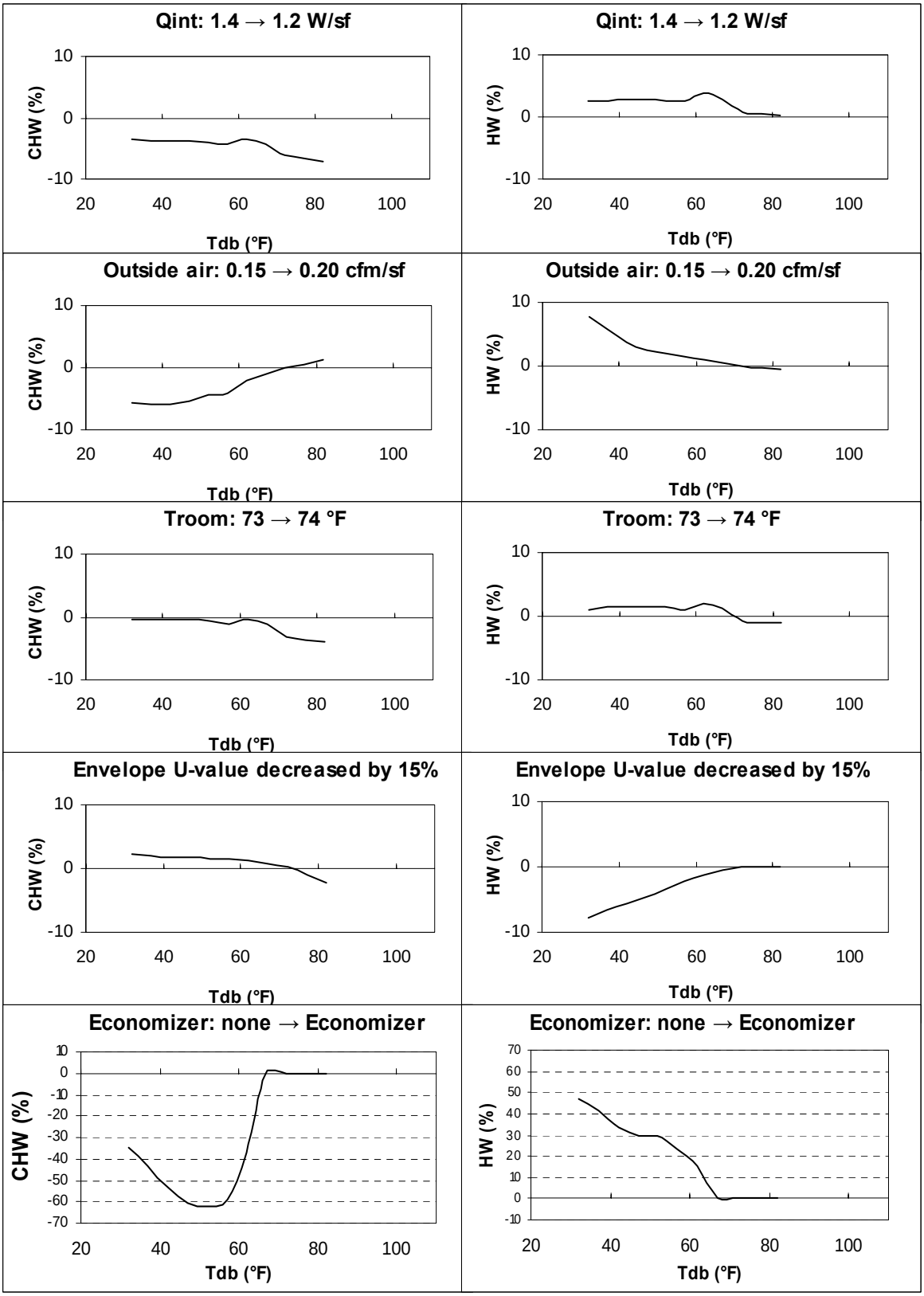

Figure 24. Continued

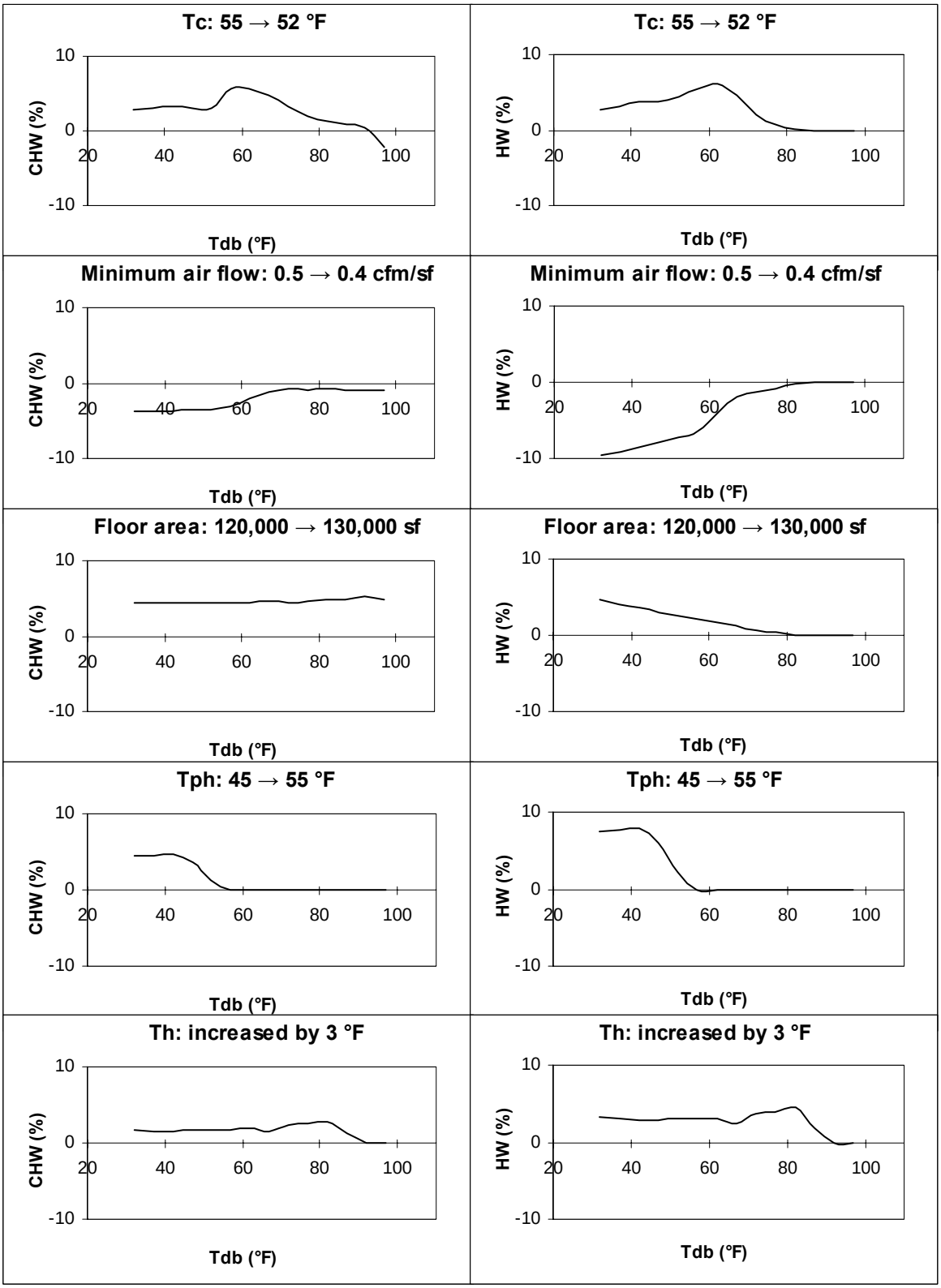

Figure 25. Characteristic signatures for DDVAV systems in Pasadena

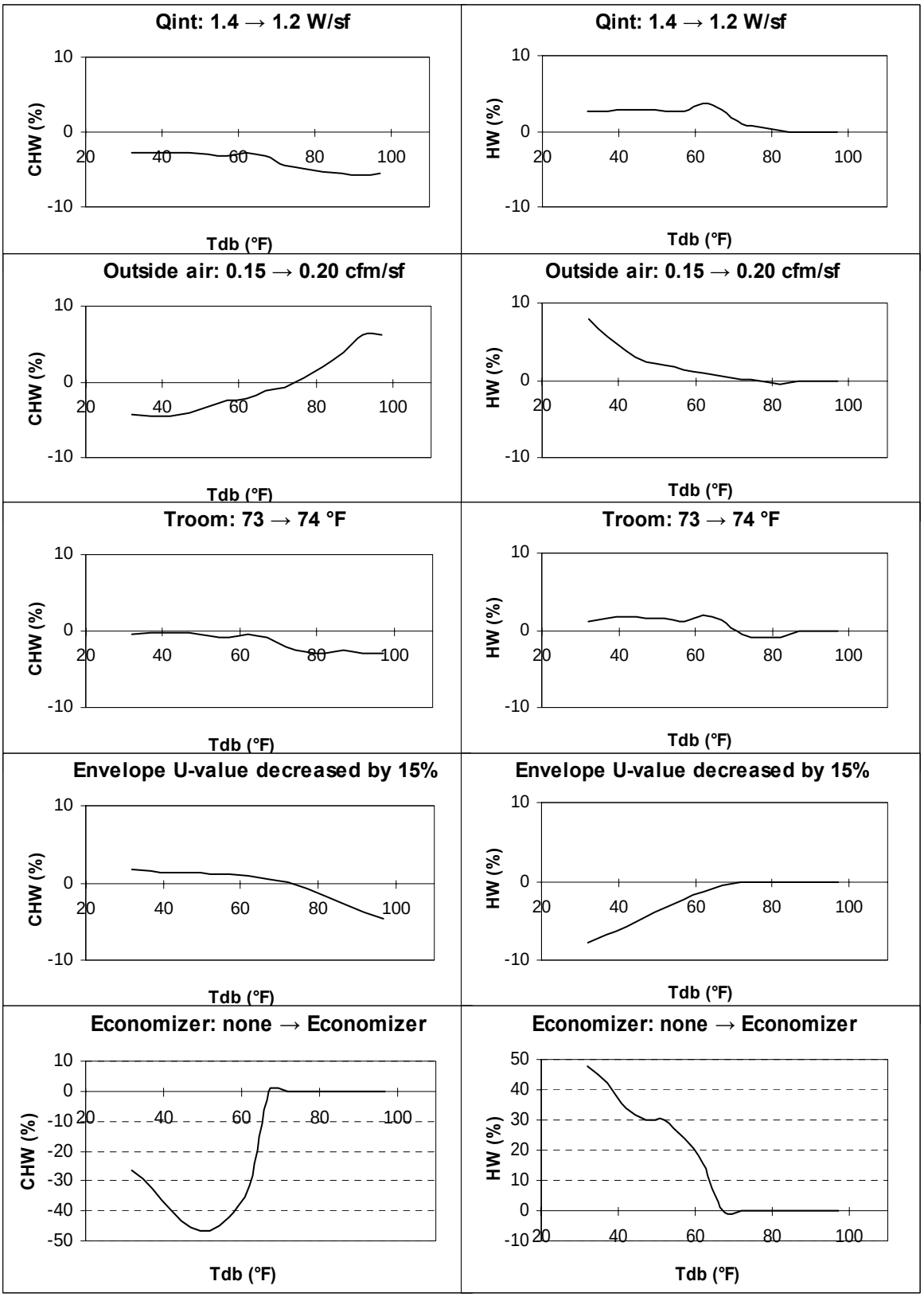

Figure 25. Continued

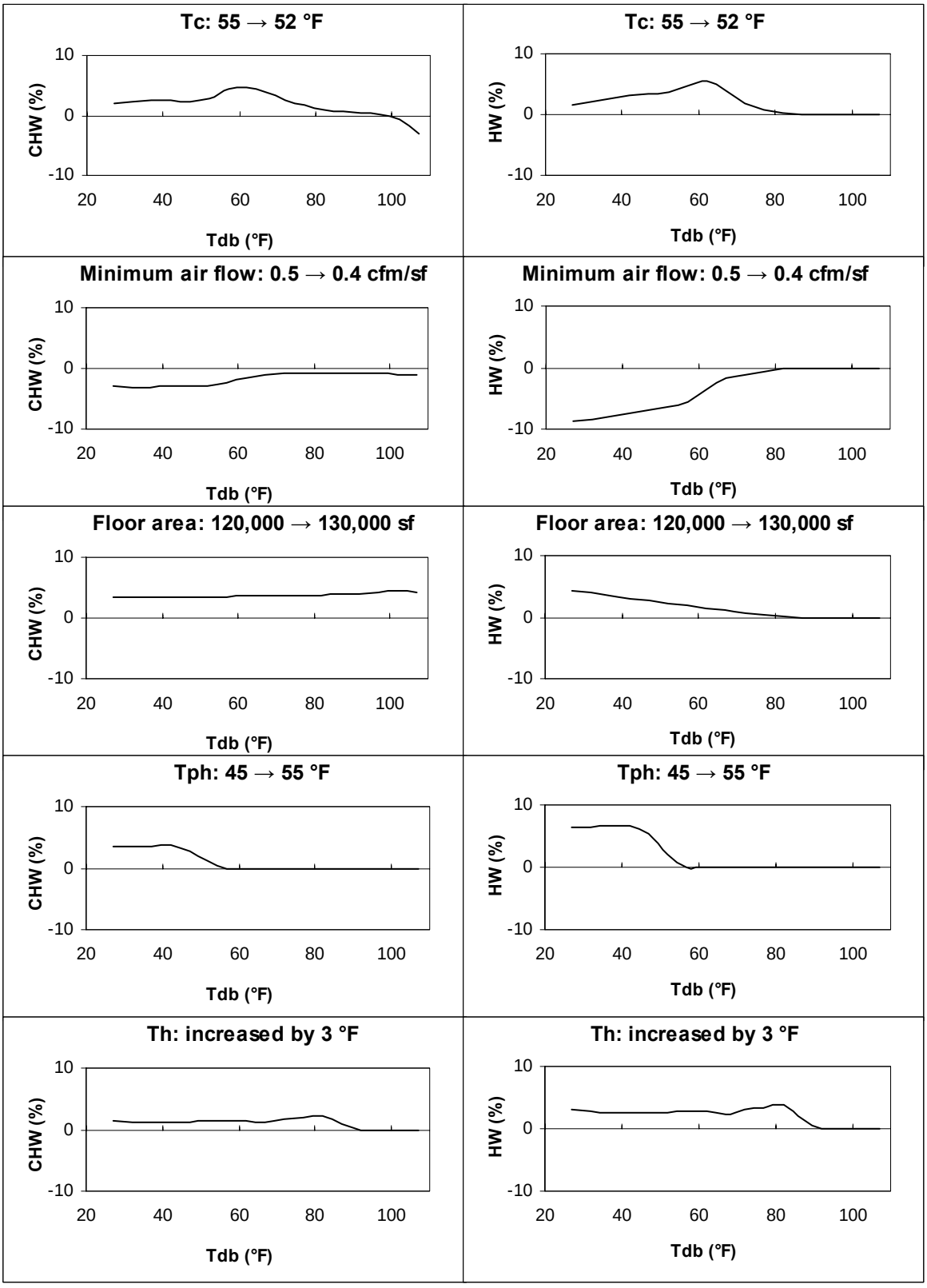

Figure 26. Characteristic signatures for DDVAV systems in Sacramento

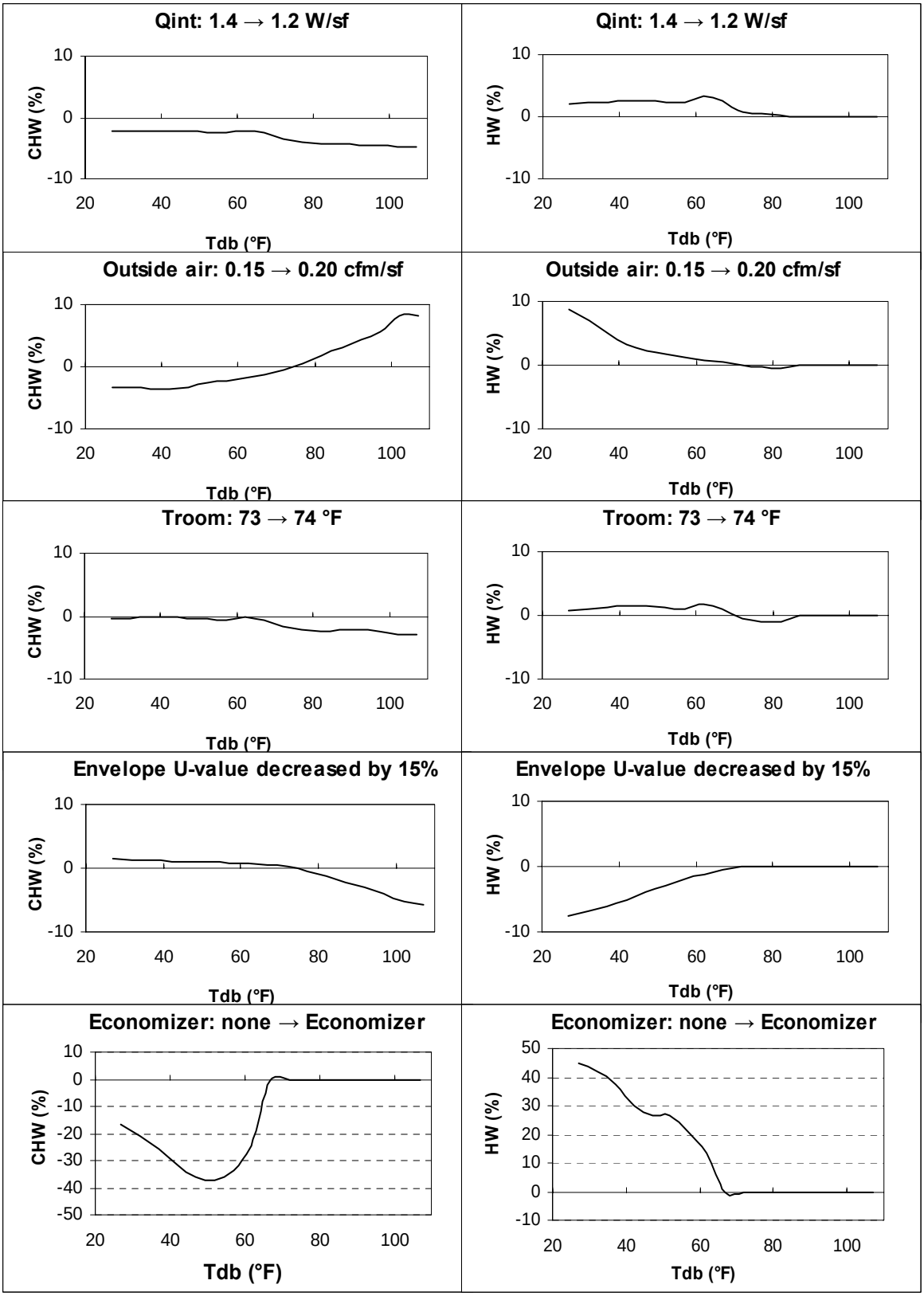

Figure 26. Continued

III.6 Characteristic signatures for air handling units with preheating after mixing

As shown in Figure 27, the preheat coil can be located in the outside air stream (a), or in the mixed air stream (b).

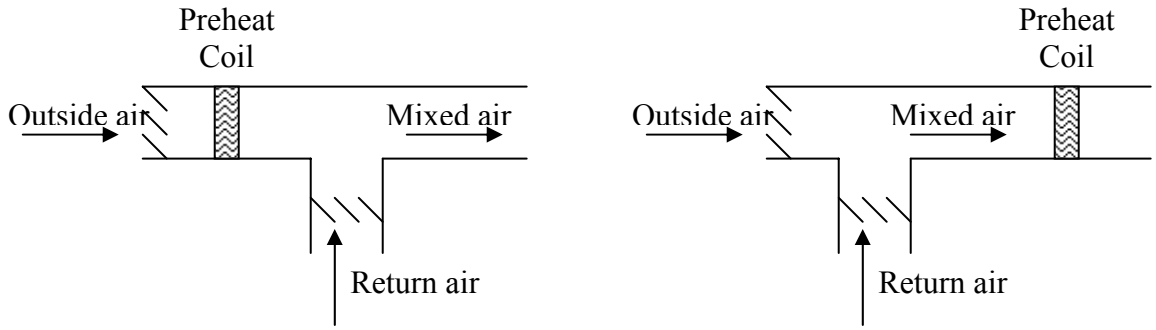

a. Preheat located in outside air stream b. Preheat located in mixed air stream

Figure 27. Preheat locations

Systems used to generate characteristic signatures in this thesis have preheating in the outside air stream as shown in Figures 8 and 9. However, the sets of characteristic signatures provided in this thesis can still be used for systems with preheat in either location. The main differences occur at the lower range of outside air temperatures where the preheating temperature setpoint can be higher than the outside air temperature but lower than the mixed air temperature. Figure 28 shows the characteristic signatures that differ between a Single Duct Constant Volume system with preheat at the outside air stream and the same system type with preheat at the mixed air stream for Pasadena weather. The other characteristic signatures are similar.

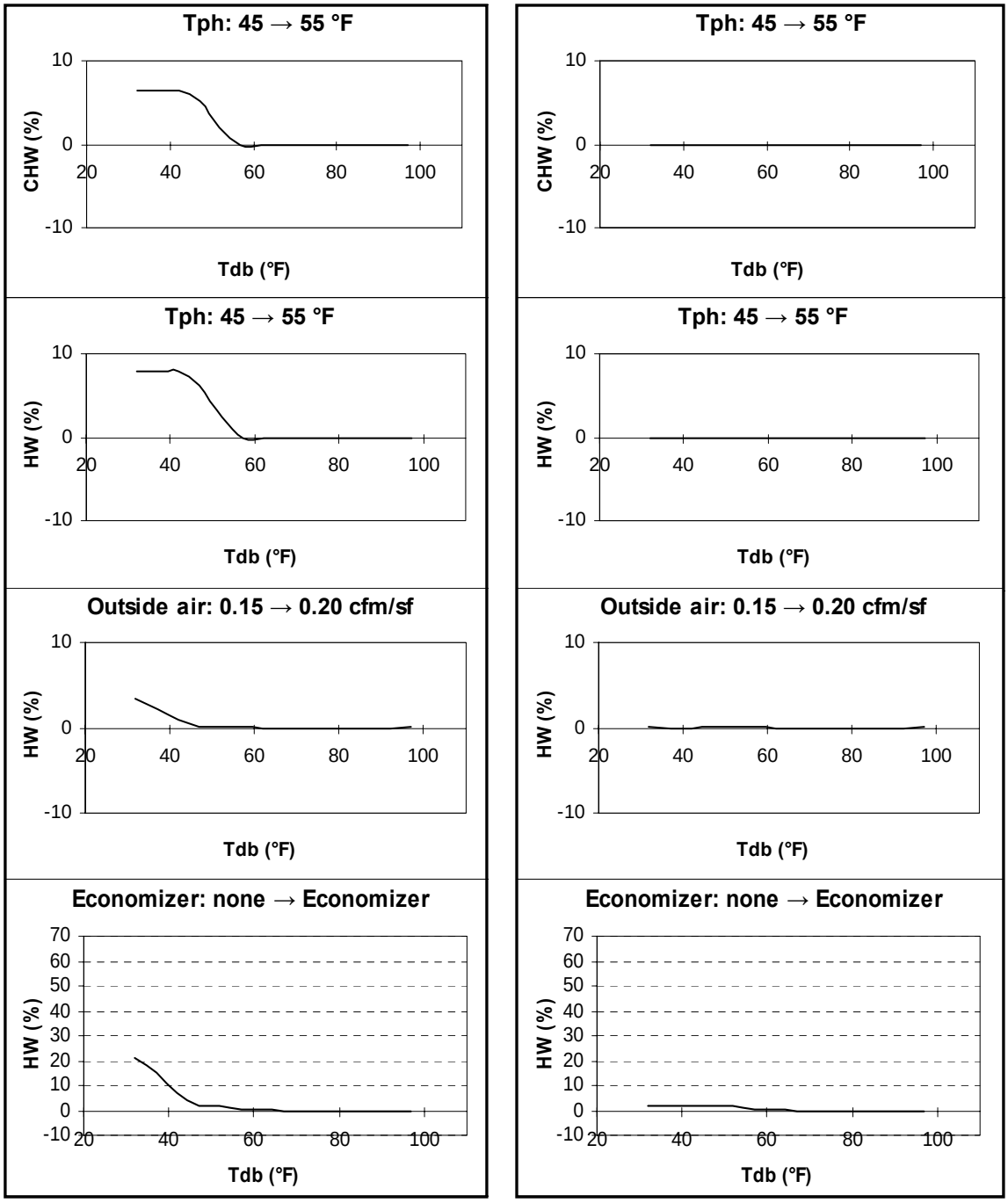

a. SDCV system with preheat at outside air stream

b. SDCV system with preheat at mixed air stream

Figure 28. Comparison of characteristic signatures for different preheat locations

III.7 Creating your own characteristic signatures

Sets of calibration signatures have been provided for the four major air handling unit types for three California weather conditions. There may be a need to create one's own calibration signatures for other weather conditions or other variations of air handling unit types, or to test the sensitivity of other input parameters not tested in the provided sets.

It is preferable to use the initial simulation, which is based on the best approximation of input parameters, as the baseline for characteristic signatures. Figure 29 illustrates how a calibration signature is created for an input parameter "ip" using a spreadsheet. MS Excel was used for this purpose.

Any simulation program may be used. Simulated data is then copied and pasted in the spreadsheet to create the signature. In Figure 29, dry-bulb temperatures were pasted in column B for the corresponding time steps in column A. Weather data can be hourly, daily… or bin data. The baseline simulation data was pasted in column C with the caption Q_{bl}. It could be either cooling or heating energy consumption. In this initial simulation, the input parameter "ip" had an initial value ip_0. To create the calibration signature for this parameter, its value was altered in the input file from ip_0 to ip_1 and the simulation was rerun. Simulated data was then pasted in column D with the caption Q_{ip} and the characteristic signature was calculated in column E for line "i" as:

$$\textit{Characteristic Signature for input parameter "ip"} = \frac{Q_{ip}(i) - Q_{bl}(i)}{Max\,(Q_{bl})} \quad x\ 100\%$$

Max (Q_{bl}) is the maximum baseline simulated value for the entire simulation period. Note that it would be different for cooling and heating. The input parameter is changed to an amount that gives a significant change in energy consumption, typically up to 10%.

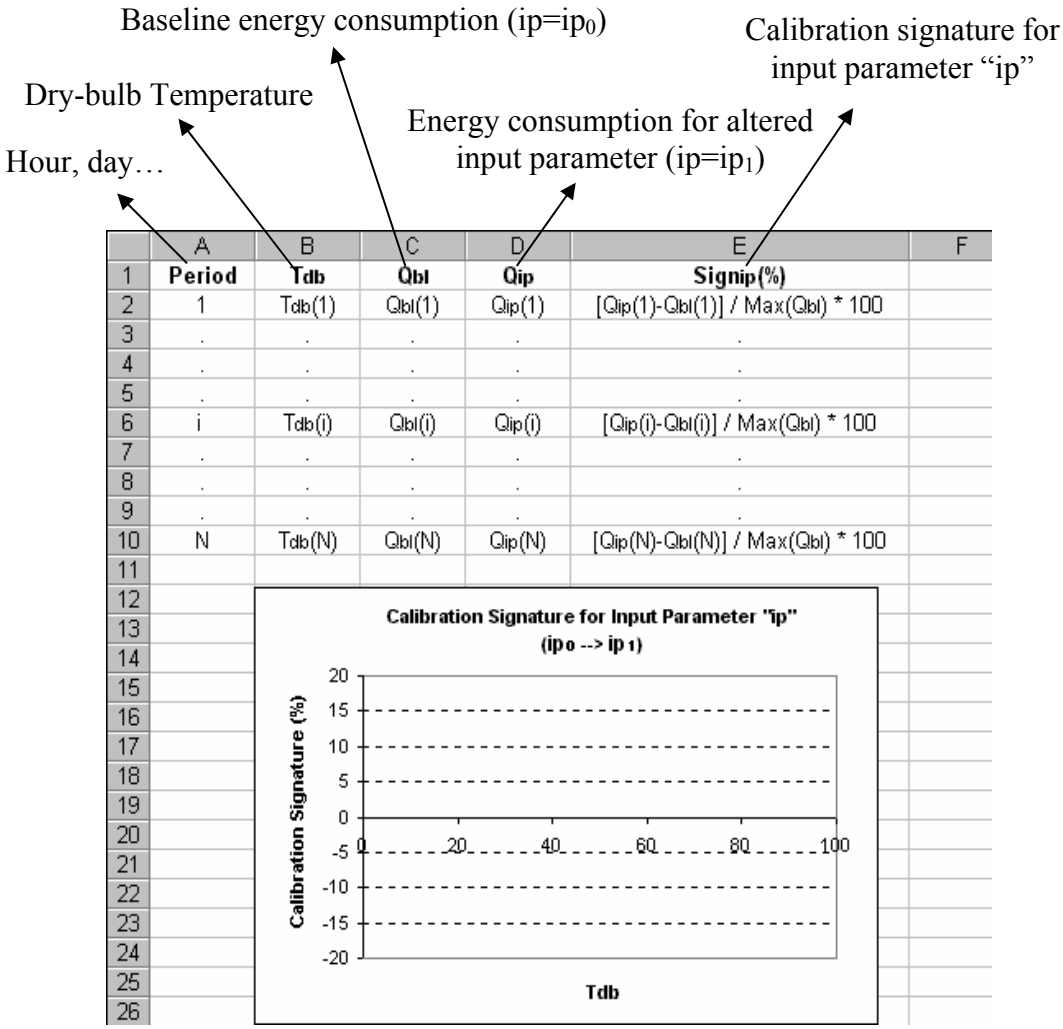

	A	B	C	D	E	F
1	**Period**	**Tdb**	**Qbl**	**Qip**	**Signip(%)**	
2	1	Tdb(1)	Qbl(1)	Qip(1)	[Qip(1)-Qbl(1)] / Max(Qbl) * 100	
3	.	.	.	.	.	
4	.	.	.	.	.	
5	.	.	.	.	.	
6	i	Tdb(i)	Qbl(i)	Qip(i)	[Qip(i)-Qbl(i)] / Max(Qbl) * 100	
7	.	.	.	.	.	
8	.	.	.	.	.	
9	.	.	.	.	.	
10	N	Tdb(N)	Qbl(N)	Qip(N)	[Qip(N)-Qbl(N)] / Max(Qbl) * 100	

Figure 29. Creation of a characteristic signature for input parameter "ip"

Figure 30 shows the calculation of the cooling characteristic signature of the supply air flow rate for a SDCV system. This simulation uses bin data. The baseline simulation was run with a supply air flow rate of 1 cfm/ft^2 and the second simulation was run with a

value of 1.08 cfm/ft^2. Characteristic signature data points were connected with a smoothed line to show the impact of the input parameter over the entire range of dry-bulb Temperatures.

	A	B	C	D	E
1	**Period**	**Tdb**	**Q-baseline**	**Q-supply air**	**Sign-supply air(%)**
2		32	1.854	1.998	4.86
3		37	1.856	2	4.86
4		42	1.857	2.001	4.86
5		47	1.896	2.043	4.96
6		52	1.993	2.147	5.19
7		57	2.089	2.251	5.46
8		62	2.204	2.371	5.63
9		67	2.357	2.536	6.04
10		72	2.415	2.598	6.17
11		77	2.57	2.766	6.61
12		82	2.721	2.928	6.98
13		87	2.815	3.03	7.25
14		92	2.966	3.193	7.65
15		97	2.857	3.08	7.52

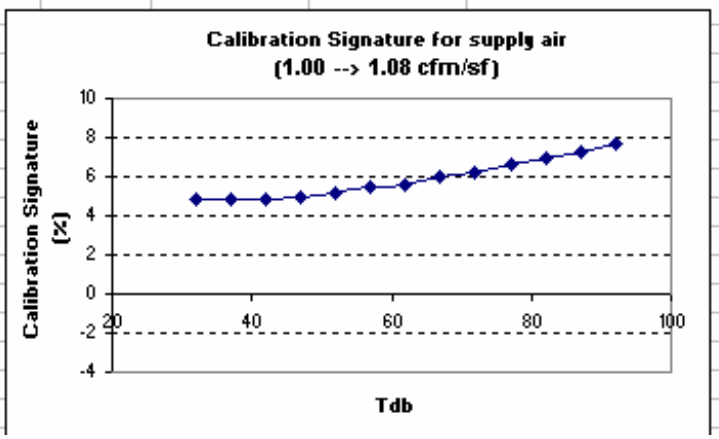

Figure 30. Characteristic signature for supply air flow rate for a SDCV system

CHAPTER IV

CALIBRATION USING CHARACTERISTIC SIGNATURES

IV.1 Calibration process

The steps to follow to calibrate cooling and heating simulations using characteristic signatures are as follows:

- ***Step 1***. Collect measured consumption and weather data over a period of uniform HVAC system operation.
- ***Step 2***. Perform an initial simulation using the best estimates of your system parameters.
- ***Step 3***. Make any necessary conversions of weather data, measured consumption data and simulated results to daily averages or another time step, or temperature bins. It may be necessary to adopt guidelines to deal with missing measured data (e.g. interpolate up to a critical number of missing data points per time step and disregard the whole time step if more data points are missing).
- ***Step 4***. Calculate the residuals, the RMSE and the cooling and heating calibration signatures according to equations 3, 6, 1 and 2 respectively.
- ***Step 5***. Plot measured data, simulated results and residuals in the same chart as a function of outside air dry-bulb temperature and plot the calibration signature on the same or a separate chart. It may be helpful to perform some type of best fit regression to the calibration signature data points to help detect the overall trend of the signature.

- ***Step 6***. Compare cooling and heating calibration signatures with the characteristic signatures available in appendices C, D, E or F for the corresponding system type and climate and try to find the best match or matches. If there is a need to create your own characteristic signatures for other weather conditions or other variations of air handling unit types or to test the sensitivity of other input parameters not tested in the signatures provided, follow the procedure described in section III.7. In comparing the pair of cooling and heating calibration signatures with pairs of cooling and heating characteristic signatures, things to look for include signs (positive or negative), intercepts, slopes and bulges. This will identify an input or inputs that, when changed, are the most likely to minimize the residuals over the targeted range or ranges of outside air temperature.

  If two or more pairs of characteristic signatures have similar shapes (e.g. the floor area and the total supply air characteristic signatures in Figure 16a), conduct field measurements or use your own judgment to estimate which one is the most likely to be inaccurate in the initial simulation. It's possible that more than one needs to be changed.

  If the calibration signatures do not strongly resemble any pair of characteristic signatures, try to use characteristic signatures to reduce cooling and heating calibration signatures at their maximum magnitudes or to remove any irregular shapes in either calibration signature over a certain range of outside air temperature. It is possible to alter two or more inputs simultaneously when each one of them targets a different range of outside air temperature or targets more specifically either the cooling or the heating calibration signature.

- ***Step 7***. Alter the identified input parameter and rerun the simulation. The change should be made in the same direction as in the identified pair of characteristic signatures (e.g. increase or decrease). The amount of change should be estimated by comparing the magnitudes of the cooling and heating calibration signatures with the magnitudes of the cooling and heating characteristic signatures. Different values may be tested and the value with optimum results can be selected.
- ***Step 8***. Evaluate the new RMSE, residuals and cooling and heating calibration signatures. If the results of the calibration are not satisfactory, repeat from step 6 and iterate until the RMSE is minimal, the residuals are randomly scattered around zero and the calibration signature is flat and shows no trend with temperature.
- ***Step 9***. If daily data was used for the calibration, fine-tune the calibration by calibrating the simulation of hourly data. This can be achieved by introducing a daily load profile describing load variation during HVAC operating hours.

IV.2 Evaluating the adequacy of a calibration

There are several metrics to use in evaluating whether or not a simulation is sufficiently calibrated, or in comparing two possible calibration adjustments.

a. Root Mean Square Error

The Root Mean Square Error (RMSE) is defined as:

$$RMSE = \sqrt{\frac{\sum_{i=1}^{n} Residual_i^2}{n-2}} \tag{6}$$

where n is the number of data points. The RMSE is a good measure of the overall magnitude of the errors. It reflects the size of the errors and the amount of scatter, but does not reflect any overall bias in the data. For example, if large errors are randomly distributed both above and below zero, you would have a large RMSE. Similarly, if all the errors are positive, you might have the same RMSE. Thus, the RMSE would be a good metric of how "good" the simulation is for calibration purposes. It is generally difficult to achieve a value of the RMSE that is less than 5 to 10% of the mean value of the larger of the heating and cooling consumption. The minimum RMSE will sometimes be significantly larger, particularly when heating and cooling consumption are small relative to total internal gains.

b. Mean Bias Error

The Mean Bias Error (MBE) is defined as:

$$MBE = \frac{\sum_{i=1}^{n} Residual_i}{n} \quad (7)$$

where n is the number of data points. With the MBE, positive and negative errors cancel each other out, so the MBE is an overall measure of how biased the data is. The MBE is also a good indicator of how much error would be introduced into annual energy consumption estimates, since positive and negative daily errors are cancelled out.

A simulation with a small RMSE, but with a significant MBE, might indicate an error in simulation inputs. A simulation with a large RMSE but a small MBE, might have no errors in simulation inputs, but building performance may reflect some other un-modeled behavior (such as occupant behavior) that is difficult to simulate, or it may have significant input errors. Minimizing mean bias error is very important if a calibrated simulation is to be used as a baseline for determining savings from retrofits or commissioning.

Calibration using characteristic calibration signatures involves estimating both cooling and heating energy use. A separate RMSE can be calculated for each. It is common that making a specific change to simulation inputs will increase a heating RMSE while decreasing a cooling RMSE, or vice versa. In this case, the two RMSE values may be summed, and a minimum value may be sought.

CHAPTER V

EXAMPLES OF USE OF CHARACTERISTIC SIGNATURES

Two examples are presented to illustrate the application of the calibration process described in section IV.1. The first example illustrates the basic calibration steps using the signatures. The second is a more complex example in which more judgment must be used to perform the calibration. Both examples are based on a simulated building (i.e., the "measured" data used for the calibration is actually output from a simulation). The case studies presented in section IV show the use of this method with data from real buildings.

The two examples that follow use the DDCV system model described in section III.3 and the building model described in section III.4. They were simulated using AirModel and Pasadena weather data.

V.1 A simple example

- ***Step 1***. The results of an "accurate" or "baseline" simulation were used in this example as the "measured" data. Then, a set of "errors" was introduced into the simulation inputs to represent an uncalibrated simulation. The example illustrates the use of characteristic signatures to identify what these errors were. Pasadena weather data will be used.
- ***Step 2***. The uncalibrated simulation was conducted with hourly data.

- ***Step 3***. Hourly weather and cooling and heating data were converted to daily averages.
- ***Step 4***. The residuals, the RMSE and the calibration signatures were calculated for the initial simulation. The RMSE was found to be 0.05 MMBtu/hr and 0.07 MMBtu/hr respectively for cooling and heating energy consumption.
- ***Step 5***. Measured data (Meas), simulation results (Sim), residuals (Res) and calibration signatures (Sign) were plotted versus outside air dry-bulb temperature (T_{db}), as shown in Figure 31, for cooling (left) and heating (right). The signature magnitudes are shown on the right hand side y-axis. Note that the symbols for the simulated and measured results overlap, so they cannot be readily distinguished over much of the range.

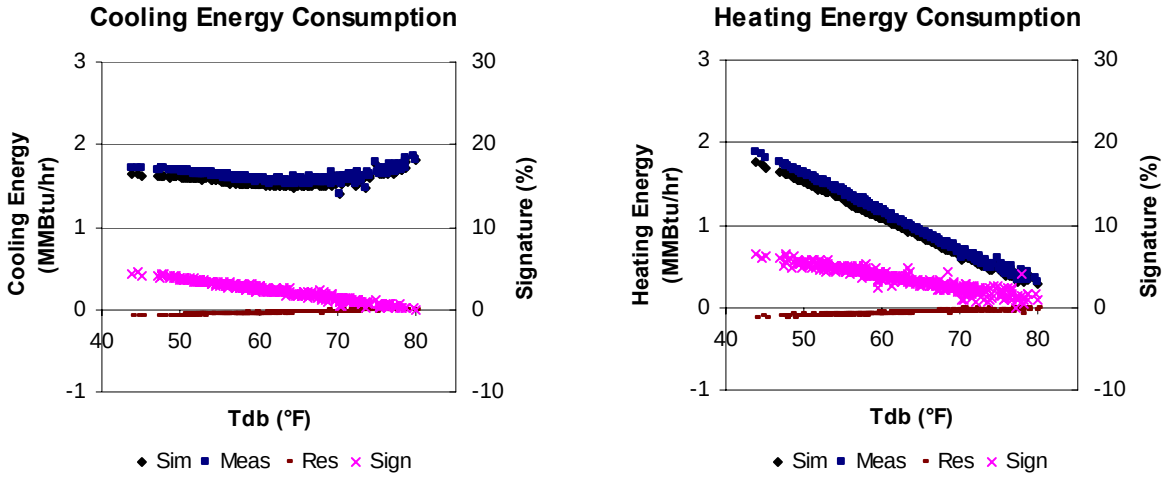

Figure 31. Initial simulation for Example 1 including calibration signatures

- ***Step 6***. The calibration signatures in Figure 31 should be compared to the characteristic signatures in Figure 22 corresponding to DDCV systems in

Pasadena. It can be noticed that the calibration signatures have positive values and negative slopes. They start at about 4% and 7% at low temperatures respectively for cooling and heating energy consumption, and approach zero at higher temperatures. They are comparable to the characteristic signatures of cold deck temperature, supply air flow rate and floor area for the characteristic signatures of Figure 22. Floor area was excluded because the cooling energy signature does not approach zero at high temperatures. In a real building simulation, site measurements of cold deck temperature and supply air flow may be used to determine which was not simulated accurately in the initial simulation. In this illustrative example, it was decided to change the cold deck temperature.

- ***Step 7***. In the characteristic signature of Figure 22, the cold deck temperature was decreased by 2 °F, which caused an increase of about 7% at low temperatures for both cooling and heating. Since the increase is of about 4% and 7% respectively for the cooling and heating calibration signatures, the cold deck temperature should be decreased by about 1 to 2 °F. Different values between 53 °F and 54 °F were tested during the first iteration and the cooling and heating RMSE values were summed and a minimal value was sought. The best result was obtained by decreasing the cold deck temperature from 55 to 53.6 °F.
- ***Step 8***. After this change, the RMS errors have both dropped considerably to 0.020 MMBtu/hr and 0.016 MMBtu/hr respectively for cooling and heating energy consumption. Figure 32 shows simulation charts after this first iteration.

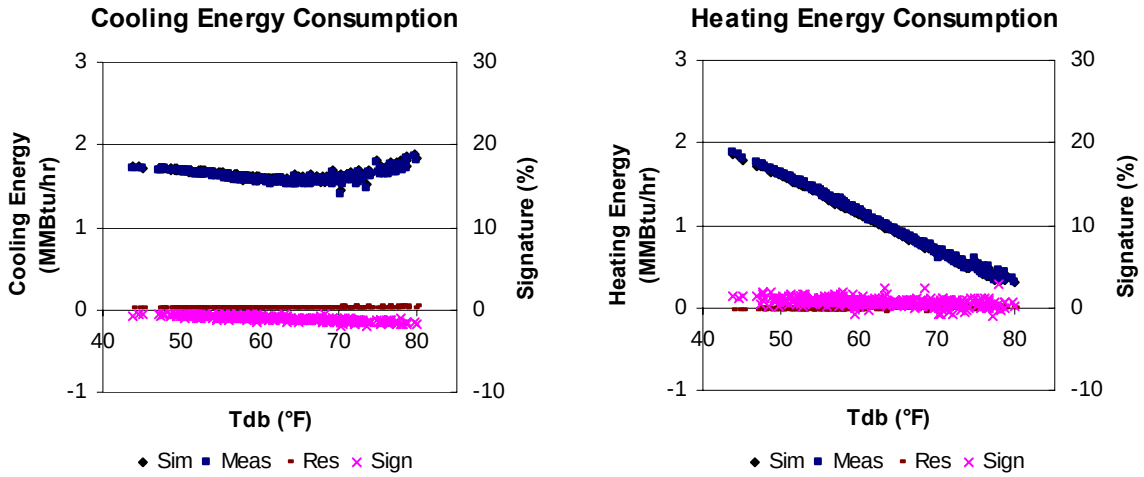

Figure 32. Simulation charts for Example 1 after the first iteration

The choice of the above mentioned value of the cold deck temperature was aimed to optimize both RMS errors for cooling and heating energy consumption. A higher value of 53.8 °F gave RMS errors of 0.013 and 0.024 MMBtu/hr, and a lower value of 53.4 °F gave RMS errors of 0.028 and 0.010 MMBtu/hr, respectively for cooling and heating energy consumption. The results of these simulations are shown in Figures 33 and 34.

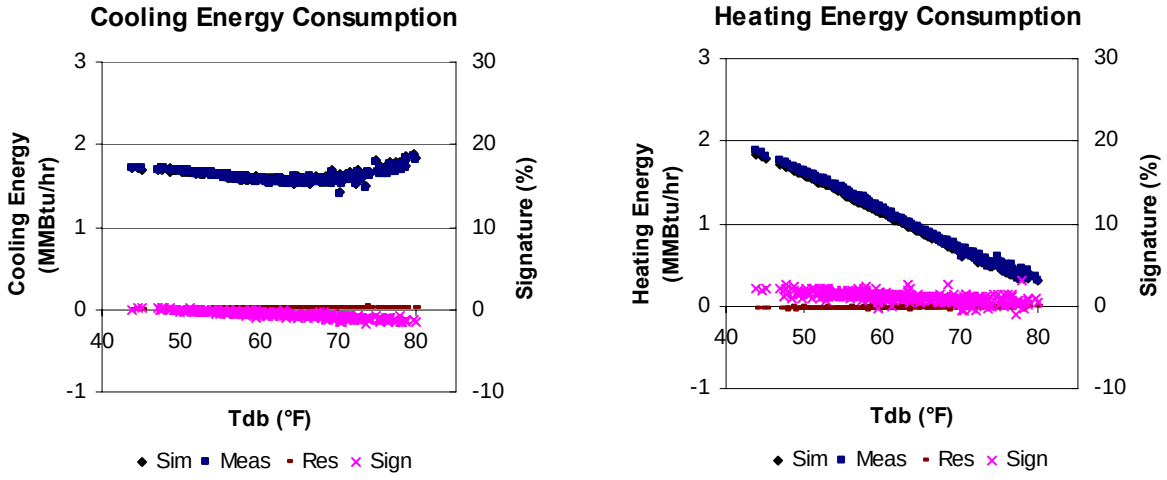

Figure 33. Simulation charts for Example 1 during first iteration with T_C = 53.8 °F

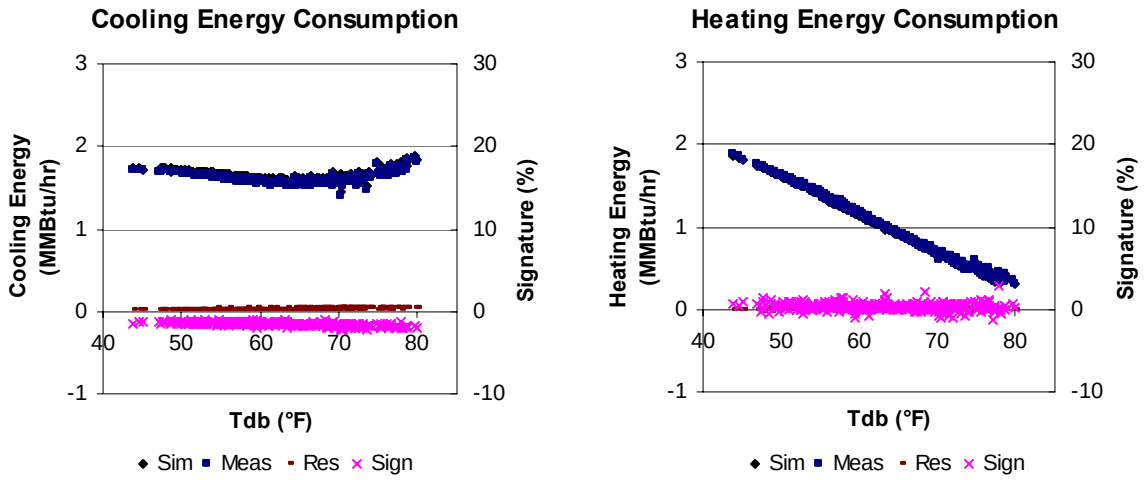

Figure 34. Simulation charts for Example 1 during first iteration with T_C = 53.4 °F

After the first iteration of the calibration process, the calibration signatures show improvement, but there are still significant errors, and the shape of the calibration signatures still show a detectable trend.

- ***Iteration 2.*** The calibration signatures in Figure 32 have negative values for cooling and positive values for heating. They have negative slopes and approach zero at low temperatures for cooling, and at high temperatures for heating. Referring again to Figure 22, it can be noticed that the characteristic signatures for decreasing the internal gain have the same characteristics. In the characteristic signature, a decrease of 0.4 W/ft^2 in internal gains caused maximum changes of about -9% and 7% respectively in cooling and heating energy use. The magnitude of the calibration signatures in Figure 32 reaches about –2% and 2% respectively for cooling and heating energy use, so internal gains should be decreased by about

0.1 W/ft^2. Different values between 0.65 and 0.85 W/ft^2 were tested and the best result was obtained by decreasing internal gains from 0.8 to 0.72 W/ft^2.

After this iteration, the calibration signatures and RMS errors dropped to zero. Figure 35 shows calibrated simulation charts.

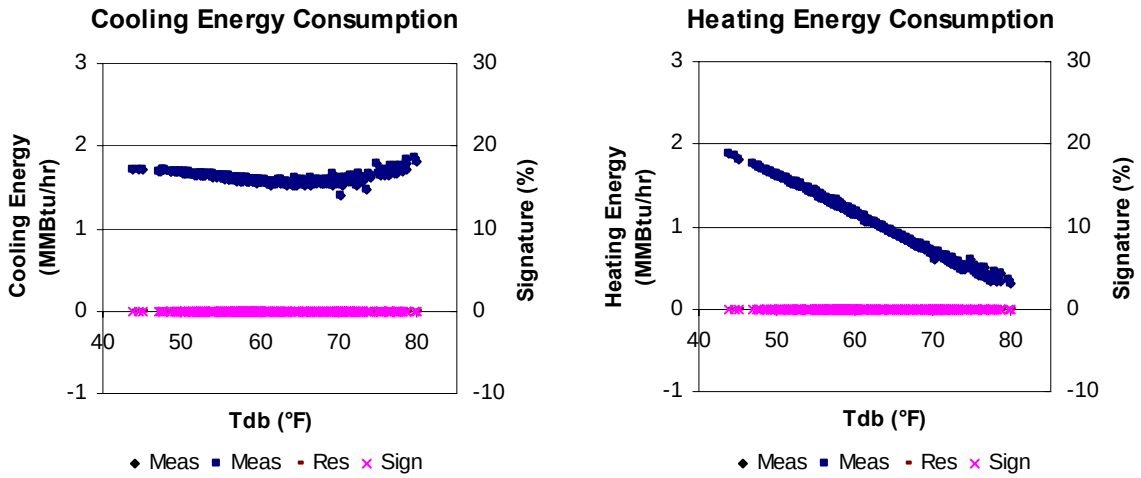

Figure 35. Calibrated simulation for Example 1

V.2 A more complex example

This example utilizes the same building system used in the previous example and described in section III.4. In this example, a more complex set of differences were introduced into the "uncalibrated" simulation to increase the difficulty of the calibration process. In addition, the person who devised the baseline simulation that produced the synthetic "measured" data was not the same individual who conducted the calibration. It was therefore possible at the end of the process to compare the final inputs that were selected through the calibration process with the "real" inputs that had been used, and to comment on how successfully the simulation was calibrated.

- ***Step 1***. The results of a "baseline" simulation were used in this example as the "measured" data. Then, the individual who conducted the calibration was given a different set of inputs as the inputs for the "uncalibrated" simulation. The example illustrates the use of characteristic signatures to identify the changes needed to calibrate the simulation. Pasadena weather data was used.
- ***Step 2***. The uncalibrated simulation was conducted with hourly data.
- ***Step 3***. Hourly weather and cooling and heating data were converted to daily averages.
- ***Step 4***. The residuals, the RMSE and the calibration signatures were calculated for the initial simulation. The RMSE was found to be 0.07 MMBtu/hr and 0.18 MMBtu/hr respectively for cooling and heating energy consumption.
- ***Step 5***. Measured data (Meas), simulation results (Sim), residuals (Res) and calibration signatures (Sign) were plotted versus outside air dry-bulb temperature (T_{db}), as shown in Figure 36, for cooling (left) and heating (right). Signature magnitudes are shown on the right hand side y-axis.

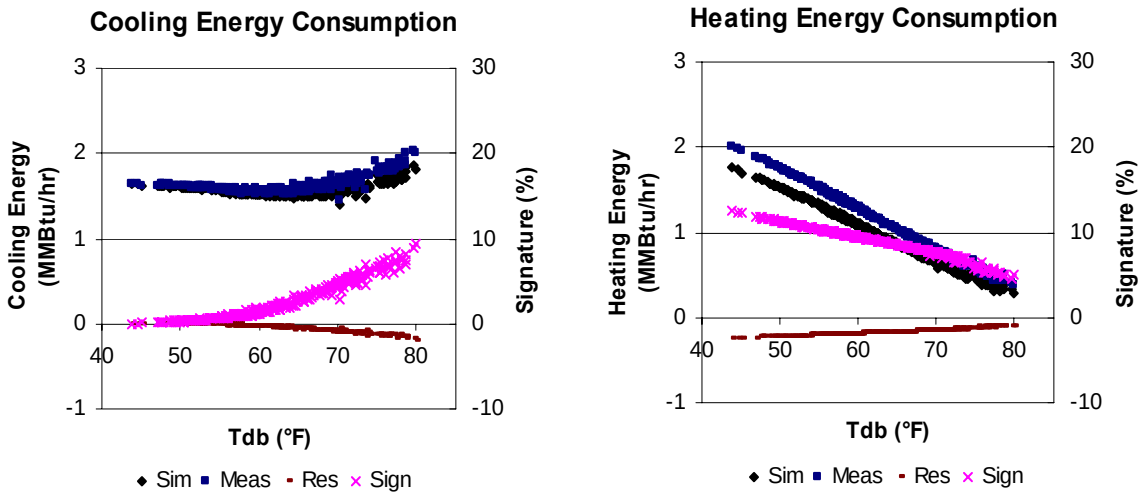

Figure 36. Initial simulation for Example 2 including calibration signatures

- ***Step 6***. Examining the calibration signatures of the first simulation indicates that the cooling signature is almost 10% at high temperatures, but close to zero at low temperatures. While the heating signature always has significant positive values, it has the opposite slope. Examining the characteristic signatures in Figure 22 indicates that only outside air and envelope U-value have this combination of opposite slopes. Neither has a strong positive value throughout the range of outside temperatures, so it can be assumed that the calibration signatures represent a combination of multiple characteristic signatures. I chose to modify the outside air quantity, since both calibration signatures reach large values at extreme temperatures, more like those of the outside air signatures than the envelope U-values.
- ***Step 7***. In the characteristic signature of Figure 22, the outside air flow rate was increased by 0.05 cfm/ft^2, which caused an increase of about 15% in cooling and a decrease of about 8% in heating across the entire range of ambient temperature. In the calibration signatures the change was about 10% and -8% respectively for cooling and heating. This suggests that the outside air flow rate should be increased by about 0.05 cfm/ft^2 or less. Different increments ranging from 0.02 to 0.06 cfm were tested and the best result was obtained by increasing the outside air flow rate from 0.10 to 0.14 cfm/ft^2.
- ***Step 8***. After this change, the calibration signature approached zero at high temperatures for cooling, but increased at low temperatures. The cooling RMSE remained at 0.07 MMBtu/hr, but the signature became more uniform across the entire temperature range. For heating, the signature is noticeably smaller at low

temperatures, but has changed little at high temperatures. The heating RMSE decreased from 0.18 to 0.16 MMBtu/hr. Figure 37 shows simulation charts after this first iteration.

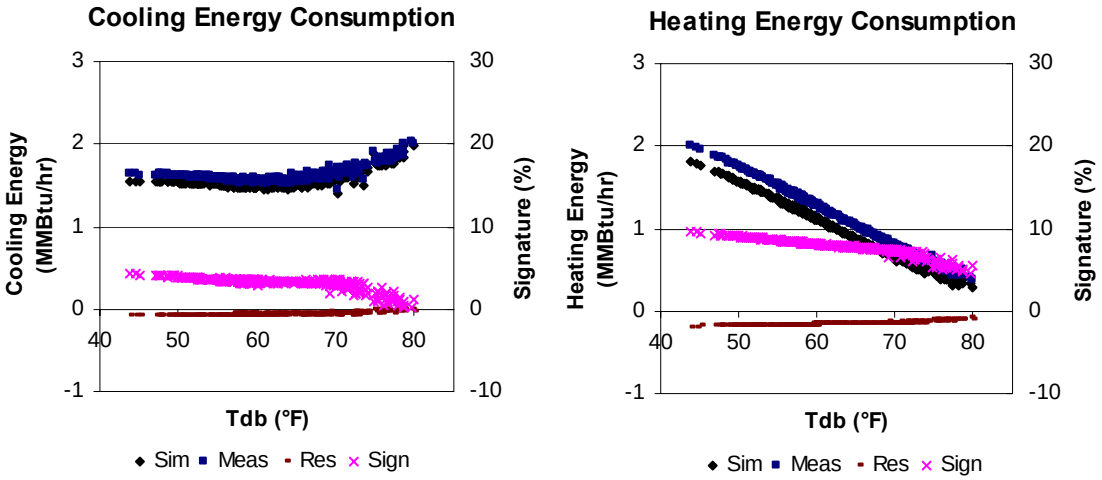

Figure 37. Simulation charts for Example 2 after the first iteration

- ***Iteration 2***. It is needed to alter a calibration parameter so that both cooling and heating energy consumption increase over the entire range of outside air temperature, and the characteristic signatures for both cooling and heating should have negative slopes. Examining the characteristic signatures of Figure 22 indicates that decreasing the cold deck temperature, increasing the supply air, or increasing the floor area all have these general characteristics. It can also be noted increasing the floor area had a fairly large cooling characteristic signature at high temperatures, while the cooling calibration signature of Figure 37 is near zero at high temperatures, so it is possible to consider only cold deck temperature or supply air flow rate at this point. This is often true - the calibration signatures will not suggest a single option, but will point toward a small number of options. It is

relatively easy to measure cold deck temperatures, so that would be a logical step at this point if one has access to the building. In this illustrative example, I chose to decrease the cold deck temperature because its cooling characteristic signature reaches zero at high temperatures.

It was not possible to bring both cooling and heating calibration signatures to zero by decreasing the cold deck temperature, but I found that when the cold deck temperature was decreased from 55 to 54 °F, the cooling RMSE dropped considerably from 0.07 to 0.02 MMBtu/hr. Both cooling and heating calibration signatures dropped over almost the entire range of outdoor temperatures as shown in Figure 38. The heating RMSE decreased from 0.16 to 0.12 MMBtu/h.

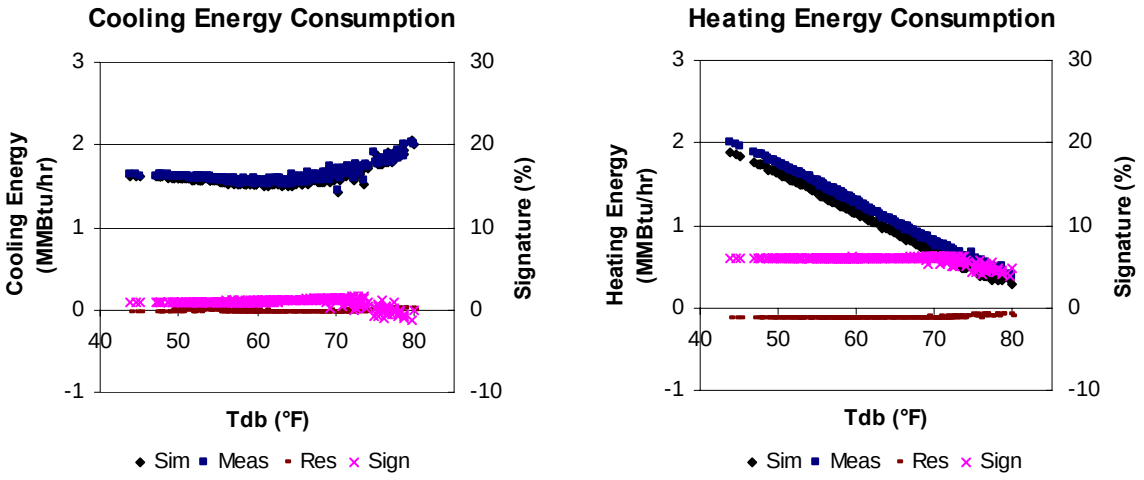

Figure 38. Simulation charts for Example 2 after iteration 2

- ***Iteration 3***. The calibration signatures are now both positive, but the heating signature is considerably larger than the cooling signature. None of the characteristic signatures match these characteristics, but room temperature

characteristic signatures are both positive at low temperatures and the heating characteristic signature is twice as large as that of cooling. This calibration step will target the low temperature range assuming that the calibration signatures of Figure 38 require a set of combined characteristic signatures. In the characteristic signature, increasing the room temperature from 73 °F to 74 °F caused energy use to increase by 2% and 4% at low temperatures respectively for cooling and heating, while the calibration signatures are at 1% and 6% at low temperatures respectively for cooling and heating. This suggests that increasing room temperature by about 0.5 °F should bring the cooling calibration signature to zero at low temperatures, and increasing it by 1.5 °F should bring the heating calibration signature to zero at low temperature. It was decided to increase room temperature by only 0.5 °F to avoid too much effect on the high temperature side. The room temperature setpoint was therefore increased from 73 °F to 73.5 °F. Figure 39 shows simulation charts after this change. As expected, the cooling calibration signature has approached zero at low temperatures, but the cooling RMSE has actually increased slightly from 0.02 to 0.03 MMBtu/hr due to the slight increase at high temperatures. The heating RMSE has decreased slightly from 0.12 to 0.11 MMBtu/hr.

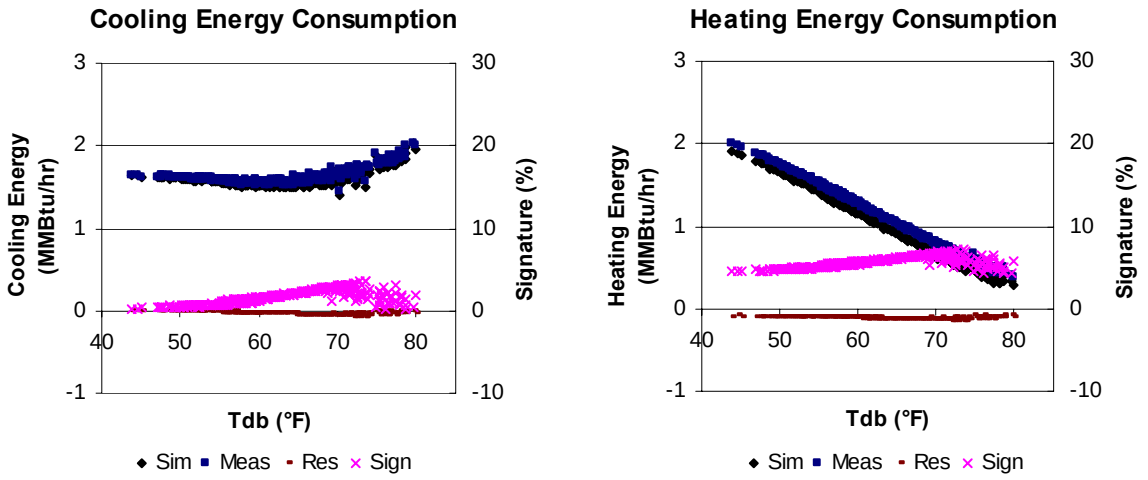

Figure 39. Simulation charts for Example 2 after iteration 3

- ***Iteration 4***. There are now peaks in the middle range of high temperatures in both the cooling and heating calibration signatures. Examination of the characteristic signatures of Figure 22 indicates that the hot deck temperature characteristic signatures have a similar trend. I found out that increasing the hot deck temperature to remove the peaks caused the RMSE to decrease for heating and increase for cooling, so both RMSE values were summed and a minimum value was sought. The best result was obtained by increasing the hot deck temperature by 2 °F. The heating RMSE dropped sharply from 0.11 MMBtu/hr to 0.04 MMBtu/hr and the cooling RMSE increased slightly from 0.03 to 0.05 MMBtu/hr. After this alteration, the peaks have been removed as shown in Figure 40.

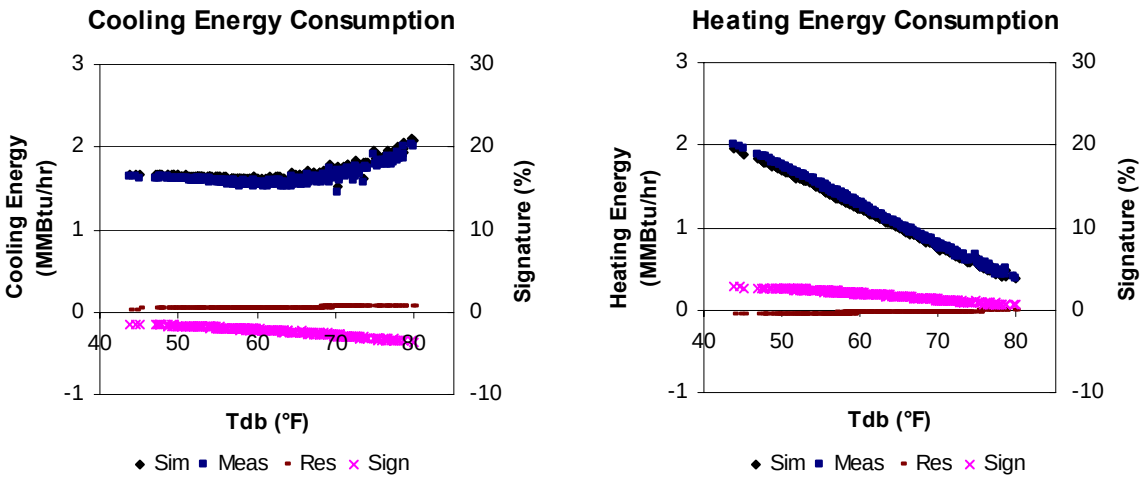

Figure 40. Simulation charts for Example 2 after iteration 4

- ***Iteration 5***. The calibration signature for cooling is now negative with a negative slope while the heating signature is positive with a negative slope. Alternatively, it can be said that cooling energy consumption needs to be decreased, and heating energy consumption increased over the entire temperature range. The change should tend to zero at lower temperatures for cooling consumption, and at higher temperatures for heating consumption. Examining the signatures of Figure 22 indicates that only a decrease in internal gain level has a similar set of signatures. In this set of signatures, a decrease of 0.4 W/ft^2 in internal gains caused maximum changes of -9% and 7% respectively for cooling and heating, while the calibration signatures reach -4% and 3% respectively for cooling and heating. This suggests that internal gains have to be decreased by about 0.15 to 0.2 W/ft^2. Different values were tested and the best result was obtained by decreasing internal gains from so 0.8 to 0.6 W/ft^2. It provided an extremely good match as shown in Figure 41. The calibration signatures have dropped to near zero over the whole range of

temperatures, and the RMS errors are only 0.003 and 0.001 MMBtu/hr respectively for cooling and heating energy consumption. The simulation model is now calibrated.

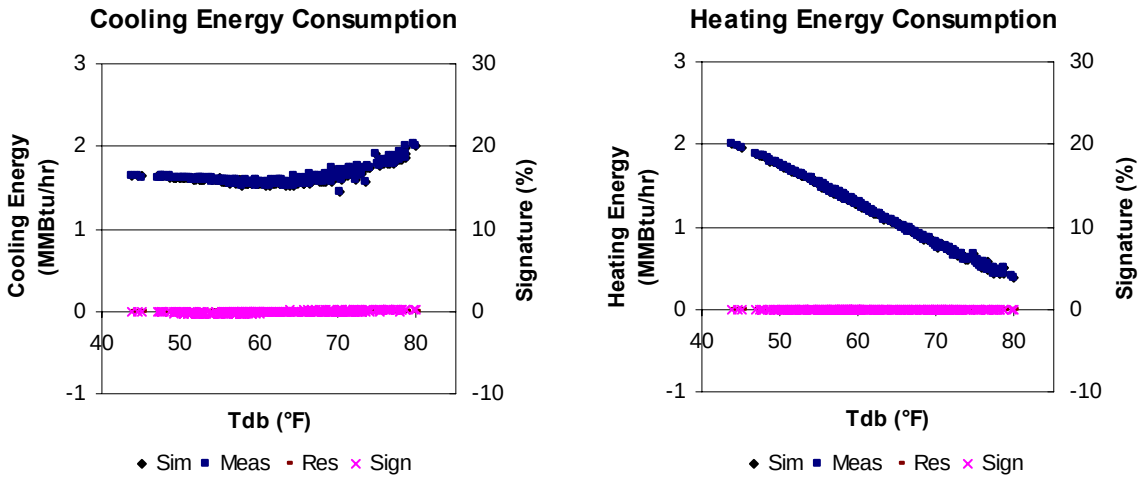

Figure 41. Calibrated simulation for Example 2

In this example, the generation of the original simulation the provided the "measured" data and the calibration process were conducted by two people. This was done to provide more realistic calibration conditions where the answer was not known by the one performing the calibration. The alterations made to generate the uncalibrated simulation and those made to calibrate the system are compared in Table 5.

Note that the changes made to input parameters to calibrate the model are close to those needed to correct the errors that were intentionally introduced to simulate the real building. Temperature differences were 0.5 °F or less, which is comparable to measurement accuracy.

Table 5. Comparison of calibration alterations with "real" errors

Input parameter	Model calibration	"Measured" Value
Outside air flow rate	0.1 → 0.14 cfm/ft^2	0.14 cfm/ft^2
Cold deck Temperature	55 → 54 °F	53.6 °F
Room Temperature	73 → 73.5 °F	73 °F
Hot deck Temperature	110 → 112 °F at T_{OA}=40 °F 80 → 82 °F at T_{OA}=70 °F 70 → 72 °F at T_{OA}=100 °F	111.5 °F at T_{OA}=40 °F 81.5 °F at T_{OA}=70 °F 71.5 °F at T_{OA}=100 °F
Internal heat gain	0.8 → 0.6 W/ft^2	0.55 W/ft^2

Step 9 (hourly fine tuning) of the calibration procedure was not used in these examples. This step is rather helpful when calibrating to real data, which typically produces somewhat more scatter in the results than shown in these examples that used "measured" data generated by a simulation program. The case studies presented in the next section show the use of this final calibration step in real buildings.

CHAPTER VI

CASE STUDY

This section describes an additional example, using data from a real building rather than simulations. This example shows that in real buildings, issues such as lack of sufficient measured data and operational changes can make the calibration process somewhat more complicated, but that the characteristic calibration signatures method still allowed the analyst to define a believable simulation with minimal effort.

VI.1 Building information

The Oakland Administration Building was constructed in 1998. It consists of two separate buildings, the Dalziel Building and the Wilson Building, with a combined gross area of 450,000 ft^2 and a relatively low whole building energy use of 50 $kBtu/ft^2/yr$ (Motegi et al. 2002).

The objective of this case study was to calibrate the simulation of cooling and heating energy consumption for Dalziel. This building, shown in Figure 42, has six floors with an estimated conditioned floor area of about 230,000 ft^2. The main HVAC system is a Single Duct Variable Air Volume (SDVAV) system with hot water reheat. Two 500-ton chillers, located in Dalziel, serve the main air handlers in both buildings, while each building has its own hot water boilers. Table 6 shows metering points in the building for the HVAC system, lighting and plug loads (Motegi 2002).

Figure 42. Picture of the Dalziel Building

Table 6. Metering points for the Dalziel building

Folder	File	Metering point	Comment	Interval
D_kw	CHWBTU	D_CHLR_BTU/HR	Chiller Btu/hr	15 mn
	CHWSYSK	D_CHLR_1&2_KW	Chillers kW	15 mn
		D_PRCHWP_4&5_KW	CHW pump 4&5 kW	15 mn
		D_CHWP_6-8_KW	CHW pump 6&8 kW	15 mn
	CWSYSKW	D_CLG_TWR_1_KW	Cooling tower 1 kW	60 mn
		D_CLG_TWR_2_KW	Cooling tower 2 kW	60 mn
		D_CWP_1-3_KW	CHW pump 1-3 kW	60 mn
	ELVKWKW	D_G_ELEV_KW	Garage elevator kW	60 mn
		D_GAR_ELEV_KWH	Garage elevator kWh	60 mn
		D_ELEVATOR_KW	Elevator kW	60 mn
		D_ELEV_KWH	Elevator kWh	60 mn
	FANKWKW	D_SF_1-4_KW	Supply fan 1-4 kW	15 mn
		D_RF_1-4_KW	Return fan 1-4 kW	15 mn
		D_SF_1-4_KWH	Supply fan 1-4 kWh	15 mn
		D_RF_1-4_KWH	Return fan 1-4 kWh	15 mn
	HHWBTU	D_HW_BTU/H	HW Btu/hr	15 mn
		D_HHW_GAS	HW gas ft^3	15 mn

Table 6. Continued

Folder	File	Metering point	Comment	Interval
D_kw	MISEFKW	EF-1_LD_DK_KW	Exhaust fan 1 kW	60 mn
		EF-2_TEF_KW	Exhaust fan 2 kW	60 mn
		EF-3_CHLRRM_KW	Exhaust fan 3 kW	60 mn
		OSA-1_KW	Outside air fan kW	60 mn
	PACKWKW	D_PAC-1_KW	(kW)	60 mn
		D_PAC-2_KW	(kW)	60 mn
		D_PAC-1_KWH	(kWh)	60 mn
		D_PAC-2_KWH	(kWh)	60 mn
D_kwh	CHW_KWH	D_CHLR_1&2_KWH	Chillers kWh	15 mn
		D_PCHWP_4&5_KWH	CHW pump 4&5 kWh	15 mn
		D_CHWP_6_8_KWH	CHW pump 6&8 kWh	15 mn
	CW_KWH	D_CT_1_KWH	Cooling tower 1 kWh	15 mn
		D_CT_2_KWH	Cooling tower 2 kWh	15 mn
		D_CWP_1_3_KWH	CW pumps1-3kWh	15 mn
	FL3VAFP	CONF_RM_D3317	Zone temp	60 mn
		CONF_RM_D	Zone temp	60 mn
		OFFICE_D4305	Zone temp	60 mn
		PO2_D4348	Zone temp	60 mn
D_sys	2	SF1/2_MA_TEMP	Mixed air temp	15 mn
	B_SF3_4	SF_3_MA_TEMP	Mixed air temp	15 mn
		SF_4_MA_TEMP	Mixed air temp	15 mn
	CH12CTL	CH#1_CHWS_TEMP	Chiller 1 CHWS temp	15 mn
		CH#2_CHWS_TEMP	Chiller 2 CHWS temp	15 mn
		BLDG_CHWS_TEMP	Building CHWS temp	15 mn
		BLDG_CHWR_TEMP	Building CHWR temp	15 mn
		CHW_FLOW	CHW gpm	15 mn
		CHILLER_#1_S/S	Chiller 1 On/off	15 mn
		CHILLER_#2_S/S	Chiller 2 On/off	15 mn
		CHWP-4_S/S	CHW pump 4 On/off	15 mn
		CHWP-5_S/S	CHW pump 5 On/off	15 mn

Table 6. Continued

Folder	File	Metering point	Comment	Interval
D_sys	CHWP6_8	CW_FRM_TWR_TEMP	CW temp from tower	15 mn
		CW_TO_TWR_TEMP	CW temp to tower	15 mn
		D_BLDG_CHWS_DP	Building CHWS DP	15 mn
		CHWP-6_S/S	CHW pump 6 On/off	15 mn
		CHWP-7_S/S	CHW pump 7 On/off	15 mn
		CHWP-8_S/S	CHW pump 8 On/off	15 mn
	CWP1_3	MIX_VLV_FDBK	Mixing valve %	15 mn
		CHWP-1_S/S	CHW pump 5 On/off	15 mn
		CHWP-2_S/S	CHW pump 5 On/off	15 mn
		CHWP-3_S/S	CHW pump 5 On/off	15 mn
	DBOILER	BLR_FLOW	Boilers gpm	15 mn
		BLR#1_HHWS_TEMP	Boiler 1 HWS temp	15 mn
		BLR#2_HHWS_TEMP	Boiler 1 HWS temp	15 mn
		HWP-9_S/S	HW pump 9 On/off	15 mn
		HWP-10_S/S	HW pump 10 On/off	15 mn
	SF1_2	SF_1/2_SA_TEMP	(°F)	15 mn
		SF_1/2_RA_TEMP	(°F)	15 mn
		SF_1/2_DUCT_ST	Static pressure	15 mn
		SF_1/2_DMPRS	Dampers %	15 mn
		OPEN_OFFC_D6303	Zone temp	60 mn
		OFFICE_D6307	Zone temp	60 mn
		GENERAL_MANAGER	Zone temp	60 mn
	Slab	FLR_5_MASS_TEMP	Slab temp	60 mn
Dlitekw	DELITE	D_ELITE_RSR_KW	(kW)	60 mn
	DWLITE	D_WLITE_RSR_KW	(kW)	60 mn
	LTKWKWH	D_INT_LITE_KW	Interior light kW	60 mn
		D_INT_LITE_KWH	Interior light kWh	60 mn
	XLKWKWH	D_EXT_LITE_KW	Exterior light kW	60 mn
		D_EXTERIOR_LITE	Exterior light kWh	60 mn
		D_EXTERIOR_LT	Exterior light On/off	60 mn

Table 6. Continued

Folder	File	Metering point	Comment	Interval
Dlite	DELITE	D_E_LIGHTING_KWH	East light kWh	60 mn
	DWLITE	D_W_LIGHTING_KWH	West light kWh	60 mn
kwh Dplugkw	DFLR1A	DFLR1A_PLUG_KW	Flr 1 Plug (kW)	60 mn
	DFLR2E	DFLR2E_PLUG_KW	Flr 2 East Plug (kW)	60 mn
	DFLR2W	DFLR2W_PLUG_KW	Flr 2 West Plug (kW)	60 mn
	DFLR3E	DFLR3E_PLUG_KW	Flr 3 East Plug (kW)	60 mn
	DFLR3W	DFLR3W_PLUG_KW	Flr 3 West Plug (kW)	60 mn
	DFLR4E	DFLR4E_PLUG_KW	Flr 4 East Plug (kW)	60 mn
	DFLR4W	DFLR4W_PLUG_KW	Flr 4 West Plug (kW)	60 mn
	DFLR5E	DFLR5E_PLUG_KW	Flr 5 East Plug (kW)	60 mn
	DFLR5W	DFLR5W_PLUG_KW	Flr 5 West Plug (kW)	60 mn
	DFLR6E	DFLR6E_PLUG_KW	Flr 6 East Plug (kW)	60 mn
	DFLR6W	DFLR6W_PLUG_KW	Flr 6 West Plug (kW)	60 mn
		D_TTL_PLG_KWH	Total Plug (kW)	60 mn
Dplugkwh	CUNION	CUNION_PLUG_KWH	(kWh)	60 mn
	DFL1E_W	DFL1W&E_PLUGS	Flr 1 Plug (kWh)	60 mn
	DFLR2E	DFL2E_PLUG_KWH	Flr 2 East Plug (kWh)	60 mn
	DFLR2W	DFLR2W_PLUG_KWH	Flr 2 West Plug (kWh)	60 mn
	DFLR3E	DFL3E_PLUG_KWH	Flr 3 East Plug (kWh)	60 mn
	DFLR3W	DFLR3W_PLUG_KWH	Flr 3 West Plug (kWh)	60 mn
	DFLR4E	DFL4E_PLUG_KWH	Flr 4 East Plug (kWh)	60 mn
	DFLR4W	DFLR4W_PLUG_KWH	Flr 4 West Plug (kWh)	60 mn
	DFLR5E	DFL5E_PLUG_KWH	Flr 5 East Plug (kWh)	60 mn
	DFLR5W	DFLR5W_PLUG_KWH	Flr 5 West Plug (kWh)	60 mn
	DFLR6E	DFL6E_PLUG_KWH	Flr 6 East Plug (kWh)	60 mn
	DFLR6W	DFLR6W_PLUG_KWH	Flr 6 West Plug (kWh)	60 mn

VI.2 Calibration process

- ***Step 1***. The major difficulty encountered in calibrating the Dalziel Building was frequent changes in the operating schedule of the building systems. In the interest of avoiding this issue, this case study considers only a 3-month period when the schedule was consistent, i.e. March 5 to June 2, 2000.
- ***Step 2***. AirModel was used for the simulation. The main input parameters for the initial simulation are shown in Table 7. They were taken or calculated from a report on the Oakland Administration Building (Eley Associates 2001), as well as a set of files that includes measured data and input and output files from an earlier DOE-2 simulation provided by Motegi (2002). These input parameters were considered to be representative of expected operation of the building. Monthly solar gains were calculated using the Klein-Theilacker method (Duffie and Beckman 1991) described in Appendix A. The months of December and July were established as having respectively the minimum and maximum solar gains. These two months were therefore used as the maximum and minimum solar gain inputs as required by AirModel as shown in Table 7. AirModel approximates solar gains as a linear function of outside air temperature (Knebel 1983).

  Site measured weather data was used for the simulation. Figure 43 shows daily average ambient temperature variations and daily average dry-bulb temperatures versus daily average wet-bulb temperatures for the simulation period.

Table 7. Initial AirModel simulation parameters for the case study

Parameter	Value
Conditioned floor area	231,557 ft^2
Interior zone ratio	0.2
Occupied period	6 am to 6 pm on weekdays only
Exterior wall and roof area	91.982 ft^2
Average exterior wall and roof U-value	0.073 $Btu/ft^2.hr.°F$
Window area	19,339 ft^2
Window U-value	0.34 $Btu/ft^2.hr.°F$
Room temperature setpoint T_{room}	72 °F
Minimum air flow rate	0.34 cfm/ft^2
Outside air flow rate	0.28 cfm/ft^2
Economizer range	40 - 70 °F
Average internal heat gain Q_{int}	1.8 W/ft^2
Solar gains	0.078 MMBtu/h at 42 °F, and 0.138 MMBtu/h at 88 °F
Air infiltration	None
Average occupancy	356 ft^2/person
Difference between return and room air temperatures	2 °F
Cold deck temperature T_c	64 °F
Preheat location	Outside air
Preheat temperature T_{ph} schedule	45 °F for T_{OA}<45 °F

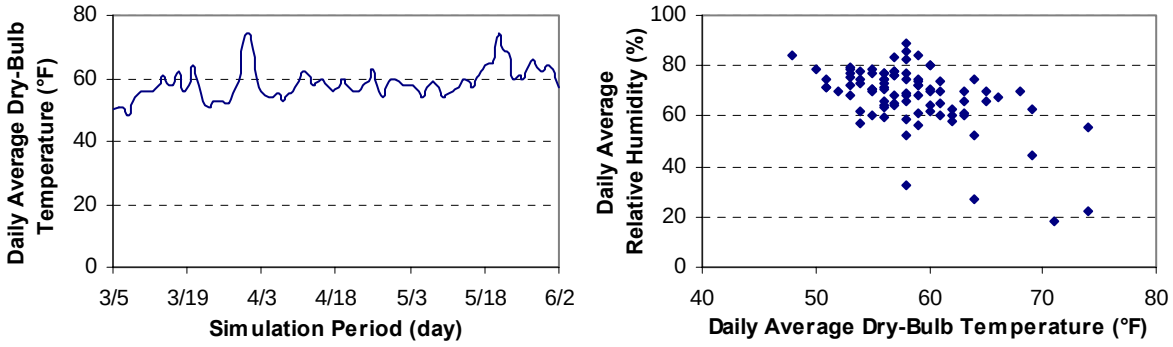

Figure 43. Weather conditions for the simulation period

- ***Step 3***. Daily average values were used for this simulation. Using daily averages helps eliminate dynamic effects and reduce the scatter. The major difficulty was the small number of cooling data points. The number of hourly cooling data points was very small because chillers were turned off whenever the ambient temperature was less than 65°F; a large number of hourly measurements were also missing, so a number of days with insufficient hourly data were eliminated. In the absence of reliable cooling data, a model was created for cooling energy consumption using measured data from the period between June 5 and August 7, 2001, for which considerably more daily average cooling energy consumption (Q_{cool}) data points could be generated. The 3-parameter change point linear regression model of cooling consumption generated from this data was:

$$Q_{cool}\ (\text{MMBtu/hr}) = 0 \qquad \text{for } T_{db}\ (°\text{F}) < 59.63\ °\text{F}$$

$$= 0.0737\ T_{db}\ (°\text{F}) - 4.3949 \qquad \text{for } T_{db}\ (°\text{F}) \geq 59.63\ °\text{F}$$

- ***Step 4***. The RMS errors for the initial simulation were 0.13 and 0.36 MMBtu/hr respectively for cooling and heating energy consumption.
- ***Step 5***. Cooling and heating simulation charts for the initial simulation are illustrated in Figure 44. This figure consists of four charts. The two charts on the left hand side are cooling charts and the two charts on the right hand side are heating charts. The upper ones show simulated (sim) and measured (meas) daily average energy consumption, as well as residuals (res) as defined in equation 3. The building operates only on weekdays as shown in Table 7. Therefore, weekends, as well as holidays, were removed from the simulation. The lower graphs show calibration signatures as defined in equations 1 and 2. The purpose

of the solid line in the calibration signatures is to reveal the trend of the scattered data points, which makes it easier to compare the calibration signature to characteristic signatures. The trend line is a moving average of 6 points for cooling and 9 points for heating. Groups of an equal number of points have been used rather than temperature bins because data points were not distributed uniformly over the temperature range, and more points were used per group for heating than for cooling because there were considerably more heating than cooling data points.

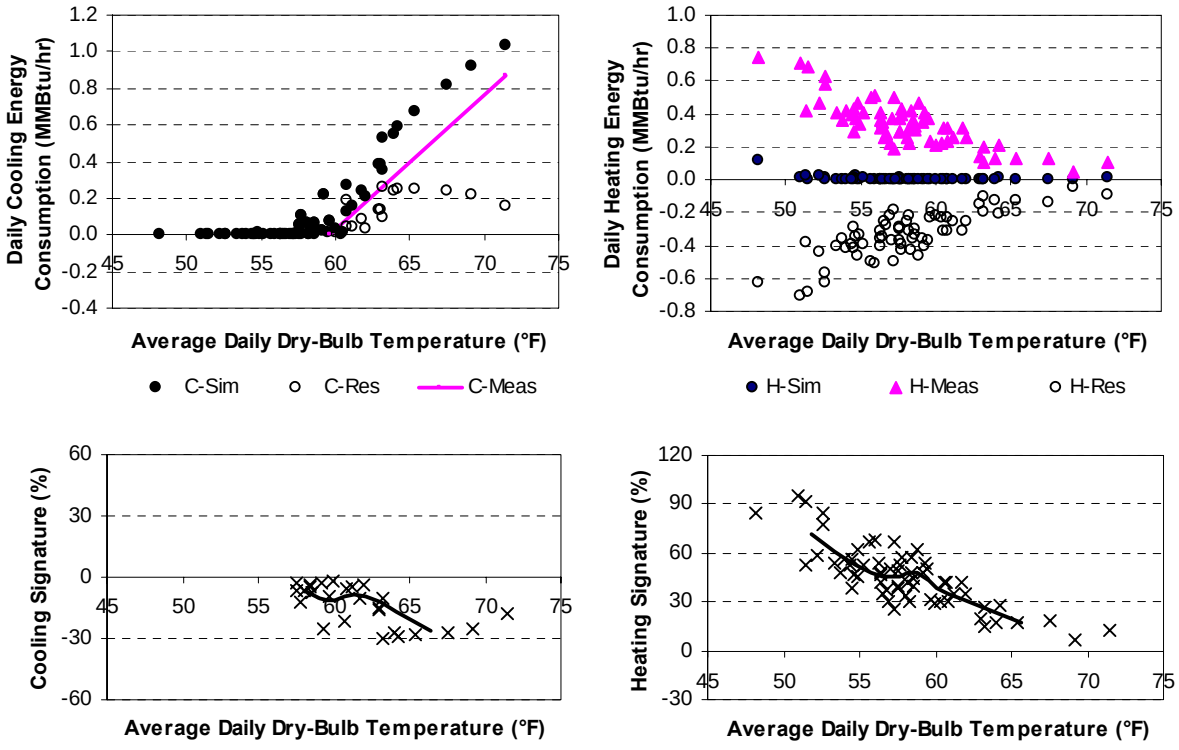

Figure 44. Initial simulation charts for the case study

- ***Step 6***. After running the initial simulation, the major remark is that heating energy consumption is simulated to be zero, while the cooling simulation signature is relatively small. The objective of the first input change should be to produce heating energy consumption over the entire temperature range. The characteristic signatures in Figure 18, corresponding to SDVAV systems in Oakland, will be used for this case study. Examining these characteristic signatures indicates that decreasing the cold deck temperature, increasing the minimum air flow rate, increasing the floor area, decreasing internal gains or increasing room temperature would cause heating to increase uniformly over the entire temperature range. Since the objective of this input change is to increase heating consumption as much as possible, the parameter to be altered for Iteration 1 will be chosen as the most sensitive among those mentioned above. The minimum air flow rate seems to be the most sensitive, since a decrease of as little as 0.03 cfm/ft^2 caused heating energy use to decrease by about 6% over the entire temperature range.
- ***Step 7***. The minimum air flow rate characteristic signature for heating is negative, while the heating calibration signature is positive, so the input parameter should be altered in the opposite sense, i.e. increased. The minimum air flow rate was increased to 0.8 cfm/ft^2.
- ***Step 8***. Figure 45 shows simulation charts after this change. The heating RMSE has decreased considerably from 0.36 to 0.28 MMBtu/hr. The effect of increasing the minimum air flow rate was more pronounced in the lower temperature range, while there was not much effect at higher temperatures, which explains why the

cooling RMSE remained at 0.13 MMBtu/hr as there is no cooling energy consumption at low temperatures.

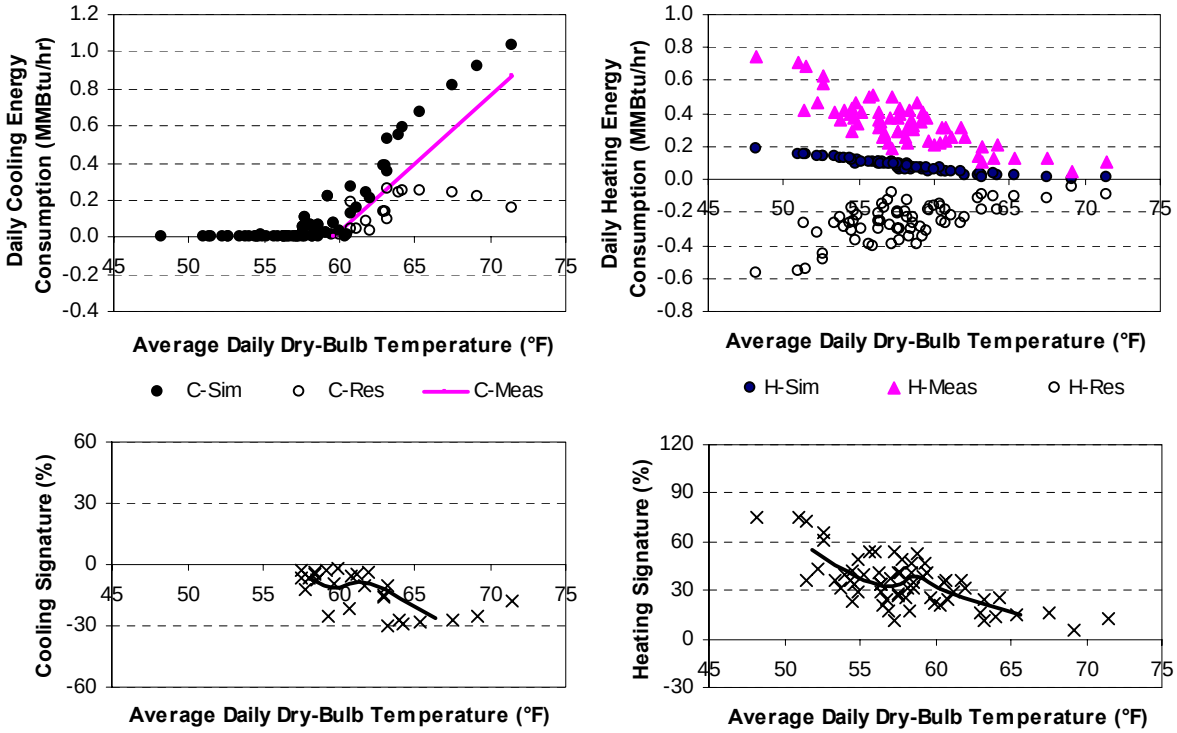

Figure 45. Cooling and heating simulation charts after the first iteration

- ***Iteration 2***. The calibration signature was considerably decreased for heating in Iteration 1. However, it still remains as large as 75% at low temperatures, while the cooling simulation signature is within -30%. This calibration step will focus again on heating energy consumption. Examining the characteristic signatures in Figure 18 indicates that decreasing the internal gain should decrease the heating calibration signature over the total temperature range without much effect on cooling. It should even decrease the cooling calibration signature at high temperatures since the cooling characteristic signature also has a negative slope at

high temperatures. The best result was obtained by decreasing the internal heat gain from 1.8 to 1.25 W/ft^2. Figure 46 shows simulation charts after this change. The RMS errors have decreased from 0.13 to 0.11 MMBtu/hr for cooling and from 0.28 to 0.12 MMBtu/hr for heating.

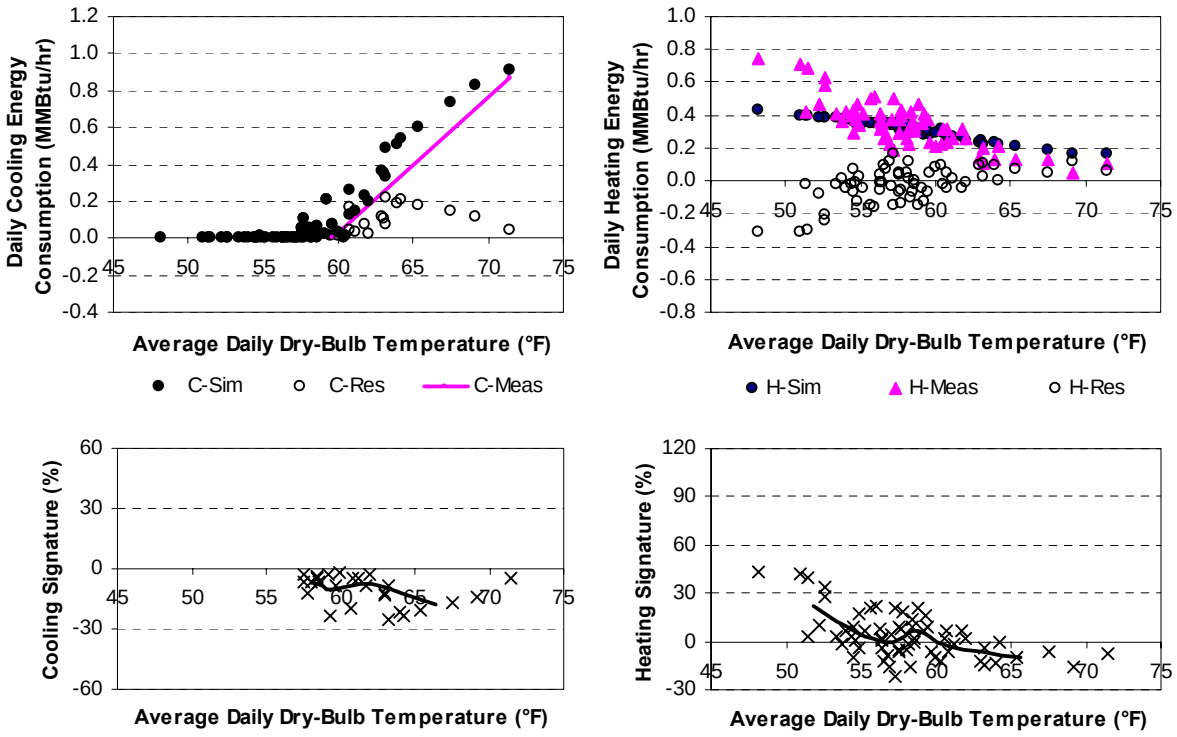

Figure 46. Cooling and heating simulation charts after iteration 2

- ***Iteration 3***. Both cooling and heating RMS errors have decreased after Iteration 2. But, the heating calibration signature still has a steep negative slope at low temperatures. Examining the characteristic signatures in Figure 18 indicates that the heating characteristic signature for outside air is comparable to the heating calibration signature in Figure 46. Therefore, increasing the outside air flow rate should neutralize or reduce the negative slope at low temperatures in the heating

calibration signature. The calibration and characteristic signatures for cooling do not match. In order to reduce the effect on the cooling calibration signatures, the outside air flow rate was increased to partially neutralize the negative slope at low temperatures for heating and make it uniform with the rest of the signature. The outside air flow rate was increased from 0.28 to 0.42 cfm/ft^2. Figure 47 shows simulation charts after this alteration. The RMSE has decreased from 0.12 to 0.10 MMBtu/hr for heating and increased slightly from 0.11 to 0.12 MMBtu/hr for cooling.

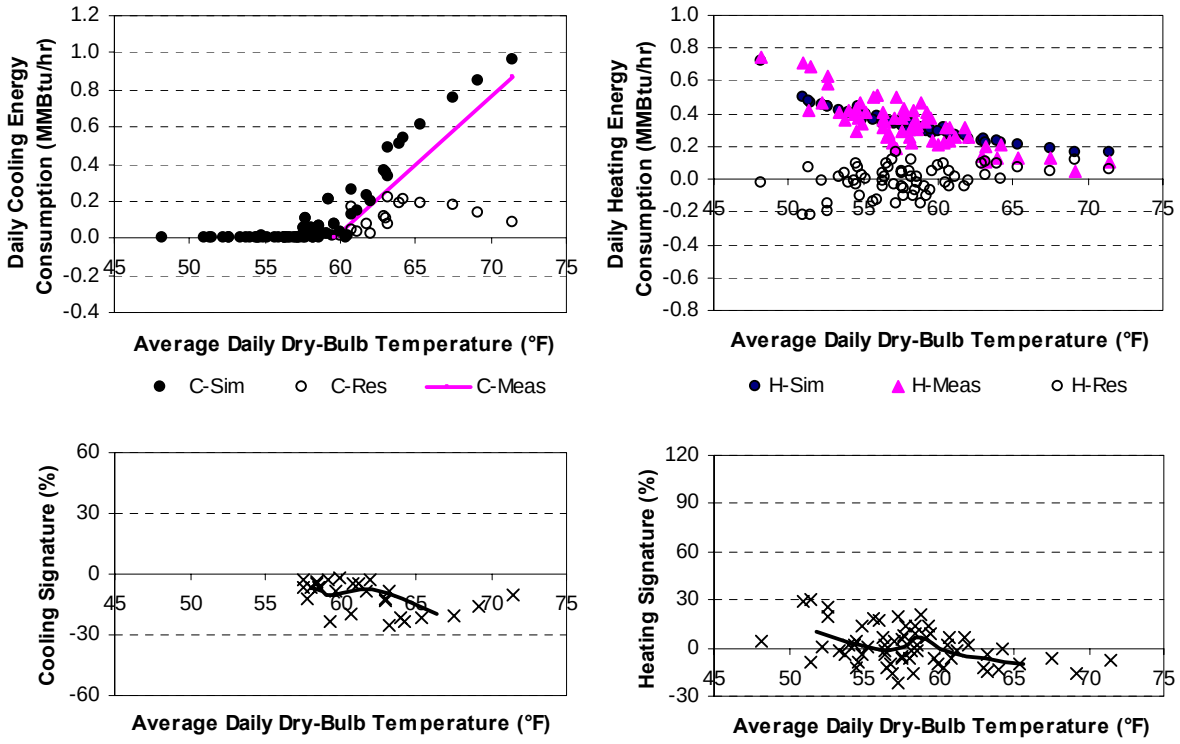

Figure 47. Cooling and heating simulation charts after iteration 3

- ***Iteration 4***. Now that the heating simulation signature has been reduced to reasonable values, the purpose of this calibration step is to reduce the cooling simulation signature over the entire temperature range. The cooling calibration signature in Figure 47 is negative over the total temperature range. It is almost constant at lower temperatures and has a negative slope at high temperatures. Examining the characteristic signatures in Figure 18 indicates that the cooling characteristic signatures for the cold deck temperature (T_c) and the room temperature setpoint (T_{room}) have similar trends and are both positive. Therefore, decreasing the cold deck temperature and/or increasing the room temperature setpoint should neutralize the negative slope at high temperatures, but would increase cooling energy consumption at lower temperatures instead of decreasing it. Similarly, increasing the cold deck temperature and/or decreasing the room temperature setpoint should decrease cooling energy consumption, but would make the negative slope at high temperatures even steeper. In order to decreasing cooling energy consumption and at the same time neutralize the negative slope at high temperatures, both the cold deck temperature and the room temperature setpoint have to be altered, one in the same direction as in the characteristic signature and one in the opposite direction, i.e. both increased or decreased. The best result was obtained by increasing the cold deck temperature from 64 °F to 66 °F and the room temperature setpoint from 72 °F to 73.5 °F. Figure 48 shows simulation charts after this iteration. The RMSE has decreased considerably for cooling from 0.12 to 0.06 MMBtu/hr. It has decreased slightly for heating from 0.10 to 0.09 MMBtu/hr.

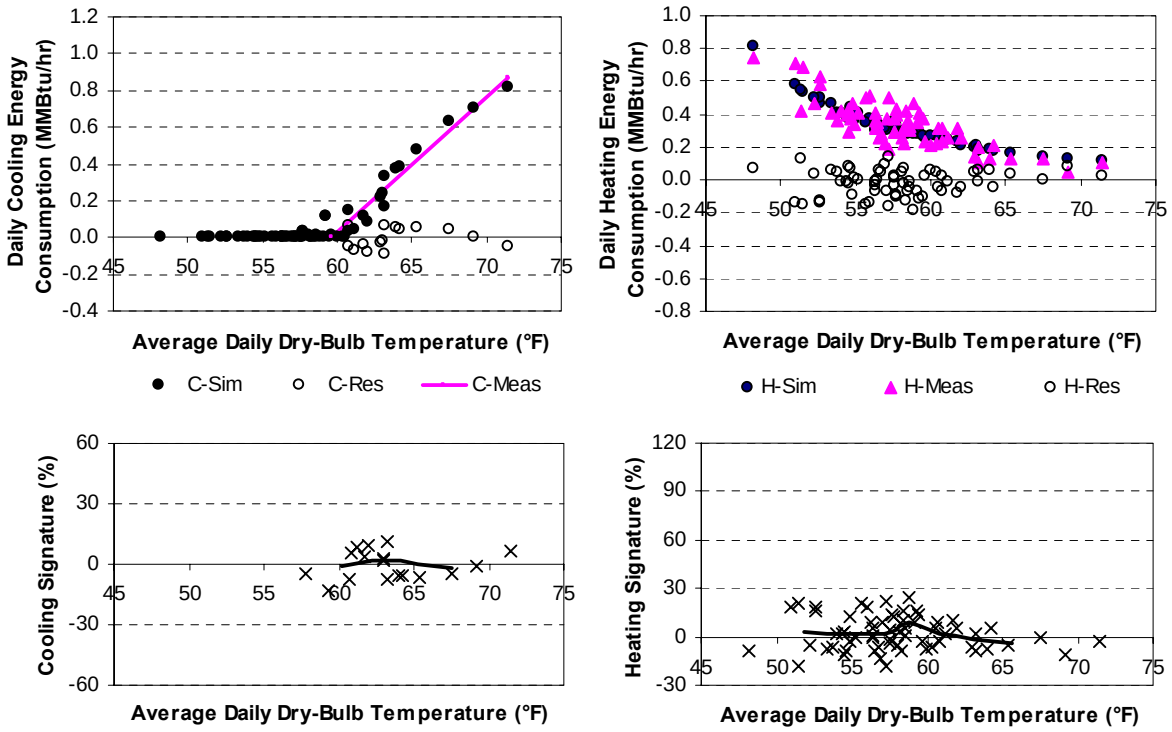

Figure 48. Cooling and heating simulation charts after iteration 4

- ***Iteration 5.*** Both cooling and heating RMS errors have decreased to reasonable values in the previous simulation. But, it can be noticed that the heating calibration signature in Figure 48 still has a slightly negative slope. Examining Figure 18 indicates that the heating characteristic signature for the envelope U-value has a constant positive slope. This characteristic signature was obtained by decreasing the envelope U-value. Therefore, the envelope U-value has to be increased in this calibration step to match the negative slope of the heating calibration signature. The best result was obtained by increasing the U-value by 20%. Consequently the exterior wall and window U-values were increased respectively from 0.073 to 0.088 Btu/ ft^2.hr.°F and from 0.34 to 0.41 Btu/ ft^2.hr.°F.

Figure 49 shows simulation charts after this iteration. The RMSE has slightly decreased for heating from 0.09 to 0.08 MMBtu/hr and remained at 0.06 MMBtu/hr for cooling.

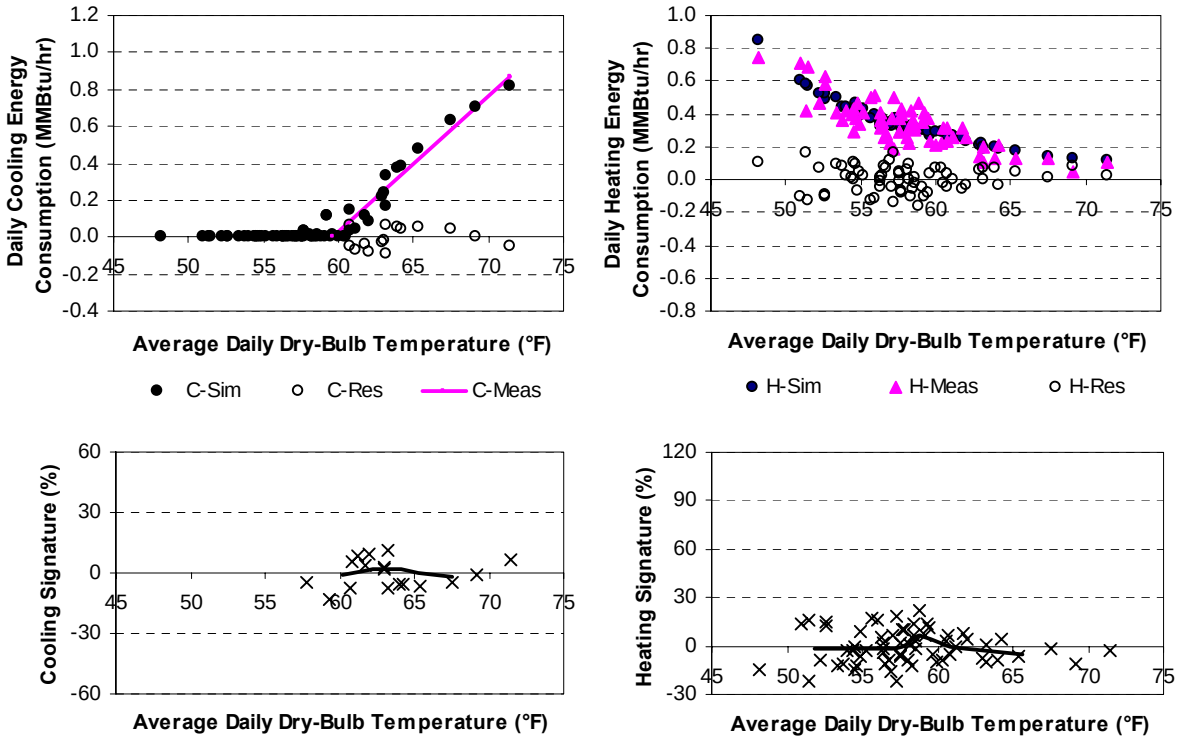

Figure 49. Cooling and heating simulation charts after iteration 5

- ***Step 9***. The objective is to fine-tune the calibration by calibrating the simulation of hourly data. This is achieved by introducing the daily internal gain profile, shown in the right hand side of Figure 50, and calculated from the hourly variations of light and plug loads in the building, shown in the left hand side of Figure 50. The daily internal gain profile was defined for each hour as the ratio of the internal gain to the maximum internal gain. It was calculated for weekdays

only as there were no vacation periods and the HVAC system was shut off on weekends during the calibration period.

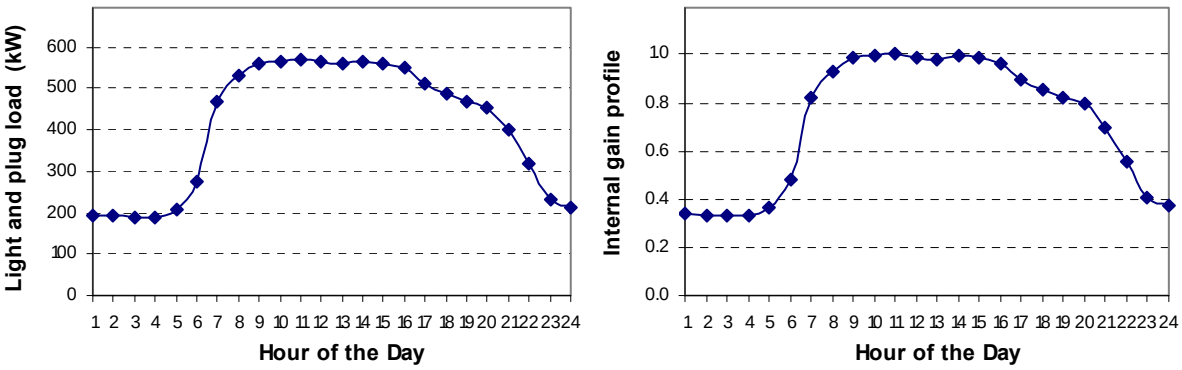

a. Hourly light & plug load

b. Internal heat gain

Figure 50. Internal load and heat gain profiles

Therefore, instead of using an average heat gain of 1.25 W/ft^2 for each hour of the day, a maximum internal gain will be used along with the internal gain profile of Figure 50. The only parameter that needs to be adjusted is the maximum internal gain. Different values were tested and the best result was obtained with 1.42 W/ft^2.

Figure 51 shows calibrated simulation charts. Note on the heating calibration signature that the hourly calibration has reduced the negative slope at high temperatures. The heating RMSE has actually decreased from 0.08 to 0.07 MMBtu/hr while the cooling RMSE has remained at 0.06 MMBtu/hr.

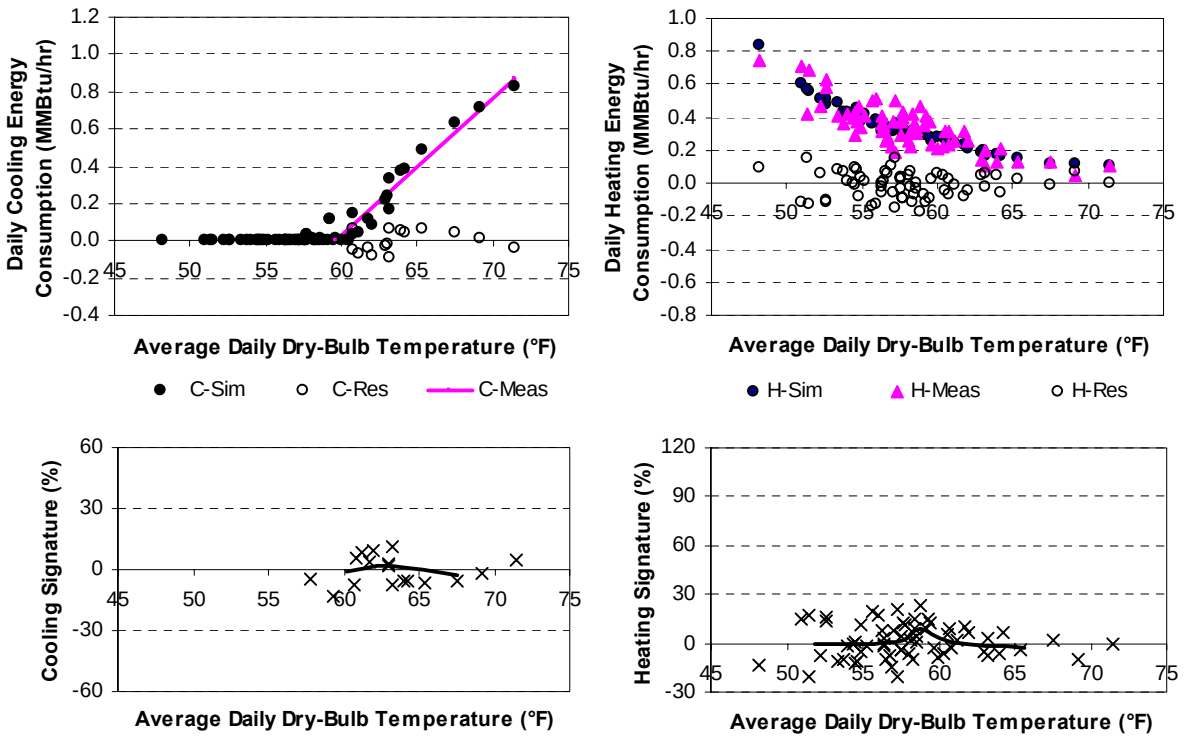

Figure 51. Calibrated simulation charts for the case study

The bulge in the middle of the heating calibration signature is due to the way the temperature range was divided into small intervals of equal numbers of data points. It turned out that the bulge corresponded to an interval where most of the signature data points were higher than the neighboring data points. They would have cancelled out within a larger or shifted temperature interval.

Otherwise, the residuals are randomly scattered around zero and calibration signatures show no trend with temperature for both cooling and heating. The RMS errors have also been reduced to very small values, i.e. 0.06 and 0.07 MMBtu/hr respectively for cooling and heating. Table 8 shows a summary of the calibration steps. The Mean Bias Error (MBE) is shown for each calibration step

for both cooling and heating. It has been reduced from 0.12 to 0.004 MMBtu/hr for cooling and from -0.33 to 0.005 MMBtu/hr for heating during the calibration process.

Table 8. Summary of case study calibration steps

Simulation parameter and alteration	Heating (MMBtu/hr)		Cooling (MMBtu/hr)	
	RMSE	**MBE**	**RMSE**	**MBE**
Initial simulation	0.36	-0.33	0.13	0.12
Minimum air flow rate: 0.34 → 0.8 cfm/ft^2	0.28	-0.25	0.13	0.12
Internal gain (average): 1.8 → 1.25 W/ft^2	0.12	-0.016	0.11	0.09
Outside air flow rate: 0.28 → 0.42 cfm/ft^2	0.10	0.003	0.12	0.10
Cold deck temperature: 64 → 66°F, and room temperature: 72 → 73.5°F	0.09	-0.009	0.06	0.004
Envelope U-value: Increased by 20% ◆ Exterior wall and roof: 0.073 → 0.088 Btu/ft^2.hr.°F ◆ Window: 0.34 → 0.41 Btu/ft^2.hr.°F	0.08	0.012	0.06	0.005
Hourly calibration ◆ Internal gain: 1.25 av. → 1.42 W/ft^2 max. ◆ Internal gain profile: Figure 50 (right)	0.07	0.005	0.06	0.004

Notice that the calibration process in this case study was rather focused on heating energy consumption. This was due to the large heating RMSE in the initial simulation (0.36 MMBtu/hr compared to 0.13 MMBtu/hr for cooling). It took two calibration steps to bring it down to the level of the cooling RMSE. This is because reasonable alterations in input parameters produce limited changes in total energy consumption (expect for adding or removing an economizer as can be seen in Figure 18).

The calibrated simulation RMS errors were very low for this case study. But, simulation signature data points were quite high (± 10 % for cooling and ± 25 % for heating). This is due to the low energy consumption. In fact, the maximum daily average energy consumption was 0.8 MMBtu/hr for cooling and heating. For the sake of comparison, the maximum daily average energy consumption for a building with a comparable conditioned floor area in College Station, TX - namely the Zachry Engineering Center - is 6.5 MMBtu/hr for cooling and 2.5 MMBtu/hr for heating. This consumption level would have produced signatures in the range of ± 1 % for cooling and ± 9 % for heating with the RMS errors of this case study.

CHAPTER VII

CONCLUSIONS

VII.1 Summary

This thesis describes a method that can be used to facilitate the calibration of a building system simulation to measured data. The method uses a graphical format that intuitively summarizes and describes the differences between the simulation results and the measured data, referred to as a calibration signature. By creating a library of shapes for certain known errors, clues can be provided to the analyst to use in identifying what simulation input errors may be causing the discrepancies. These are referred to as characteristic calibration signatures.

This thesis defines calibration and characteristic signatures and illustrates how they are used in calibration. Two fairly simple examples of their use, based on synthetic "measured" data, are provided, as well as a real-world case study that illustrated how to handle additional challenges in the calibration process. The characteristic signatures were provided for four major system types, and for three different California climates.

This method is found to be quite useful, and its use should enable a broader array of analysts to produce better quality building simulations. These more reliable simulations can be used for a host of purposes, including analysis of expected savings, building optimization, commissioning, and fault detection.

VII.2 Future work

This work has extended and formalized the energy signature method. The main recommendation for future research on the signature method is to test the robustness of characteristic signatures by examining their dependence on building characteristics, and weather and baseline conditions. It would also be valuable to determine if the proposed calibration process can help determine the existence of hot deck, cold deck, or temperature reset schedules.

REFERENCES

Ahmad, M., 2003, "Systematic Time-Based Study for Quantifying the Uncertainty of Uncalibrated Models in Building Energy Simulations," M.S. thesis, Texas A&M University, College Station, TX.

Baltazar-Cervantes, J., 2000, "Study of Cubic Spines and Fourier Series as Interpolation Techniques for Filling in Short Periods of Missing Building Energy Use and Weather Data," M.S. thesis, Texas A&M University, College Station, TX.

Bronson, D., Hinchey, S., Haberl, J., and O'Neal, D., 1992, "A Procedure for Calibrating the DOE-2 Simulation Program to Non-Weather-Dependent Measured Loads," *ASHRAE Transactions*, Vol. 98, Part 1, pp. 636-652. Paper number AN-92-1-5.

Building Systems Laboratory (BSL), 1999, "BLAST 3.0 Users Manual," Department of Mechanical and Industrial Engineering, Building Systems Laboratory, University of Illinois, Urbana-Champaign, IL.

Chen, H., 1999, "Rehabilitating Missing Energy Use and Weather Data When Determining Retrofit Energy Savings in Commercial Buildings," M.S. thesis, Texas A&M University, College Station, TX.

Claridge, D., 1998, "A Perspective on Methods for Analysis of Measured Energy Data from Commercial Buildings," *Transactions of the ASME*, Vol. 120, pp. 150-155.

Clark, D.R., and May, W.B., 1985, "HVACSIM+ Building Systems and Equipment Simulation Program - Users Guide," Performer: National Bureau of Standards (NEL), Gaithersburg, MD. Building Equipment Div., Sponsor: Department of Energy, Washington, DC, Office of Building and Community Systems, Civil Engineering Lab. (Navy), Port Hueneme, CA. Sep 1985. 203p. Report: NBSIR-85 /3243.

Crawley, D. B., Lawrie, L. K., Winkelmann, F.C., Buhl, W.F., Huang, Y.J., Pedersen, C. O., Strand, R. K., Liesen, R. J., Fisher, D. E., Witte, M. J., and Glazer, J., 2001, "EnergyPlus: Creating a New-Generation Building Energy Simulation Program," *Energy and Buildings Journal*, Vol. 33, No. 4, pp. 319-331.

Diamond, S., and Hunn, B., 1981, "Comparison of DOE-2 Computer Program Simulations to Metered Data from Seven Commercial Buildings," *ASHRAE Transactions*, Vol. 87, Pt. 1, pp. 1222-1231.

Duffie, J.A., and Beckman, W.A., 1991, *Solar Engineering of Thermal Processes*, 2nd edition. John Wiley & Sons, New York.

Eley Associates, 2001, "Oakland Administration Building Energy Performance Contract," San Francisco, CA.

Energy Information Administration (EIA), 1997, "Commercial Buildings Characteristics 1995," US Department of Energy, Washington, DC.

Fleming, W.S., and Associates, Inc., 1983, "ASEAM: A Simplified Energy-Analysis Method. Microcomputer Program Users Manual," Department of Energy, Washington, DC. Report: DOE/CE/20286-T1.

Haberl, J., Bronson, D., and O'Neal, D., 1995, "Impact of Using Measured Weather Data vs. TMY Weather Data in a DOE-2 Simulation," *ASHRAE Transactions*, Vol. 101, Pt 2, 1995, pp. 558-576.

Haberl, J. and Bou-Saada, T., 1998, "Procedures for Calibrating Hourly Simulation Models to Measured Building Energy and Environmental Data," *ASME Journal of Solar Energy Engineering*, Vol. 120, pp. 193-204, August.

Huang, Y.J. and Crawley, D.B., 1996, "Does It Matter Which Weather Data You Use in Energy Simulations?," *Proceedings of the ACEEE 1996 Summer Study on Energy Efficiency in Buildings*, Vol. 4, pp. 183-192, Washington, DC, August 25 - 31, 1996.

International Performance Measurement and Verification Protocol (IPMVP), 2001, "Concepts and Options for Determining Energy and Water Savings," DOE/GO-102001-1187, U.S. Dept. of Energy, Washington, DC.

Kaplan, M., McFerran, J., Jansen, J., and Pratt, R., 1992, "Reconciliation of a DOE2.1c Model With Monitored End-use Data from a Small Office Building," *ASHRAE Transactions*, Vol. 96, Pt 1, pp.981-993.

Knebel, D.E., 1983, *Simplified Energy Analysis Using the Modified Bin Method*, American Society of Heating, Refrigerating, and Air-Conditioning Engineers, Inc, Atlanta, GA.

Kusuda, T., 2001, "Building Environment Simulation Before Desktop Computers in the USA Through a Personal Memory," *Energy and Buildings Journal*, Vol. 33, No. 4, pp. 291-302.

Liu, M., 1997, *User's Manual for Air Side Simulation Programs (AirModel)*, Energy Systems Laboratory, Texas A&M University, College Station, TX.

Liu, M., and Claridge, D.E., 1998, "Use of Calibrated HVAC System Models to Optimize System Operation," *ASME Journal of Solar Energy Engineering*, Vol. 120, pp. 131-138.

Liu, M., Wei, G. and Claridge, D. E., 1998, "Calibrating AHU Models Using Whole Building Cooling and Heating Energy Consumption Data," *Proceedings of the ACEEE 1998 Summer Study on Energy Efficiency in Buildings*, Vol. 3, pp. 229-241, Washington, DC, American Council for an Energy Efficient Economy, .

Liu, M., 2001, Personal communication, August 2001. Energy Systems Laboratory, University of Nebraska.

Manke, J., and Hittle, D., 1996, "Calibrating Building Energy Analysis Models Using Short-Term Test Data," *Proceedings of the 1996 International Solar Energy Conference*, pp. 369-378, San Antonio, TX, March 31-April 3, 1996.

Motegi, N., Piette, M.A., and Wentworth, S., 2002, "From Design Through Operations - Multi -Year Results from a New Construction Performance Contract," *Proceedings of the 2002 ACEEE Summer Study on Energy Efficiency in Buildings*, pp. 291-302, Pacific Grove, CA, August 18-23, 2002.

Motegi, N., 2002, Personal communication, February 2002. Lawrence Berkeley National Laboratory, Berkeley, CA.

Norford, L. K., Socolow, R. H., Hsieh, E. S., and Spadaro, G. V., 1994, "Two-to-One Discrepancy Between Measured and Predicted Performance of a `Low-Energy' Office Building: Insights from a Reconciliation Based on the DOE-2 Model," *Energy and Buildings Journal*, Vol. 21, No. 2, pp. 121-131.

Subbarao, K., 2000, "Method and Apparatus for Improving Building Energy Simulations". United States patent number 6,134,511.

Thamilseran, S., 1999, "An Inverse Bin Methodology to Measure the Savings from Energy Conservation Retrofits in Commercial Buildings," Ph.D. dissertation, Texas A&M University, College Station, TX.

Wei, G., Liu, M., and Claridge, D.E., 1998, "Signatures of Heating and Cooling Energy Consumption for Typical AHUs," *Proceedings of the Eleventh Symposium on Improving Building Systems in Hot and Humid Climates*, pp. 387-402, Fort Worth, TX, June 1-2, 1998.

Winkelmann, F.C., Birdsall, B.E., Buhl, W.F., Ellington, K.L., Erdem, A.E., Hirsch, J.J., and Gates, S., 1993, *DOE-2 Supplement, Version 2.1E*, LBL-34947. Lawrence Berkeley National Laboratory, National Technical Information Service, Springfield, VA.

APPENDIX A

SOLAR HEAT GAIN CALCULATIONS

According to Knebel (1983), solar gains may be approximated as a linear function of ambient temperature between the minimum solar gain, represented by the monthly average solar gain for the month of December, and the maximum solar gain, represented by the monthly average solar gain for the month of June.

This appendix presents monthly average solar gain calculations. The minimum and maximum solar gains will be identified and a linear approximation will be made.

Solar gain calculations in this appendix use the Klein-Theilacker method presented in Duffie & Beckman (1991). This method calculates monthly average daily radiation on a tilted surface ($\overline{H}_T$), in this case vertical windows, using monthly average daily radiation on a horizontal surface ($\overline{H}$). Solar gain is then calculated for each building exposure using window areas, shading coefficients, and a/c system runtime. The total solar gain is the sum of solar gains for each building exposure. The results of these calculations are presented for the three California cities used in this thesis: Oakland, Pasadena, and Sacramento.

The data used to carry out monthly average solar gain calculations and determine the minimum and maximum solar gains are:

- $\overline{T}$ (°C), the 24-hour monthly average ambient temperature for 12 months.

- $\overline{H}$ (MJ/m^2), the monthly average daily radiation on a horizontal surface for 12 months.

These data are available for more than 240 locations in the United States in Duffie & Beckman (1991).

The calculations are described below.

$\overline{H}_0$ (MJ/m^2), the monthly average daily extraterrestrial radiation on a horizontal surface.

$$\overline{H}_0 = \frac{24x3600G_{sc}}{\pi}\ (1 + 0.033 \cos\frac{360n}{365}) \text{ x } (\cos\phi \cos\delta \sin\omega_s + \frac{\pi\omega_s}{180}\sin\phi \sin\delta)$$

where

■ G_{sc} (W/m^2) is the solar constant. It is the energy from the sum, per unit time, received on a unit area of surface perpendicular to the direction of propagation of the radiation, at mean earth-sun distance, outside of the atmosphere.

$$G_{sc} = 1367 \text{ W/m}^2$$

■ n is the average day of the month as shown in Table A-1.

Table A-1. Average day of the month

Month	1	2	3	4	5	6	7	8	9	10	11	12
n	17	47	75	105	135	162	198	228	258	288	318	344

■ ϕ (°) is the latitude. It is defined as the angular location North or South of the equator. North is positive and South is negative. $-90° \le \phi \le +90°$.

■ δ (°) is the declination. It is defined as the angular position of the sun at solar noon (i.e., when the sun is on the local meridian) with respect to the plane of the equator. North is positive and South is negative. $-23.45° \le \phi \le +23.45°$.

$$\delta = 23.45 \sin(360 \frac{284 + n}{365})$$

■ ω_s (°) is the sunset hour angle. It is the angle between the local meridian and the sun at sunset.

$$\cos \omega_s = - \tan \phi \tan \delta$$

$\overline{K}_T$ (dimensionless), the monthly average clearness index.

$$\overline{K}_T = \frac{\overline{H}}{\overline{H}_0}$$

$\overline{H}_T$ (MJ/m^2), the monthly average daily radiation on a vertical exposure.

$$\overline{H}_T = \overline{H} \left[D + \frac{\overline{H}_d}{\overline{H}} \frac{1 + \cos \beta}{2} + \rho_g \frac{1 - \cos \beta}{2}\right]$$

where

■ $$\frac{\overline{H}_d}{\overline{H}} = \begin{cases} 1.391 - 3.560\ \overline{K}_T + 4.189\ \overline{K}_T^2 - 2.137\ \overline{K}_T^3 & \text{if } \omega_s \le 81.4° \text{ and } 0.3 \le \overline{K}_T \le 0.8 \\ 1.311 - 3.022\ \overline{K}_T + 3.427\ \overline{K}_T^2 - 1.821\ \overline{K}_T^3 & \text{if } \omega_s > 81.4° \text{ and } 0.3 \le \overline{K}_T \le 0.8 \end{cases}$$

■ β is the surface tilt angle. It is defined as the angle between the plane of the surface and the horizontal. $0 \le \beta \le 180°$, with $\beta > 90°$ for downward facing surfaces. $\beta = 90°$ for vertical window surfaces.

■ ρ_g is the ground reflectance. It depends on the condition of the ground surface, and therefore on the season. ρ_g can vary from 0.2 for a rocky surface to 0.7 for a snowy surface.

■ $$D = \begin{cases} \max\{0, G(\omega_{ss}, \omega_{sr})\} & \text{if } \omega_{ss} \ge \omega_{sr} \\ \max\{0, [G(\omega_{ss}, -\omega_s) + G(\omega_s, \omega_{sr})\} & \text{if } \omega_{ss} < \omega_{sr} \end{cases}$$

where

· $$|\omega_{ss}| = \min\left\{\omega_s, \cos^{-1}\frac{AB - C\sqrt{(A^2 - B^2 + C^2)}}{A^2 + C^2}\right\}$$

$$\text{and } \omega_{ss} = \begin{cases} +|\omega_{ss}| & \text{if (A>0 and B>0) or (A}\ge\text{B)} \\ -|\omega_{ss}| & \text{otherwise} \end{cases}$$

· $$|\omega_{sr}| = \min\left\{\omega_s, \cos^{-1}\frac{AB + C\sqrt{(A^2 - B^2 + C^2)}}{A^2 + C^2}\right\}$$

$$\text{and } \omega_{sr} = \begin{cases} -|\omega_{sr}| & \text{if (A>0 and B>0) or (A}\ge\text{B)} \\ -|\omega_{sr}| & \text{otherwise} \end{cases}$$

· $$G(\omega_1, \omega_2) = \frac{1}{2d}\left[\left(\frac{bA}{2} - a'B\right)(\omega_1 - \omega_2)\frac{\pi}{180} + (a'A - bB)(\sin\omega_1 - \sin\omega_2) - a'C(\cos\omega_1 - \cos\omega_2)\right.$$
$$\left. + \left(\frac{bA}{2}\right)(\sin\omega_1\cos\omega_1 - \sin\omega_2\cos\omega_2) + \left(\frac{bC}{2}\right)(\sin^2\omega_1 - \sin^2\omega_2)\right]$$

· $A = \cos\beta + \tan\phi\cos\gamma\sin\beta$

· $B = \cos \omega_s \cos \beta + \tan \delta \sin \beta \cos \gamma$

· $C = \dfrac{\sin \beta \sin \gamma}{\cos \phi}$

· γ (°) is the surface azimuth angle. It is defined as the deviation of the projection on a horizontal plane of the normal to the surface from the local median, with 0° due South, East negative, and West positive. $-180° \le \gamma \le +180°$.

· $a' = a - \dfrac{\overline{H}_d}{\overline{\overline{H}}}$

· $a = 0.409 + 0.5016 \sin(\omega_s - 60)$

· $b = 0.6609 - 0.4767 \sin(\omega_s - 60)$

· $d = \sin \omega_s - \dfrac{\pi \omega_s}{180} \cos \omega_s$

$Q_{sol,i}$ (MJ/hr/m^2), building solar gain for exposure i.

$$Q_{sol,i}\,(\text{MJ/hr/m}^2) = \overline{H}_T\,(\text{MJ/m}^2) \times \frac{\text{Window area on building exposure i (m}^2\text{) x SC}}{\text{a/c runtime (hr) x Building conditioned floor area (m}^2\text{)}}$$

where SC (dimensionless) is the shading coefficient.

Notice that $\overline{H}_T$ is in MJ per m^2 of window area, and that $Q_{sol,i}$ is in MJ per hour per m^2 of conditioned floor area.

Q_{sol} (MJ/hr/m^2), total building solar gain.

$$Q_{sol}\,(\text{MJ/hr/m}^2) = \sum_i Q_{sol,i}$$

Q_{sol} can be converted to I-P units as follows:

$$Q_{sol}\,(\text{Btu/hr/ft}^2) = 88.09\; Q_{sol}\,(\text{MJ/hr/m}^2)$$

Results

Figure A-1 shows solar gain, Q_{sol} in Btu/hr/ft^2, as a function of $\overline{T}$, the 24-hour monthly average ambient temperature in °F. These results were obtained using the prototypical building described in section III.4. The labels on data points represent the corresponding months. Notice that the curves have elliptic shapes, with the data points going clockwise from January to December. The solid line and the equation represent the linear fit. The solid bold line represents the linear approximation that was made using the linear fit. The dashed lines represent the minimum and maximum solar gains, and the minimum and maximum ambient temperatures obtained from the hourly data in the weather files.

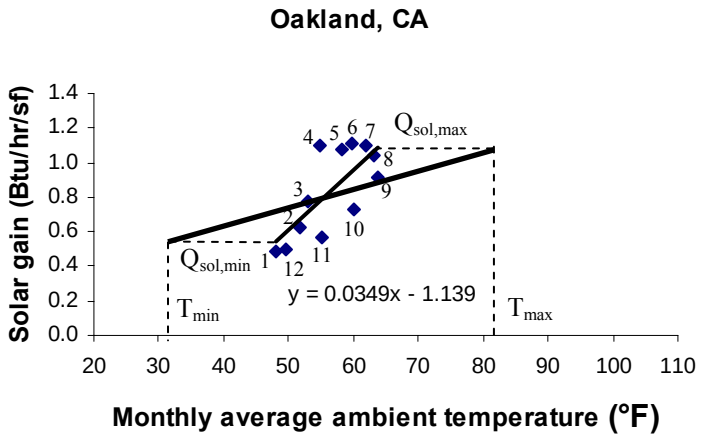

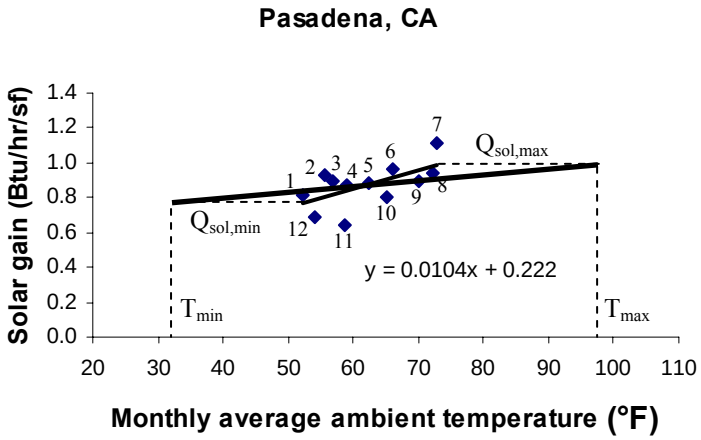

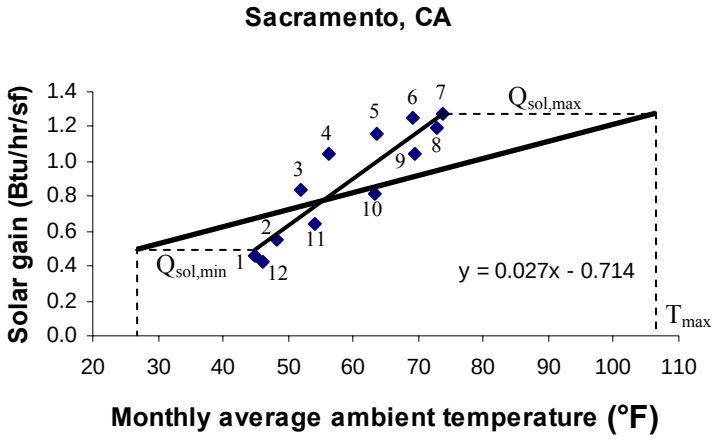

Figure A-1. Solar gain graphs for the three California cities

As stated by Knebel (1983), solar gains may be approximated as a linear function of ambient temperature between the minimum solar gain, represented by the month of December, and the maximum solar gain, represented by the month of June. The monthly average solar gains for the months of December and June, respectively, appear to be a good estimation for the minimum and maximum solar gains, as determined by the linear fit shown in Figure A-1.

Table A-2 shows the minimum and maximum solar gains and ambient temperatures used in AirModel for the three California cities.

Table A-2. Linear approximation of solar gain for the three California cities

	T_{min} (°F)	$Q_{sol,min}$ (Btu/hr/ft^2)	T_{max} (°F)	$Q_{sol,max}$ (Btu/hr/ft^2)
Oakland	32	0.54	82	1.08
Pasadena	32	0.77	97	0.98
Sacramento	27	0.49	107	1.27

VITA

NABIL BENSOUDA

Address: Mimosa, Imm 1, Apt 4
Fes, Morocco

Email:
nabil@fulbrightweb.org

EDUCATION

- **08/2004** Texas A&M University, College Station, TX
  Department of Mechanical Engineering
  MASTER OF SCIENCE IN MECANICAL ENGINEERING
- **08/2004** Texas A&M University, College Station, TX
  Department of Architecture
  FACILITY MANAGEMENT CERTIFICATE
- **06/1996** Ecole des Mines, Rabat, Morocco
  Department of Materials Engineering
  BACHELOR OF SCIENCE IN MATERIALS ENGINEERING

WORK EXPERIENCE

- **07/1996- 05/1999** Alakhawayn University, Ifrane, Morocco
  School of Science & Engineering
  LECTURER

SCHOLARSHIPS

- **08/1999- 07/2001** Sponsor: US Information Agency
  FULBRIGHT SCHOLARSHIP
- **05/2004** Sponsor: American Society of Heating, Refrigerating and Air Conditioning Engineers
  ASHRAE SCHOLARSHIP

ASSISTANTSHIPS

- 09/2003-08/2004 Sponsor: Energy Office, Texas A&M university
  Project: Continuous Commissioning of the main Texas A&M campus
- **01/2001- 08/2003** Sponsor: California Energy Commission
  - Project: High Efficiency Commercial Buildings (through Berkeley National Lab.)
  - Publication: "Manual of procedures for calibrating simulations of building systems" (HPCBS#E5P23T2b). [Online]: http://buildings.lbl.gov/hpcbs/pubs/E5P23T2b.pdf
- **07/2000-12/2000** Sponsor: Rebuild America
  Project: Continuous Commissioning of two College Station ISD schools

MEMBERSHIPS

- **09/1999-** American Society of Mechanical Engineers
- **04/2000-** American Solar Engineers Society
- **09/2000-** American Society of Heating, Refrigerating and Air Conditioning Engineers